Geology and Metallogeny
of the upper mantle rocks from the
Serranía de Ronda

Fernando Gervilla
José María González-Jiménez
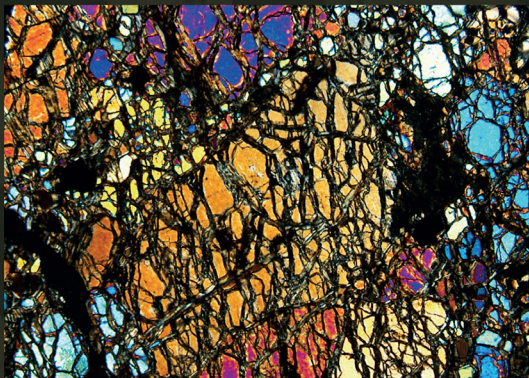Károly Hidas
Claudio Marchesi
Rubén Piña

Fernando Gervilla serves as Professor of Mineralogy in the Department of Mineralogy and Petrology of the University of Granada. He received his degree in Geology in 1984 and his PhD in Sciences (Geology) in 1989, both from the University of Granada, and completes his formation on experimental mineralogy during a postdoctoral stay in the University of Copenhagen (Denmark) in 1990. Since his PhD research project on the metallogeny of the ultramafic massifs of the Serranía de Ronda, Fernando's research activities continue focusing on the mineralogy of ore deposits related with mafic and ultramafic rocks, mainly on the role played by arsenic on the behavior of platinum-group elements in magmatic systems, the genesis of ophiolite-related chromite ores and the causes of fluid-induced chromite alteration during metamorphism.

José María González-Jiménez currently works at the Department of Mineralogy and Petrology, University of Granada. He received his PhD in Earth Sciencies in 2009 from University of Granada and worked as Postdoctoral researcher in Maquarie University in Australia (2010-2013) and Assistant Professor at University of Chile (2014-2017). José María has focused his research on the mineralogy and geochemistry of ores associated with mafic and ultramafic rocks, specializing in the use of trace elements and radiogenic isotopes to track the mobility and concentration of precious metals during magmatic and metamorphic processes. He currently develops innovative approach to decipher the impact of nanoscale processes on the geochemical evolution and metallogeny of the Earth's lithosphere.

Károly Hidas is a petrologist and is currently a postdoctoral researcher at the Instituto Andaluz de Ciencias de la Tierra (Granada, Spain). He studied geology and holds a PhD degree in Earth sciences awarded by the Eötvös Loránd University (Budapest, Hungary) in 2010. His expertise is microstructural analysis of endogenous rocks, and he is striving to understand the feedback of fluids/melts on textural evolution, with particular interest in deformation processes and annealing phenomena in the mantle. He will be appointed tenured researcher of the Instituto Geológico y Minero de España (Madrid, Spain) from 2020.

Claudio Marchesi is a researcher of the Department of Mineralogy and Petrology, University of Granada. He got his PhD in Earth Sciences in 2006 from the University of Granada and moved as Postdoctoral researcher to the Macquarie University in Australia (2008) and Géosciences Montpellier in France (2009-2010). Claudio´s research mainly consists in the study of the geochemical, petrological and mineralogical processes that control the formation and evolution of the Earth´s crust, the upper mantle and the associated ore deposits. To achieve these goals, he performs mineral and whole-rock analyses of major, trace elements and radiogenic isotopes in volcanic, plutonic and metamorphic rocks from the lithosphere of different geodynamic settings.

Rubén Piña is associate professor at the Department of Mineralogy and Petrology of the University Complutense of Madrid (Spain). He teaches Ore Geology and Ore Exploration Models. Rubén obtained his PhD at the same University working on the metallogenesis of the Ni-Cu Aguablanca ore deposit. His main research interests have been related to ore-forming processes of mineralizations associated with mafic-ultramafic rocks. Currently, his research focuses on the role of arsenide melts as collectors of PGE in magmatic systems, the genesis of sulfide-matrix breccias and the PGE distribution in sulfides from Ni-Cu mineralizations using LA-ICP-MS.

Geology and metallogeny of the upper mantle rocks from the Serranía de Ronda

Fernando Gervilla
José María González-Jiménez
Károly Hidas
Claudio Marchesi
Rubén Piña

Acknowledgements

Contents

Preface

The ultramafic massifs exposed in orogenic belts are an unequal window to access directly the study of the Earth's upper mantle. The Serranía de Ronda in the Málaga province in southern Spain exposes the world's largest outcrops of mafic and ultramafic rocks corresponding to a former upper lithospheric mantle once beneath a continent, i.e., subcontinental lithospheric mantle (SCLM). These Ronda's special rocks are not only interesting in terms of the petrological processes they preserve but also in terms of their metallogeny that is unique in the world. The study of the upper mantle rocks from the Serranía de Ronda by many authors of diverse background have fructified in many technical and scientific reports that have served as continuous source of inspiration for the study of other mantle rocks worldwide. The main target of this monographic book is to provide a state-of-the-art of this knowledge, emphasizing on the tectonic, petrological and geochemical evolution of the ultramafic massifs and their links to the genesis of a very unique assemblage of metallic mineral deposits.

We the authors invite readers to digging deeper the chapters of this book with a challenging eye, looking beyond their own experience to see how ideas and concepts on the origin of the Ronda's upper mantle rocks and associated mineral deposits have evolved over the past two hundred years. We, of course, could not feature the entire spectrum of the authors have worked in the Serranía de Ronda, and many geological aspects of these rocks are not covered in this publication. However, the chapters of this book are concise, detailed, and filled with specifics of multidisciplinary geosciences. The inquires in the book open the door to other inquires and suggest new benchmarks that have potential to enrich and broaden our current understanding of Earth's upper mantle processes and metallogeny overall.

Chapter 1 introduces the book reviewing the mining history of the ultramafic massifs of the Serranía de Ronda. Chapter 2 provides a brief summary of the Geology of the Betic Cordillera to which the Serranía de Ronda belongs. Chapter 3 and Chapter 4 focus on the tectonics, petrology and geochemistry of the three main mantle massifs in the Serranía de Ronda. Chapter 5 gives knowledge on the geochronology of these rocks since their formation in the SCLM to final exhumation into the continental crust. The metallogeny of these mantle massifs is described and discussed in Chapters 6 and 7. Finally, Chapter 8 provides an independent field-trip guide. This guide focuses on specific aspects of the tectonic and petrological evolution of the mafic and ultramafic

rocks, having a specific stop where the characteristics and genesis of a very peculiar chromitite ore is described in relation with the petro-structural evolution of its host rocks. The guide is intended to be a track-map for the readers willing to explore the geology of the Serranía de Ronda.

Chapter 1
Introduction

1.1   The ultramafic massifs of the Serranía de Ronda: a window to the Earth's upper mantle

Our current view of the Earth's formation and subsequent evolution envisions repeated cycles of melt extraction from a convecting fertile mantle, producing mafic magmas that rise to the crust and a complementary residual depleted mantle. Each episode of crust formation is usually followed by recycling, by which the crust is partially or totally mixed back into the convecting mantle or stored deeper in the Earth. Geochemists have defined a number of proxies that track these processes, many of them based on elemental and isotopic analyses of magmas generated in the convecting mantle (e.g., Griffin et al., 2002; Rudnick and Walker, 2009). However, the best materials for the study of mantle processes are ultramafic and mafic rocks from the mantle itself, which can be sampled in very different geological settings. For example, kimberlites and related magmas usually enclose xenocrysts and xenoliths that have sampled the subcontinental lithospheric mantle (SCLM) beneath Archean-Proterozoic, thick cratons. Likewise, alkali basalts often host xenocrysts-xenoliths from thinner (i.e., off-craton), Phanerozoic tectonic domains or regions where older SCLM has been substantially thinned (e.g., O'Reilly and Griffin, 2013). Subcontinental, suboceanic and subarc mantle rocks may also be tectonically emplaced into the continental crust and form variably sized ultramafic bodies, which are widespread along suture zones and/or orogenic belts originated by closure of oceans and/or continent-continent collision (e.g., Bodinier and Godard 2014).

The study of ultramafic massifs in orogenic belts, namely orogenic peridotites (Bodinier and Godard, 2014), is of particular interest because it provides crucial understanding about the processes active under continents that is complementary to the information conveyed by xenoliths. Most orogenic peridotite massifs show the predominance of lherzolites equilibrated in the garnet-, spinel-, or plagioclase-peridotite facies defined by O'Hara (1967). The world's best examples of orogenic peridotites recording all these mineralogical facies crop out in the Betic–Rif orogenic belt (western Mediterranean) (see Chapters 2 and 3). In this region, fragments of an ancient Proterozoic SCLM (Fig. 1.1) occur as scattered ultramafic bodies that
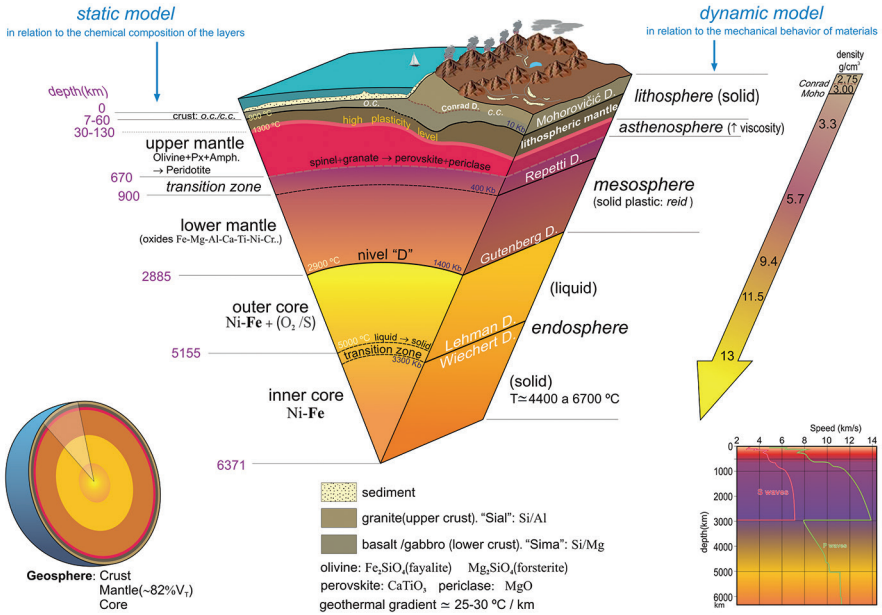
Figure 1.1. The internal structure of the Earth (Geosphere) is layered in spherical shells, consisting of an outer silicate solid crust, a highly viscous asthenosphere and mantle, a liquid outer core that is much less viscous than the mantle, and a solid inner core. This figure shows this layered structure in terms of chemistry and mineralogy (static model) and mechanical behavior of the constituent rocks (dynamic model). The crust is subdivided into continental (*cc*) and oceanic (*oc*). The picture also includes some physical properties of the different layers, including temperature, pressure, density and speed of P and S seismic waves.

include the massifs of Ronda, Ojén and Carratraca in the Serranía de Ronda, at the westernmost part of the Betic Cordillera in southern Spain (Orueta-Duarte, 1917; Hernández-Pacheco, 1967; Obata, 1980; Frey et al., 1985; Suen and Frey, 1987; Reisberg et al., 1991; Remaidi, 1993; Reisberg and Lorand, 1995; Van der Wal, 1993; Targuisti, 1994; Van der Wal and Visser, 1993, 1996; Van der Wal and Bodinier, 1996; Garrido, 1995; Garrido and Bodinier, 1999; Lenoir et al., 2001), the Beni Bousera massif in northern Morocco (Kornprobst, 1969; Kornprobst et al, 1990; Targuisti, 1994; Frets, 2012; Frets et al., 2012, 2014) and the Collo massif in Little Kabylia, Algeria (Leblanc and Temagoult, 1989). In particular, the Ronda ultramafic massif is the largest exposure of SCLM on the Earth's surface (~300 km^2) and one of the most studied orogenic peridotite massifs in the world. A number of investigations on this massif over the past few decades (see Chapters 4 and 5) have provided benchmarks for the interpretation of Earth's mantle processes at the global scale. These studies show that the Betic-Rif-Tell mantle peridotites constitute a unique window on mantle dynamics and lithosphere-asthenosphere interaction in very fast spreading environments.

1.2   A world's unique assemblage of magmatic ores in the SCLM

A unique assemblage of magmatic Cr, Ni, Cu, platinum-group elements (PGE: Os, Ir, Ru, Rh, Pt and Pd) and Au ores crops out in the ultramafic massifs of the Serranía de Ronda (southern Spain) and Beni Bousera (northern Morocco) (Gervilla, 1990; Gervilla and Leblanc, 1990; Gutiérrez-Narbona, 1999; Gervilla et al., 2002; González-Jiménez et al., 2013, 2017; Hajjar et al., 2017). Three unusual ore types have been found within the peridotites (see Chapter 6): (1) *Chromium-Nickel (Cr-Ni) ores* consisting of chromite and Ni-arsenides singularly enriched in PGE and gold, which are frequently associated with magmatic orthopyroxenites and/or cordieritites; (2) *Sulphide-Graphite (S-G) ores* consisting of Fe-Ni-Cu sulphides (pyrrhotite, pentlandite, chalcopyrite and cubanite) with graphite and minor chromite; and (3) *Chromium (Cr) ores* consisting of chromite with scarce Ni arsenides and olivine, orthopyroxene and/or clinopyroxene, which resemble the typical podiform-like chromitites in ophiolites. This assemblage of magmatic ores has not been recognized in other upper mantle rocks and its distribution within the massifs is closely related to the petrological zoning of enclosing peridotites (see Chapter 4), attesting for a link between the origin of the ores and the tectonomagmatic processes that affected this volume of SCLM.

   In addition to the ores mentioned above, several small magnetite deposits occur along the contact between the peridotite massifs and the underlying crustal units or within them (Orueta-Duarte, 1917, Leine, 1967; Westerhof, 1975). Besides the detailed research carried out by Westerhof (1975) on the *El Peñoncillo Mine* (also known as *La Concepción Mine*), the mineral assemblages and origin of these ores are not well constrained (see Chapter 6). Westerhof (1975) considered that the formation of iron ore at El Peñoncillo took place owing to metamorphism linked with the intrusion of basic sills, predating the Alpine emplacement of peridotites. However, preliminary data on *Mina San Manuel* (north to Estepona) and *El Robledal* and *La Víbora mines* (south to Ronda) point to skarn-type genetic processes linked with the crustal emplacement of peridotites. The genesis of this type of mineralization is not treated in this book because there is still little available scientific knowledge about these ores.

   In summary, the ultramafic massifs of the Serranía de Ronda are unusual examples of SCLM not only in terms of the petrological processes they preserve (Chapters 4 and 5) but also in terms of their metallogeny that is unique in the world (Chapters 6 and 7).

1.3   Mining history of the ultramafic massifs of the Serranía de Ronda

Mining activities in the ultramafic massifs of the Serranía de Ronda began in the middle of the 19th Century. This mining mainly targeted nickel and iron, the former extracted from orebodies hosted within the ultramafic rocks (i.e., Cr-Ni ores) and the latter from magnetite skarn deposits found at the contact between the ultramafic bodies and the underlying crustal metamorphic rocks (e.g., San Manuel, El Peñoncillo and El Robledal mines). Accurate data about the mining history and ore production in that time are lacking. Álvarez de Linera (1851) wrote the first technical report

about ores associated with these ultramafic massifs, and described about five hundred small occurrences of Ni mineralization exploited a decade earlier. Based on this knowledge, artisanal mining was resumed at the beginning of the 20th Century when new exploration campaigns discovered additional resources. Detailed information about the ore reserves and amount of exploited mineral during this period can be found in Orueta-Duarte (1917). Mining stopped during the first quarter of the 20th Century, coinciding with the Great Depression at the end of the twenties, and during the Second Spanish Republic and the Civil War in the thirties. Exploration studies were resumed during the forties by the COMEIN (Consejo Ordenador de Minerales Estratégicos de Interés Militar), leading to intensive mining of the largest Cr-Ni orebodies (e.g., Los Jarales district in the Carratraca massif and La Gallega in the Ojén massif) that continued up to the end of the fifties when reserves were almost exhausted. A revival of exploration took place at the end of the sixties when the INI (Instituto Nacional de Industria), in coordination with the Spanish-Belgium-Canadian holding PLANT, investigated areas close to the mines already exploited by the COMEIN. In the next decade, different public and private companies conducted exploration studies, although none of these investigations yield satisfactory results and no further mining works were developed. In the last three decades, the IGME (Instituto Geológico Minero de España), in collaboration with other institutions, put efforts into the discovery of new resources of noble metals (e.g., Castroviejo, 1998) and the potential use of ultramafic rocks as reservoir for CO_2 storage (Zapatero et al., 2009). To date, no active mining exists in the area.

References

Alvarez de Linera, A. (1951). Descripción del criadero de níquel de Carratraca. Málaga. Imprenta del Comercio.

Bodinier, J.L. and Godard, M. (2014). Orogenic, ophiolitic and abyssal peridotites. In Turekian, K.K. and Holland, H.D. Editors. The Mantle and Core: Treatise on Geochemistry (2nd Edition). Oxford, UK, Elsevier, 103-167.

Castroviejo, R. (1998). Nuevas aportaciones a la tipologia de metales preciosos para exploracion en España. *Boletín Geológico y Minero* 109-5, 497-520.

Frets, E. C. (2012). Thermo-mechanical evolution of the subcontinental lithospheric mantle in an extensional environment. Ph.D. Thesis, University of Granada. Spain.

Frets, C., Tommasi, A., Garrido, C.J., Padrón-Navarta, J.A., Amri, I and Targuisti, K. (2012). Deformation processes and rheology of pyroxenites under lithospheric mantle conditions. *Journal of Structural Geology* 26, 1401-1418.

Frets E.C., Tommasi, A. Garrido, C.J., Vauchez, A., Mainprice, D., Targuisti, K. and Amri, I. (2014). The Beni Bousera peridotite (Rif Belt, Morocco): an oblique-slip low-angle shear zone thinning the subcontinental mantle lithosphere. *Journal of Petrology* 55 (2), 283–313

Frey, F.A., Suen, J. and Stockman, H.W. (1985). The Ronda high temperature peridotite: geochemistry and petrogenesis. Geochimica et Cosmochimica Acta 49, 2469-2491.

Garrido, C.J. (1995). Estudio geoquímico de las capas máficas del Macizo Ultrmáfico de Ronda. Ph. D. Thesis, University of Granada. Spain.

Garrido, C.J. and Bodinier, J.L. (1999). Diversity of mafic rocks in the Ronda peridotite: evidence for pervasive melt/rock reaction during heating of subcontinental lithosphere by upwelling asthenosphere. *Journal of Petrology* 40, 729-754.

Gervilla, F. (1990). Mineralizaciones magmáticas ligadas a la evolución de las rocas ultramáficas de la Serranía de Ronda (Málaga, España). Ph. D. Thesis, University of Granada. Spain.

Gervilla, F., Gutiérrez-Narbona, R. y Fenoll Hach-Alí, P. (2002). The origin of different types of magmatic mineralizations from small-volume melts in the lherzolite massifs from the Serranía de Ronda (Málaga, Spain). *Boletín de la Sociedad Española de Mineralogía* 25, 79-96.

Gervilla, F. and Leblanc, M. (1990). Magmatic ores in high-temperature Alpine-type lherzolite massifs (Ronda, Spain) and Beni Bousera, Morocco). *Economic Geology* 85, 112-132.

González-Jiménez, J.M., Marchesi, C., Griffin, W.L., Gervilla, F., Belousova, E.A., Garrido, C.J., Romero, R., Talavera, C., Leisen, M., O'Reilly, S.Y., Barra, F. and Martin, L. (2017). Zircon recycling and crystallization during formation of chromite- and Ni-arsenide ores in the subcontinental lithospheric mantle (Serranía de Ronda, Spain). *Ore Geology Reviews* 90, 193-209.

González-Jiménez, J.M., Marchesi, C., Griffin, W.L., Gutiérrez-Narbona, R., Lorand, J.P., O'Reilly, S.Y., Garrido, C.J., Gervilla, F., Pearson, N.J. and Hidas, K. (2013). Transfer of Os isotopic signatures from peridotite to chromitite in the subcontinental mantle: insights from in situ analysis of platinum-group and base-metal minerals (Ojén peridotite massif, southern Spain). *Lithos* 164-167, 74-85.

Griffin, W.L., Spetius, Z.V., Pearson, N.J. and O'Reilly, S.Y. (2002). In situ Re– Os analysis of sulfide inclusions in kimberlitic olivine: new constraints on depletion events in the Siberian lithospheric mantle. Geochemistry, Geophysics and Geosystems 3(11), doi:10.1029/2001GC000287

Gutiérrez-Narbona, R. (1999). Implicaciones metalogénicas (cromo y elementos del grupo del platino) de los magmas/fluidos residuales de un proceso de percolación a gran escala en los macizos ultramáficos de Ronda y Ojén (Béticas, Sur de España). Ph. D. Thesis, University of Granada. Spain.

Hajjar, Z., Gervilla, F., Essaifi, A. and Wafik, A. (2017). Mineralogical and geochemical features of the alteration processes of magmatic ores in the Beni Bousera Ultramafic Massif (North Morocco). *Journal of African Earth Sciences* 132, 47-63.

Hernández- Pacheco, A. (1967). Estudio petrofráfico y geoquímico del macizo ultramáfico de Ojén (Málaga). *Estudios Geológicos* XXIII, 85-143.

Kornprobst, J. (1969). Le massif ultrabasique de Beni Bouchera (Rif Interne, Maroc): Étude des péridotites de haute température et de haute pression, et des pyroxénolites, à grenat ou sans grenat, qui leur son associées. Contributions to Mineralogy and Petrology 23, 283-322.

Kornprobst, J., Piboule, M. and Tabit, A. (1990). Corundum-bearing garnet clinopyroxenites at Beni Bousera (Morocco): Original plagioclase-rich gabbros recrystallized at depth within the mantle? Journal of Petrology 31, 717-745.

Leblanc, M. and Temagoult, A. (1989). Chromite pods in a lherzolite massif (Collo, Algeria): Evidence of oceanic-type mantle rocks along the West Mediterranean Alpine Belt. *Lithos* 23, 153-162

Leine, L. (1967). Geology of a magnetite deposit of the Mg-Skarn type near Marbella, Spain. *Economic Geology* 62, 926-931.

Lenoir, X., Garrido, C.J., Bodinier, J.-L., Dautria, J.-M. y Gervilla, F. (2001). The recrystallization front of the Ronda peridotite: Evidence for melting and thermal erosion of subcontinental lithospheric mantle beneath the Alborán basin. *Journal of Petrology,* 42 (1), 141-158.

Obata, M. (1980). The Ronda peridotite: Garnet-, spinel-, and plagioclase-lherzolite facies and the P-T trajectories of a high-temperature mantle intrusión. *Journal of Petrology* 21, 533-572.

O'Hara, M.J. (1967). Mineral facies in ultrabasic rocks. In: Wyllie P.J. (ed.), Ultramafic and Related Rocks. New York: Wiley & Sons, 7-18.

O'Reilly, S.Y. and Griffin, W.L. (2013). Mantle metasomatism. In: Harlov DE, Austrheim H (eds) Metasomatism and the chemical transformation of rock: lecture notes in earth system sciences. Springer,Berlin, pp 467–528.

Orueta-Duarte, D. (1917). Estudio geológico y petrográfico de la Serranía de Ronda. *Memorias del Instituto Geológico y Minero de España* 32, 571 pp.

Reisberg, L. and Lorand, J.-P. (1995). Longevity of sub-continental mantle lithosphere from osmium isotope systematics in orogenic peridotite massifs. *Nature* 376, 159–162.

Reisber, L.C., Allègre, C.J. and Luck, J.M. (1991). The Re-Os systematics of the Ronda ultramafic complex of southern Spain. *Earth and Planetary Science Letters* 105, 196-213.

Remaïdi, M. (1993). Etude petrologique et goechimique d'une association peridotites refractaires-pyroxenites dans le massif de Ronda (Spagne). Ph. D. Thesis, University of Montpellier. France.

Rudnick, R.L. and Walker, R.J. (2009). Interpreting ages from Re–Os isotopes in peridotites. Lithos 112:1083–1095.

Suen, C.J. and Frey, F.A. (1987). Origin of the mafic and ultramafic rocks in the Ronda peridotite. Earth and Planetary Science Letters 85, 183-202.

Targuisti, K. (1994). Petrología y geoquímica de los macizos ultramáficos de Ojén (Andalucía) y Beni Bousera (Rif septentrional, Marruecos). Ph. D. Thesis, University of Granada. Spain.

Van der Wal, D. (1993). Deformation processes in mantle peridotites. Ph. D. Thesis, University of Utrech. The Netherlands.

Van der Wal, D. and Bodinier, J.L. (1996). Origin of the recrystallization front in the Ronda peridotite by km-scale pervasive porous flow. *Contributions to Mineralogy and Petrology* 122, 387-405.

Van der Val, D. and Vissers, R.L.M. (1993). Uplift and emplacement of upper mantle rocks in the western Mediterranean. *Geology* 21, 1119-1122.

Van der Val, D. and Vissers, R.L.M. (1996). Structural petrology of the Ronda peridotite SW Spain: deformation history. *Journal of Petrology* 37, 23-43.

Westerhof, A.B. (1975). Genesis of magnetite ore near Marbella, Southern Spain: Formation by oxidation of silicates in polymetamorphic gedrite-bearing and other rocks. *GUA papers of geology*. Amsterdam. 216 pp.

Zapatero, M.A., Reyes, J.L., Martínez, R., Suárez, I., Arenillas, A., Perucha, M.A. (2009). Estudio preliminary de las formaciones favorables para el almacenamiento de CO_2 en España. Instituto Geológico y Minero de España, Grupo de Almacenamiento de CO_2 135 pp.

Chapter 2
Geological setting

2.1 The Betic Orogenic Belt

The Serranía de Ronda peridotites in southern Spain crop out in the Betic orogenic belt (also known as the Betics or Betic Cordillera), which represents the westernmost part of the Alpine orogen in the Mediterranean region (Fig. 2.1). This orogenic belt, together with the Rif in north Morocco, formed due to the convergence between the Iberian and African plates from late Cretaceous to Tertiary times, coeval with the westward movement of a microcontinent known as the Alborán Domain (Andrieux et al., 1971, Durand-Delga and Fontboté 1980; Dewey et al., 1989; Balanyá and García Dueñas, 1987). The Betic orogenic belt has traditionally been subdivided into Internal (the hinterland) and External zones (the foreland), with Flysch formations sandwiched between them (see Azdimousa et al., 2019) (Fig. 2.1). The External Zones consist of Triassic to Early Miocene sedimentary rocks deposited in the Iberian continental margin, whereas the Internal Zones mostly consist of metamorphic rocks of Paleozoic and Triassic age grouped in three stacked nappe complexes. This set of complexes, from bottom to top, includes:

(1) The *Nevado-Filábride complex*. It corresponds to the lowest nappe complex and crops out in several tectonic windows below the overlying Alpujárride complex in the central and eastern zones of the Betics. Three major, tectonically superimposed units constitute this complex from bottom to top: the Veleta Unit, the Calar Alto Unit and the Bédar-Macael Unit (Martínez-Martínez and Azañón, 1997; Martínez-Martínez et al., 1997). The Veleta unit consists of Upper Carboniferous graphite schists and quartzites (Jabaloy-Sánchez et al., 2018; Rodríguez-Cañero et al. 2018; Santamaría and Sanz de Galdeano, 2018). The Calar Alto and Bédar-Macael units share a similar lithostratigraphic sequence of Upper Carboniferous graphite schists and quartzites at the bottom, and Permian-Triassic metapelites and metapsammites (Jabaloy-Sánchez et al., 2018; Santamaría and Sanz de Galdeano, 2018) topped by dolomitic and calcitic marbles of Triassic to younger ages (Jabaloy-Sánchez et al., 2018). The Calar alto and Bédar-
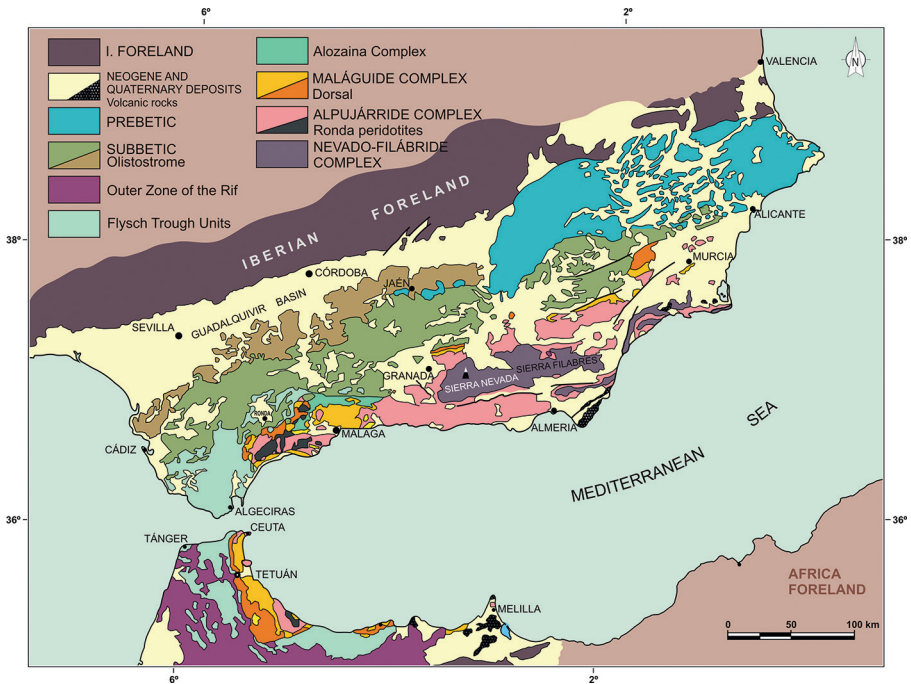
Figure 2.1. Main geological units of the Betic-Rif Orogenic Belt (modified from Sanz de Galdeano and Ruiz-Cruz, 2016).

Macael units also include orthogneisses, gabbros and ultramafic rocks (Puga et al., 1990; Trommsdorff et al., 1998; Gómez Pugnaire et al., 2012; Padrón-Navarta et al. 2010), which record higher metamorphic degree (up to 680 ºC and 1.9 GPa; Padrón-Navarta et al. 2010) than the lower Veleta Unit (350-480 ºC; Gómez-Pugnaire and Franz, 1988; Booth-Rea et al., 2003). The main metamorphic event in the Nevado-Filábride complex occurred at 18-15 Ma (López Sánchez-Vizcaíno et al., 2001; Gómez-Pugnaire et al., 2004, 2012; Platt et al., 2006).

(2) The *Alpujárride complex*. It is composed of superimposed tectonic units constituted by similar lithostratigraphic sequences. Each unit includes a lower sequence of metapelites and quartzites of Palaeozoic age, an intermediate member of Permian-Middle Triassic phyllites and quartzites with increasing amounts of calc-schists upwards, and an upper variably thick carbonate member of Middle to Upper Triassic age (Martín-Rojas et al. 2012, and references therein). The lithological sequence of the Alpujárride complex in the westernmost part of the Betic orogenic belt includes ultramafic rocks from the subcontinental lithospheric mantle, currently known as the Serranía de Ronda peridotites.

(3) The *Maláguide complex*. It consists of a weakly metamorphosed, metapelitic sequence locally intercalated with carbonates and sandstones of Silurian to Carboniferous age (Herbig, 1983), topped by a Triassic, detrital formation

covered by Jurassic to Oligocene carbonates (e.g. Geel, 1973; Martín-Algarra, 1987). According to Balanyá (1991), metamorphism in this complex is of low grade, developed during the Variscan orogeny, and mainly affects the lower members of the sequence.

The Alborán Domain (or microcontinent), as originally defined by Balanyá and García Dueñas (1987), includes all the three complexes of the Betic Internal Zones, but more recently it has been redefined comprising only the two upper tectonic complexes (Gómez-Pugnaire et al., 2012; Booth-Rea et al., 2007; Behr and Platt, 2012; Platt et al., 2013; Rodríguez-Cañero et al., 2018). Thus, the Nevado-Filábride complex is now generally considered part of the Iberian foreland that was subducted below the Alborán Domain (Booth-Rea et al., 2007; Gómez-Pugnaire et al., 2012; Behr and Platt, 2012; Platt et al., 2013; Rodríguez-Cañero et al., 2018).

2.2   The Alpujárride Complex in the western part of the Betic Orogenic Belt

The Alpujárride units are heterogeneously distributed in the Betic orogenic belt (Fig. 2.1). Up to five types of allochthonous tectonic units are identified, from bottom to top, in the eastern and central sectors of the belt: the Lújar-Gardor-type units, the Escalate-type units, the La Herradura-type units, the Salobreña-type units and the Adra-type units. These units record variable degrees of metamorphism evolving from low pressure-low temperature in the Lújar-Gador type units, to low-intermediate pressure-low temperature in the Escalate type units, and to high pressure-high temperature in the La Herradura, Salobreña and Adra type units (Tubía et al., 1992; Azañón, 1994; Martínez-Martínez and Azañón, 1997). In the western sector of the Alpujárride complex, different tectonic subdivisions have been proposed (Hoeppener et al. 1964; Dürr, 1967; Mollat, 1968; Buntfuss, 1970; Didon, et al. 1973; Navarro-Vila and Tubía, 1983; Tubía, 1988; Balanyá et al., 1987; Balanyá, 1991; Balanyá and García-Dueñas, 1991; Sánchez-Gómez, 1997). For the sake of clarity, this monography presents a simplified classification distinguishing only two crustal units according to their position relative to the peridotite bodies: (1) the Los Reales Unit, including the whole metasedimentary sequence overlying the ultramafic rocks, and (2) the Blanca Unit, grouping all metamorphic rock types that underlie the peridotites (Figure 2.2).

2.2.1   The Los Reales Unit

This unit correlates with the Adra- and Salobreña-types in the eastern and central sectors of the Betics (Azañón, 1994; Martínez-Martínez and Azañón, 1997). The Los Reales unit is a highly thinned -but complete- continental crustal section that overlies the Ronda peridotite slab. From top to bottom, the unit (≤ 5 km thick) is composed of carbonates, low-grade phyllites with relic HP-LT assemblages, graphitic mica schists, and garnet-rich porphyroclastic to mylonitic gneisses
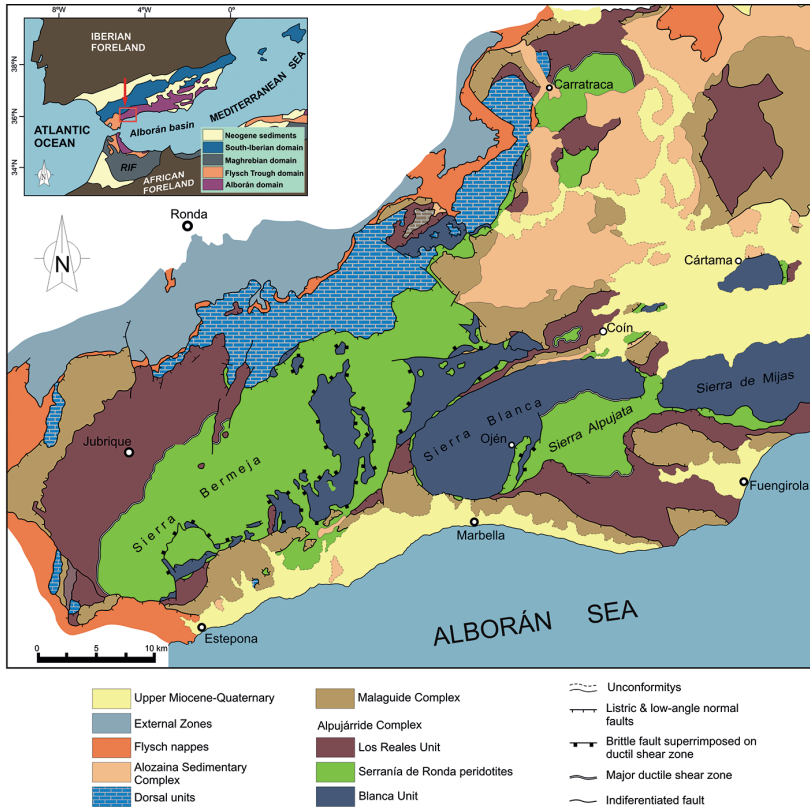
Figure 2.2. Geology of the western zone of the Betic Orogenic Belt showing the structural relationships of the ultramafic massif of the Serranía de Ronda in relation to the Los Reales and Blanca Alpujárride units (modified from Gómez-Pugnaire et al., in press).

(the latter also known as kinzigites) in contact with the peridotites. This zoned metamorphic sequence exhibits layering that is broadly parallel to layering in peridotite. Thermobarometry indicates that kinzigites record the highest peak P-T conditions (1.2-1.4 GPa and 850 ºC), overprinted by a metamorphic event at lower pressure (0.2-0.3 GPa) and temperature (~750 ºC) (Fig. 2.3) (Loomis, 1972, Torres-Roldán, 1979, 1981a; Hollerbach, 1985; Tubía 1994; García-Casco and Torres-Roldán, 1996; Bouybaouène et al. 1998, Argles et al. 1999; Platt et al., 2003; Barich et al., 2014). The P-T trajectory of the porphyroclastic garnet gneisses evolved from 1.3-1.5 GPa and 770-790 ºC to 0.3-0.4 GPa and ~700 ºC, and that of phyllites, quartzites and calc-schists from minimum 0.7 GPa to 0.4 GPa and 400 ºC (Fig. 2.3). Carbonates and phyllites at the top of the sequence record metamorphic conditions of 0.7-0.8 GPa and 200-350 ºC, followed by equilibration in the amphibolite and greenschist-facies (Torres-Roldán, 1981; Platt et al. 2003). These P-T trajectories record vertical ductile thinning and excision along low-angle normal faults or ductile shear zones by extension (Balanyá et al., 1997; Argles et al., 1999; Azañon and Crespo-Blanc, 2002; Soto
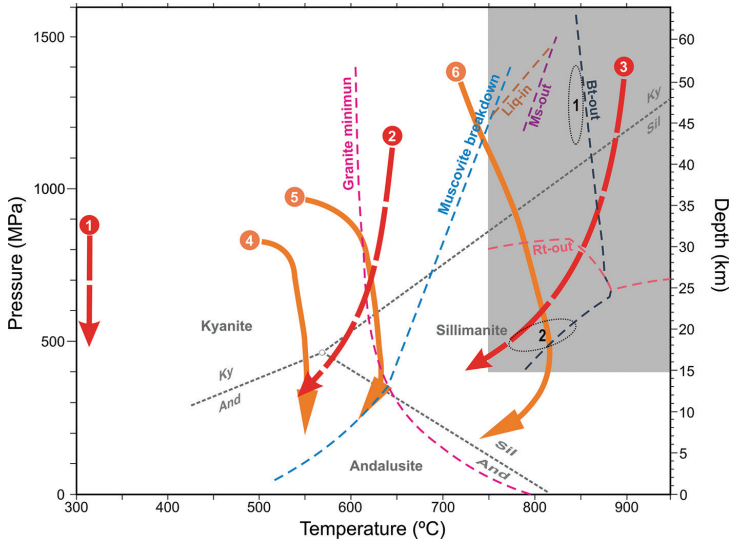
Figure 2.3. Pressure-temperature paths estimated for different metamorphic rocks from the metapelitic sequence of the Los Reales Unit above the Ronda massif (Balanyá et al., 1997; 1: phyllites, quartzites and calc-schists; 2: staurolite schists, and 3: garnet gneisses) and the Carratraca massif Argles et al. (1999) (4, 5 and 6). The plot also includes the minimum conditions for granite solidus and muscovite breakdown as well as the Liquid-in, muscovite-out (Ms-out), biotite-out (Bt-out), rutile-out (Rt-out) (the shadow area) and the peak (ellipse 1) and post-peak (ellipse 2) P-T conditions calculated by Barich et al. (2014) for a porphyroclastic gneiss of the Los Reales metapelitic sequence above the Ronda massif. Ky: kyanite; And: andalusite; Sil: sillimanite. Diagram modified after the compilation by Gómez-Pugnaire et al (in press).

and Platt, 1999; Platt et al., 2013). These tectonic events have been attributed to crustal thinning of the Alborán Domain during orogenic accretion in the Alpine orogeny (e.g., Platt et al., 2013 and references therein), although recent studies also suggest Variscan ages (Acosta-Vigil et al., 2014; Sanz de Galdeano and Ruiz-Cruz, 2016; Sánchez-Navas et al., 2017). Decompression likely took place owing to fast uplift as evidenced by textural and compositional disequilibrium in the equivalent Torrox Unit (García-Casco and Torres Roldán, 1996). Zeck et al. (1992) estimated exhumation rates of 5 to 10 km/Ma, and García-Casco and Torres-Roldán (1996) slower rates (1-3 km/Ma) during subsequent nearly isobaric cooling of 250 to 400 ºC/Ma.

2.2.2 The Blanca Unit

This unit was firstly defined by Mollat (1968) and includes a variety of metamorphic rocks, comprising a lower sequence of garnet gneisses, intrusive cordierite-bearing leucogranites, migmatite gneisses and schists, and an upper carbonate sequence of

marbles with intercalated calc-schists, metapelites, quartzites and amphibolites. The latter amphibolites locally contain relicts of eclogites (Tubía and Gil-Ibarguchi, 1991; Tubía et al., 1997). This unit hosts numerous types of granites and late metatexites and diatexites, which intrude the overlying peridotite slab and the metapelites of the Los Reales unit (Torres-Roldán, 1979; Navarro-Vila and Tubía, 1983; Balanyá and García-Dueñas, 1991). The rocks of the Blanca unit show increasing mylonitization toward the contact with peridotite and record an early HP/LT event (up to 1.7 GPa and ~800ºC in the eclogite relicts; Tubía and Gil-Ibarguchi, 1991; Sánchez-Rodríguez and Gebauer, 2000), followed by nearly isothermal decompression down to 0.3-0.5 GPa and 700-750ºC (Loomis, 1972; Torres-Roldán, 1979, 1981b), and subsequent fast cooling.

The tectonic evolution of the Blanca unit is similar to that described for the Los Reales unit and comprises three main deformational events. The early D1 is poorly preserved since it has been partly obliterated by later isothermal decompression (D2) associated with extreme crustal thinning during the Upper Oligocene (Torres-Roldán, 1981b; García-Casco and Torres Roldán, 1996, 1999). The third deformational event took place under compressive regime and mainly folded the D2-related structures. Sánchez-Gómez (1997) considered that D3 occurred at increasing pressure (up to 0.6-0.7 GPa) and temperature (up to 800 ºC) linked to the intracrustal emplacement of the peridotite slab, and was followed by retrograde evolution (D4) and a non-metamorphic stage (D5). The contact between the Serranía de Ronda peridotites and the Blanca unit is a low-angle, brittle thrust marked by extensive breccias (Lundeen, 1978) (Fig. 2.2). In some localities, this contact has been displaced by high-angle normal faults.

2.2.3   The ultramafic rocks

The ultramafic massifs of the Serranía de Ronda are dismembered portions of an independent tectonic unit placed between the Los Reales and Blanca units (Fig. 2.2). The upper and lower contacts of peridotites with the crustal units consist of high-temperature blastomilonites (e.g., Lundeen, 1978; Tubía and Cuevas, 1996; Tubía et al., 2013) variably affected by LT brittle deformation associated with late shear zones and low-angle faults (e.g., Balanyá, 1991; García-Dueñas and Balanyá, 1991). The intra-crustal emplacement of mantle peridotites has been traditionally ascribed to the Alpine orogeny (e.g., Priem et al., 1979). However, recent works have stressed that anatexis in the Blanca unit took place during the Variscan Orogeny and suggest that the emplacement of peridotites was pre-Alpine (Acosta et al 2014; Barich et al., 2014; Sanz de Galdeano and Ruiz-Cruz, 2016). These authors noted that Alpine ages in zircons collected very close to the basal contact with peridotites could reflect a resetting instead of a true crystallization age. However, zircons from most of these rocks show neo-formed rims of Alpine age (Zeck and Whitehouse, 1999; Platt and Whitehouse, 1999; Zeck and Williams, 2001; Whitehouse and Platt, 2003; Esteban et al., 2011) highlighting the role of the Alpine metamorphism in the tectono-metamorphic evolution of these Alpujárride units. Additional evidence of Alpine crustal anatexis is the presence of acid dykes (mainly leucogranites) of this age crosscutting the peridotites (Priem et al., 1979; Acosta, 1998; Sánchez-Rodríguez,

1998; Esteban et al., 2011), and magmatic zircons of ~ 20 Ma in plagioclasite and chromitite from the Ojén massif (González-Jiménez et al., 2017). These data support the Alpine intra-crustal emplacement of peridotites and suggest a genetic link between mineralizations and anatectic melts originated during such emplacement (see Chapters 6 and 7).

References

Acosta A. (1998). Estudio de los fenómenos de fusión cortical y generación de granitoides asociados a las peridotitas de Ronda. Ph. D. Thesis, University of Granada, Spain.

Acosta, A., Rubatto, D., Bartoli, O., Cesare, B., Meli, S., Pedrera, A., Azor, A. and Tajčmanová, L. (2014). Age of anatexis in the crustal footwall of the Ronda peridotites, S Spain. *Lithos* 210-211, 147-167.

Andrieux J., Fontboté J.M. and Mattauer M. (1971). Sur un modèle explicatif de l'Arc de Gibraltar. *Earth and Planetary Science Letters* 12, 191-198.

Argles, T.W., Platt, J.P, and Waters, D.J. (1999). Attenuation and excision of a crustal section during extensional exhumation: The Carratraca Massif, Betic Cordillera, southern Spain. *Journal of the Geological Society* 156, 149–162.

Azañón J.M. (1994). Metamorfismo de Alta presión/Baja Temperatura, Baja presión / Alta Temperatura y tectónica del Complejo Alpujárride (Cordilleras Bético-Rifeñas). Ph. D. Thesis. University of Granada, Spain.

Azañon, J.M. and Crespo-Blanc, A. (2000). Exhumation during a continental collision inferred from the tectonometamorphic evolution of the Alpujarride Complex in the central Betics (Alboran Domain, SE Spain). *Tectonics* 19(3), 549–565

Azañón J.M., García-Dueñas V. and Goffé B. (1998). Exhumation of high-pressure metapelites and coeval crustal extension in the Alpujárride complex (Betic Cordillera). *Tectonophysics* 285, 231-252.

Azdimousa A, Jabaloy-Sánchez A, Talavera C, Asebriy L, González-Lodeiro F and Evans NJ (2019) Detrital zircon U-Pb ages in the Rif Belt (northern Morocco): Paleogeographic implications. *Gondwana Research* 70,133–150

Balanyá J.C. (1991). Estructura del dominio de Alborán en la parte norte del Arco de Gibraltar. Ph. D. Thesis, University of Granada, Spain.

Balanyá J.C., Campos J., García-Dueñas J.M., Orozco M. and Simancas J.F. (1987). Generaciones de cabalgamientos y pliegues recumbentes en los Mantos Alpujárrides entre Ronda y Almería. Cordilleras Béticas. *Geogaceta* 2, 51-53.

Balanyá J.C. and García-Dueñas V. (1987). Les directions structurales dans le Domaine d'Alboran de part et d'autre au Détroit du Gibraltar. *Comptes Rendus de l'Academie de Sciences de París* 304, 929-933.

Balanyá J.C. and García-Dueñas V. (1991). Estructuración de los Mantos Alpujárrides al W de Málaga (Béticas, Andalucía). *Geogaceta* 9, 30-33.

Balanyá J.C., García-Dueñas J.M., Azañón J.M. and Sánchez-Gómez M. (1997). Alternating contractional and extensional events in the Alpujárride nappes of the Alborán domain (Betics, Gibraltar Arc). *Tectonics* 16 (2), 226-238.

Barich, A., Acosta-Vigil, A., Garrido, C.J., Cesare, B., Tajčmanová, L. and Bartoli, O. (2014). Microstructures and petrology of melt inclusions in the anatectic sequence of Jubrique (Betic Cordillera, S Spain): Implications for crustal anatexis. *Lithos* 206–207, 303–320.

Behr, W.M. and Platt, J.P. (2012). Kinematic and thermal evolution during two-stage exhumation of a Mediterranean subduction complex. *Tectonics* 31, TC4025.

Blumenthal M. (1927). Versuch einer tektonischen Gliederung der betischen Kordilleran von Central und Sùdwest Andalusien. *Eclogae Geologicae Helvetiae* 20, 487-592.

Booth-Rea, G., Azañón, J.M., Goffé, B., Vidal, O. and Martínez-Martínez, J.M. (2003). High-pressure, low-temperature metamorphism in Alpujarride units of southeastern Betics (Spain). *Comptes rendus de l'Académie des Sciences de Paris*, 334, 1-9.

Booth-Rea, G., Ranero, C.R. Martínez-Martínez, J.M. and Grevemeyer, I. (2007). Crustal types and Tertiary tectonic evolution of the Alborán Sea, western Mediterranean. *Geochemistry Geophysics Geosystems* 8 (10), Q10005.

Bouybaouène, M., Michard, A. and Goffé, B. (1998). High-pressure granulites on top of the Beni Bousera peridotites, Rif belt, Morocco: A record of an ancient thickened crust in the Alboran domain. *Bulletin de la Societé Geologique de France* 169(2), 153–162.

Buntfuss J.D. (1970). Die Geologie der Küstenkentten zwischen dem rio Verde und dem Campo de Gibraltar (Westliche Betische Kordillere/Südspanien). *Jahrbuch der Geologischen Bundesanstal* 88, 373-420.

Dewey, J.F., Helmann, M.L., Turco, E., Hutton, D.H.W. and Knott, S.D. (1989).Kinematics of the western Mediterranean. In: *Alpine Tectonics* (Eds. Coward, M.P., Dietrich, D. and Park, R.G.), Special Publications, Geological Society of London 45, 265-283.

Didon J., Durand-Delga M. and Kornprobst J. (1973). Homologies géologiques entre les deux rives du détroit de Gibraltar. *Bulletin de la Societé. Géologique de France* XV, 79-105.

Durand-Delga, M. and Fontboté, J.M. (1980). Le cadre structural de la Méditerranée occidentale. *Mémoires du Bureau des Recherches Géologiques et Miniéres* 115, 67–85.

Dürr S. (1967). Geologie der Serranía de Ronda und irher sudwestlichen Ausläufer (Andalousien). *Geologica Romana* 6, 1-73.

Esteban, J.J., Cuevas, J., Tubía, J.M., Sergeev, S. and Larionov, A. (2011). A revised Aquitanian age for the emplacement of the Ronda peridotites (Betic Cordilleras, southern Spain). *Geological Magazine* 148, 183-187.

García-Casco A. and Torres-Roldán R.L. (1996). Disequilibrium induced by fast decompression in St-Bt-Grt-Ky-Sil-and Metapelites from the Betic Belt (southern Spain). *Journal of Petrology* 37 (5), 1207-1239.

García-Casco A. and Torres-Roldán R.L. (1999). Natural metastable reactions involving garnet, staurolite and cordierite. Implications for petrogenetic grids and the extensional collapse of the Betic-Rif belt. *Contributions to Mineralogy and Petrology* 136, 131-156.

García-Dueñas V. and Balanyá J.C. (1991). Fallas normales de bajo ángulo a gran escala en las Béticas occidentales. *Geogaceta* 9, 33-37.

Geel T. (1973). The geology of the Betic of Málaga, the subbetic, and the zone between these two units in the Vélez-Rubio area (Southern Spain). *GUA Papers of Geology* 5, 1-131.

Gómez-Pugnaire, M.T.and Franz, G. (1988). Metamorphic evolution of the Paleozoic series of the Betic Cordilleras (Nevado-Filabride complex, SE Spain) and its relationship with the Alpine orogeny. *Geologische Rundschau* 77, 619-640.

Gómez-Pugnaire, M.T., Galindo-Zaldívar, J., Rubatto, D., González-Lodeiro, F., López Sánchez-Vizcaíno, V. and Jabaloy, A. (2004). A reinterpretation of the Nevado-Filábride and Alpujárride Complex (Betic Cordillera): field, petrography and U-Pb ages from orthogneisses western Sierra Nevada, S Spain). *Schweizerische Mineralogische und Petrographische Mitteilungen* 84, 303-322.

Gómez-Pugnaire, M.T., Nieto, F., Abad, I., Velilla, N., Garrido, C.J., Acosta-Vigil, Barich, A., Hidas, K. and López Sánchez-Vizcaino, V. (in press). Alpine Metamorphism in the Betic Internal Zones. In: *The Geology of Iberia: A geodynamic Approach.* Regional Geology Revew (Eds. Quesada, C. and Oliveira, J.T.). Springer Nature Switzerland AG 2019.

Gómez-Pugnaire, M.T., Rubatto, D., Fernández-Soler, J.M., Jabaloy, A., López Sánchez-Vizcaíno, V., González-Lodeiro, F., Galindo-Zaldívar, J. and Padrón-Navarta, J.A. (2012). U–Pb geochronology of Nevado–Filábride gneisses: evidence for the Variscan nature of the deepest Betic complex (SE Spain). *Lithos* 146-147, 93-111.

González-Jiménez, J.M., Marchesi, C., Griffin, W.L., Gervilla, F., Belousova, E.A., Garrido, C.J., Romero, R., Talavera, C., Leisen, M., O'Reilly, S.Y., Barra, F. and Martin, L. (2017). Zircon recycling and crystallization during formation of chromite- and Ni-arsenide ores in the subcontinental lithospheric mantle (Serranía de Ronda, Spain). *Ore Geology Reviews* 90, 193-209.

Herbig H.G. (1983). El Carbonífero de las Cordilleras Béticas. In : *Carbonífero y pérmico de España. X Congreso internacional de estratigrafía y Geología del carbonífero* (Ed. C. Martínez-Díaz). I.G.M.E., Madrid, 345-355

Hoeppener R., Hoppe P., Dürr S. and Mollat H. (1964). Ein Querschnitt durch die Betischen Kordilleren dei Ronda (SW Spanien). *Geologie en Mijnbouw*, 282-298.

Hollerbach R. (1985). Kontaktverhältnisse alpinotyper Peridotitemassen, Petrologische, geochemische und mineralfaziele Untersunchungen in der Casares-Einheit am ronda peridotite, Südspanien. Ph.D. Thesis, University of Wúrzburg, Germany.

Jabaloy-Sánchez, A., Talavera C, Gómez-Pugnaire, M. T., López-Sánchez-Vizcaíno, V., Vázquez-Vílchez M., Rodríguez-Peces M.J. and Evans N.J. (2018). U-Pb ages of detrital zircons from the Internal Betics: a key to deciphering paleogeographic provenance and tectono-stratigraphic evolution. *Lithos* 318–319, 244–266

Loomis T.P. (1972). Contact metamorphism of the pelitic rocks by the Ronda ultramafic intrusion, southern Spain. *Geological Society of America Bulletin* 83, 2249-2474.

López Sánchez-Vizcaíno, V., Rubatto, D., Gómez-Pugnaire, M.T., Tommsdorff, V. and Müntener, O. (2001). Middle Miocene high-pressure metamorphism and fast exhumation of the Nevado-Filábride Complex, SE Spain. *Terra Nova* 13, 327-332.

Lundeen M.T. (1978). Emplacement of the Ronda peridotite, Sierra Bermeja, Spain. *Geological Society of America Bulletin* 89, 172-180.

Martín-Algarra A. (1987). Evolución geológica alpina del contacto entre las zonas internas y las externas de la Cordillera Bética (sector central y occidental). Ph. D. Thesis, University of Granada, Spain.

Martin-Rojas I, Somma R, Delgado F, Estévez A, Iannace A and Zamparelli V (2012) The Triassic platform of the Gador-Turon unit (Alpujarride Complex, Betic Cordillera, S Spain): climate vs. tectonic factors in controlling platform architecture. *Facies* 58(2):297-323

Martínez-Martínez J.M. and Azañón J.M. (1997). Mode of extensional tectonics in the southeastern Betics (SE Spain): Implications for the tectonic evolution of the peri-Alborán orogenic system. *Tectonics* 16 (2), 205-225.

Martínez-Martínez J.M., Soto J.I. and Balanyá J.C. (1997). Crustal decoupling and intracrustal flow beneath domal exhumed core complexes, Betics (SE Spain). *Terra Nova* 9, 223-227.

Mollat H. (1965). Die Geologie der Sierra Blanca und iher Umgebung. Ph. D. Thesis, University of Bonn, Germany.

Navarro-Vilá F. and Tubía J.M. (1983). Essai d'une nouvelle différentiation des Nappes Alpujarrides dans le secteur occidental des Cordilleres Bétiques (Andalousie, Espagne). *Comptes Rendus de l'Academie de Sciences de París* 296 (Série II), 111-114.

Padrón-Navarta JA, Tommasi A, Garrido CJ, López Sánchez-Vizcaíno V, Gómez-Pugnaire MT, Jabaloy A and Vauchez A (2010) Fluid transfer into the wedge controlled by high-pressure hydrofracturing in the cold top-slab mantle. *Earth and Planetary Science Letters* 297:271-286.

Platt, J.P., Anczkiewicz, R., Soto, J.I., Kelley, S.P. and Thirlwall, M. (2006). Early Miocene continental subduction and rapid exhumation in the western Mediterranean. *Geology* 34, 981-984.

Platt, J.P., Argles, T.W. Carter, A., Kelley, S.P., Whitehouse, M.J. and Lonergan, L. (2003). Exhumation of the Ronda peridotite and its crustal envelope: Constraints from thermal modelling of a *P–T*–time array. *Journal of the Geological Society, London* 160, 655–676.

Platt, J.P., Behr, W.M., Johanesen, K. and Williams, J.R. (2013). The Betic-Rif Arc and its Orogenic Hinterland: A Review. *Annual Review of Earth Planetary Sciences* 41, 14.1-14.45.

Platt, J.P. and Whitehouse, M.J. (1999). Early Miocene high-temperature metamorphism and rapid exhumation in the Betic Cordillera (Spain): evidence from U–Pb zircon ages. *Earth and Planetary Science Letters* 171, 591–605.

Priem H.N.A.K., Boelrijk N.A.I.M., Hebeda E.H., Oen I.S., Verdurmen T.E.A. and Verschure R.H. (1979). Isotopic dating of the emplacement of the ultramafic Masses in the Serranía de Ronda, Southern Spain. *Contributions to Mineralogy and Petrology* 70, 103-109.

Puga, E. (1990) The Betic Ophiolite Association (Southern Spain). *Ophioliti* 15, 97-117.

Rodriguez-Cañero, R., Jabaloy-Sánchez, A., Navas-Parejo, P. and Martín-Algarra, A. (2018). Linking Palaeozoic palaeogeography of the Betic Cordillera to the Variscan Iberian Massif: new insight through the first conodonts of the Nevado-Filábride Complex. *International Journal of Earth Sciences (Geologische Rundschau)* 107(5), 1791-1806.

Sánchez-Gómez, M. (1997). Emplazamiento intracortical deesmembramiento extensional de los cuerpos peridotíticos de Ronda y del Rift (Arco de Gibraltar). Ph. D. Thesis, University of Granada, Spain.

Sánchez-Navas, A., García-Casco, A., Mazzoli, S. and Martín-Algarra, A. (2017). Polymetamorphism in the Alpujarride Complex, Betic Cordillera, South Spain. *The Journal of Geology* 125 (6), 637-657.

Sánchez-Rodríguez, L. (1998). Pre-Alpine and Alpine evolution of the Ronda Ultramafic Complex and its country-rocks (Betic chain, southern Spain): U–Pb SHRIMP zircon and fission-track dating. Ph.D. Thesis. ETH, Zürich, Switzerland.

Sánchez-Rodríguez, L. and Gebauer, D. (2000). Mesozoic formation of pyroxenites and gabbros in the Ronda area (southern Spain), followed by Early Miocene subduction metamorphism and emplacement into the middle crust: U–Pb sensitive high-resolution ion microprobe dating of zircon. *Tectonophysics* 316, 19–44.

Santamaría-López, A. and Sanz de Galdeano, C. (2018). SHRIMP U–Pb detrital zircon dating to check subdivisions in metamorphic complexes: a case of study in the Nevado–Filábride complex (Betic Cordillera, Spain). *International Journal of Earth Sciences*, doi: https://doi.org/10.1007/s00531-018-1613-y

Sanz de Galdeano, C. and Ruiz Cruz, M.D. (2016). Late Palaeozoic to Triassic formations unconformably deposited over the Ronda peridotites (Betic Cordilleras): Evidence for their Variscan time of crustal emplacement. *Estudios Geológicos* 72(1): e043. http://dx.doi.org/10.3989/egeol.42046.368

Torres-Roldán R.L. (1979). The tectonic subdivision of the Betic Zone (Betic Cordilleras, Southern Spain) : its significance and one possible geotectonic scenario for the western Alpine belt. *American Journal of Science* 279, 19-51.

Torres-Roldán R.L. (1981a). Plurifacial metamorphic evolution of the Sierra Bermeja Peridotite aureole (Southern Spain). *Estudios Geológicos* 37, 115-133.

Torres-Roldán R.L. (1981b). Aplicación de los geotermómetros y geobarómetros de cordierita-granate y cordierita-biotita al discernimiento de la evolución del proceso anatéctico en el complejo migmatítico de la unidad de (tipo) Blanca. *Boletín de la Sociedad Española de Mineralogía* 2, 99-118.

Trommsdorff V., López Sánchez-Vizcaíno V, Gómez-Pugnaire M.T. and Münter O. (1998). High pressure breakdown of antigorite to spinifex-textured olivine and orthopyroxene, SE Spain. *Contributions to Mineralogy and Petrology* 132, 139-148.

Tubía J.M. (1988). Estructura de los Alpujárrides occidentales. Cinemática y condiciones de emplazamiento de las peridotitas de Ronda. Publicación Espeial del *Boletín Geológico y Minero de España* 99, 1-124.

Tubía, J.M. (1994). The Ronda poridotites (Los Reales nappe): an example of the relationship between lithospheric thickening by oblique tectonics and late extensional deformation within the Betic Cordillera (Spain). *Tectonophysics* 238, 381-398.

Tubía J.M. and Cuevas J. (1986). High-temperature emplacement of the los Reales peridotite nappe (Betic Cordillera, Spain). *Journal of Structural Geology* 8, 473-482.

Tubía, J.M., Cuevas, J. and Esteban, J.J. (2013). Localization of deformation and kinematic shift during the hot emplacement of the Ronda peridotites (Betic Cordilleras, southern Spain). *Journal of Structural Geology* 50, 148-160.

Tubía J.M., Cuevas J. and Gil Ibarguchi J.I. (1997). Sequential development of the metamorphic aureole beneath the Ronda peridotites and its bearing on the tectonic evolution of the Betic Cordillera. *Tectonophysics* 279, 227-252.

Tubía J.M., Cuevas J., Navarro-Vilá F., Alvarez F. and Aldaya F. (1992). Tectonic evolution of the Alpujárride Complex (Betic Cordillera, Southern Spain). *Journal of Structural Geology* 14, 193-203.

Tubía J.M and Gil Ibarguchi J.I. (1991). Eclogites of the Ojén nappe: a record of subduction in the Alpujárride Complex (Betic Cordilleras, Southern Spain). *Journal of the Geological Society of London* 148, 801-804.

Whitehouse, M.J. and Platt, J.P. (2003). Dating high-grade metamorphism—constraints from rare-earth elements in zircon and garnet. *Contributions to Mineralogy and Petrology* 145, 61–74.

Zeck H.P., Monié P., Villa I.M. and Hansen B.T. (1992). Very high rates of cooling and uplift in the alpine belt of the Betic Cordilleras, southern Spain. *Geology* 20, 79-82.

Zeck, H.P. and Whitehouse, M.J. (2002). Repeated age resetting in zircons from Hercynian–Alpine polymetamorphic schists (Betic–Rif tectonic belt, S. Spain)—a U–Th–Pb ion microprobe study. *Chemical Geology* 182, 275–292.

Zeck, H.P. and Williams, I.S. (2001). Hercynian metamorphism in nappe core complexes of the Alpine Betic–Rif belt, western Mediterranean—a SHRIMP zircon study. *Journal of Petrology* 42, 1373–1385.

Chapter 3
The ultramafic massifs of the Serranía de Ronda

3.1 Outcrops of ultramafic rocks in the Betic-Rifean Orogenic Belt

In the Betic-Rifean orogenic belt, ultramafic rocks form coherent bodies (hereafter massifs) that are scattered along the northern and southern margins of the Alboran Sea (westernmost Mediterranean; Fig. 2.1). As noted in Chapters 1 and 2, the largest massifs of ultramafic rocks are found in the Internal Zones of the orogenic belt, namely in the Alpujárride and Nevado-Filábride complexes in the Iberian Peninsula, and in the Sebtide complex in Africa. Smaller ultramafic massifs, mainly composed of serpentinites, crop out in the External Zones (Maghrebi domain; Michard et al., 1992).

The mantle rocks in the Nevado-Filábride complex constitute small ultramafic massifs (<3 km^2) of strongly metamorphosed mantle peridotites, metaserpentinites and related metamafic rocks, interpreted as a dismembered ophiolite association or mantle portions exhumed at an ocean-continent transition zone and then subducted (Puga, 1990; Jabaloy-Sánchez et al., 2015). Field, petrological and geochemical evidence supports the exceptional nature of the rocks preserved in these massifs, particularly at Cerro del Almirez (Province of Almeria), where a unique example of antigorite-out dehydration isograd in subducted serpentinites is observed in the field (Trommsdorff et al., 1998; López Sánchez-Vizcaíno et al., 2005; Padrón-Navarta et al., 2011).

The upper mantle rocks of the Alpujárride complex are located in the western part of the Betic Cordillera, namely in the Serranía de Ronda (Province of Malaga) (Fig. 2.2). They represent large exposures (~ 450 km^2) of subcontinental mantle peridotites that crop out in three main massifs: the ***Ronda ultramafic massif*** (~300 km^2), the ***Ojén ultramafic massif*** (~70 km^2) and the ***Carratraca ultramafic massif*** (~60 km^2). Other much smaller mantle outcrops in the region include: the *Mijas ultramafic massif*, located south to the Mijas village; the *La Robla ultramafic massif*, to the east of Casarabonela (south to the larger Carratraca massif); the *Sierra Pelada ultramafic massif*, located to the west of the Coin village; and the *Dehesa del Albornoque ultramafic massif*, cropping out west to Monda. In addition, some even smaller bodies of serpentinized ultramafic rocks of few hectometers crop out north to the Sierra de Tolox and Sierra Alpujata.

The most abundant mantle rocks in the ultramafic massifs of the Serranía de Ronda are fertile lherzolites, with minor harzburgites and dunites (Fig. 3.1). The proportion of dunite is generally very low, although in some parts they are the predominant rock-type (Remaïdi, 1993). Mafic rocks, usually referred in the literature as "mafic layers" (Fig. 3.1), are also common (Garrido and Bodinier, 1999). A very interesting feature of these mantle bodies is that they host magmatic mineralizations unique in the world, which include: 1) chromium-nickel (Cr-Ni) ores, (2) sulfide-graphite (S-G) ores and (3) chromium (Cr) ores (see Chapter
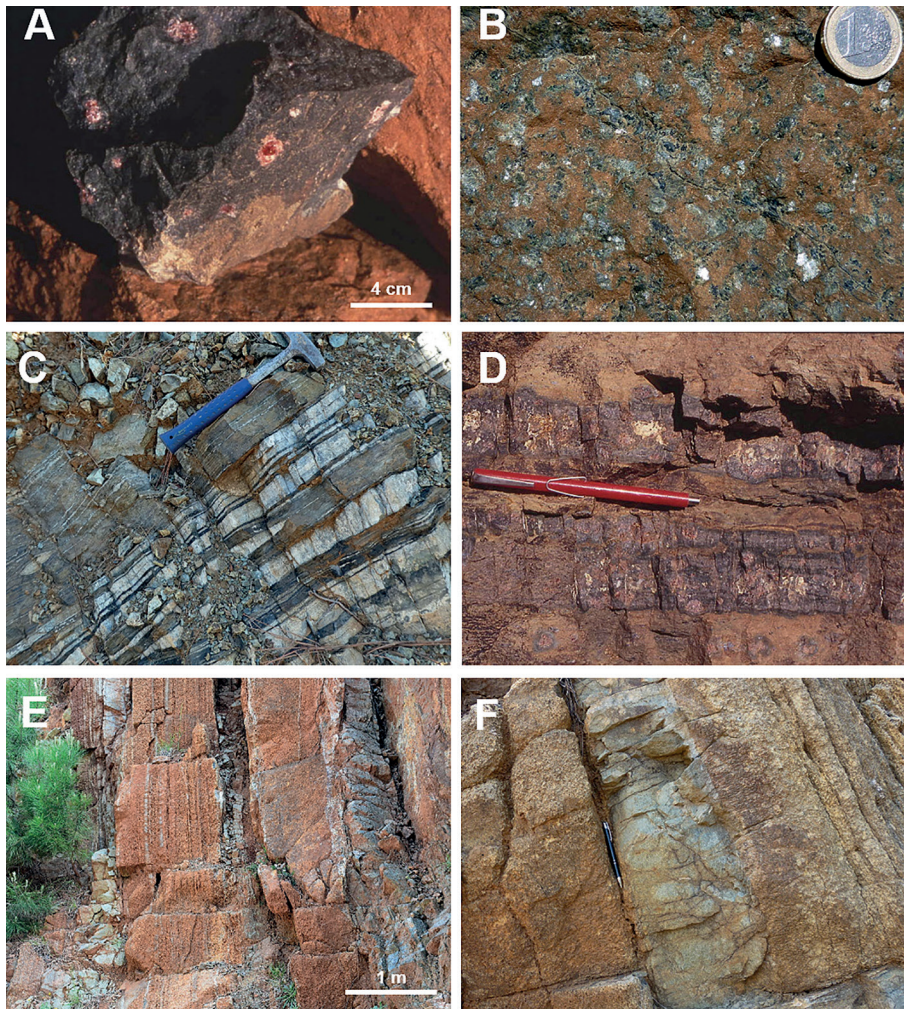
Figure 3.1. Field images of peridotites and pyroxenites from the Serranía de Ronda ultramafic massifs. A: garnet peridotite; B: granular espinel peridotite; C: deformed/boudinated garnet- and corundum-bearing pyroxenite layers; D: garnet pyroxenite layers; E: layering of peridotite and variably thick pyroxenite layers; F: chromium-rich pyroxenite layer.

6) (Gervilla, 1990; Gervilla and Leblanc, 1990). Additionally, these massifs exhibit a great variety of serpentinite rocks produced by hydrothermalism and surface weathering during the late stages of crustal emplacement. The degree of serpentinization is related to the size of the ultramafic massif, being the ultramafic rocks from Ronda the least altered.

Other lithologies spatially associated with peridotites are dykes and pods of acid rocks (i.e., leucogranites). These rocks are usually less than ten meters thick and often define stock-works that intrude the peridotites through late sets of open cracks, singularly in the proximities of the contacts between the mantle and crustal units (Hernández- Pacheco, 1967; Cuevas et al., 2006). These leucocratic dykes and pods have a wide range of compositions (i.e., granite, granodiorite, monzonite and transitional rocks between these end-members; Acosta, 1997) and they are ascribed to partial melting of underlying metapelites during the emplacement of hot mantle rocks into the crust (Acosta, 1997; Sánchez-Rodríguez and Gebauer, 2000; Pereira et al., 2003; Cuevas et al., 2006). Most of these dykes are undeformed and yield crystallization ages between 22 and 18 Ma (Priem et al., 1979; Esteban et al., 2007, 2010; González-Jiménez et al., 2017).

Most of the geological research on the Serranía de Ronda ultramafic massifs has focused on the largest Ronda massif. This massif has been the subject of pioneering petrological, igneous, metamorphic and structural studies, which have inspired investigations of other ultramafic massifs around the world. The work of scientists from tens of countries, published in hundreds of scientific papers, Master and Doctoral Theses, has defined the main features of the ultramafic massifs of the Serranía de Ronda in terms of *petrology* (e.g., Hernández-Pacheco, 1967; Obata, 1977, 1980; Targuisti, 1994), *geochemistry* (e.g., Frey et al., 1985; Suen and Frey, 1987; Remaidi, 1993; Garrido, 1995; Van der Wal and Bodinier, 1996; Garrido and Bodinier, 1999; Lenoir et al., 2001), *structure* (e.g., Darot, 1973; Tubía, 1988; Van der Wal, 1993) and *metallogeny* (e.g., Gervilla, 1990; Gervilla and Leblanc, 1990; Leblanc et al., 1990; Gutiérrez-Narbona, 1999; González-Jiménez et al. 2017). All these aspects, in particular the metallogeny, will be discussed in the following chapters of this book.

3.2 The Ronda ultramafic massif

The Ronda ultramafic massif is the largest (~300 km^2) known exposure of subcontinental mantle peridotites on Earth. It is located in the westernmost part of the Málaga province and crops out from Sierra de Torrox (to the east) to Sierra Bermeja (to the west), north to the town of Estepona (Fig. 3.2). Peridotites (including lherzolites and harzburgites with lesser amounts of dunites) constitute >90 % of the surface of the massif, whereas mafic pyroxenitic layers normally represent less than 5 % (exceptionally up to 15%). In general, the upper mantle rocks are mostly unaltered, although the degree of serpentinization increases close to crustal rocks and shear zones.

The foliation in the western part of the massif is nearly constant and strikes NE-SW. Close to the northern contact with the Los Reales unit, the foliation dips
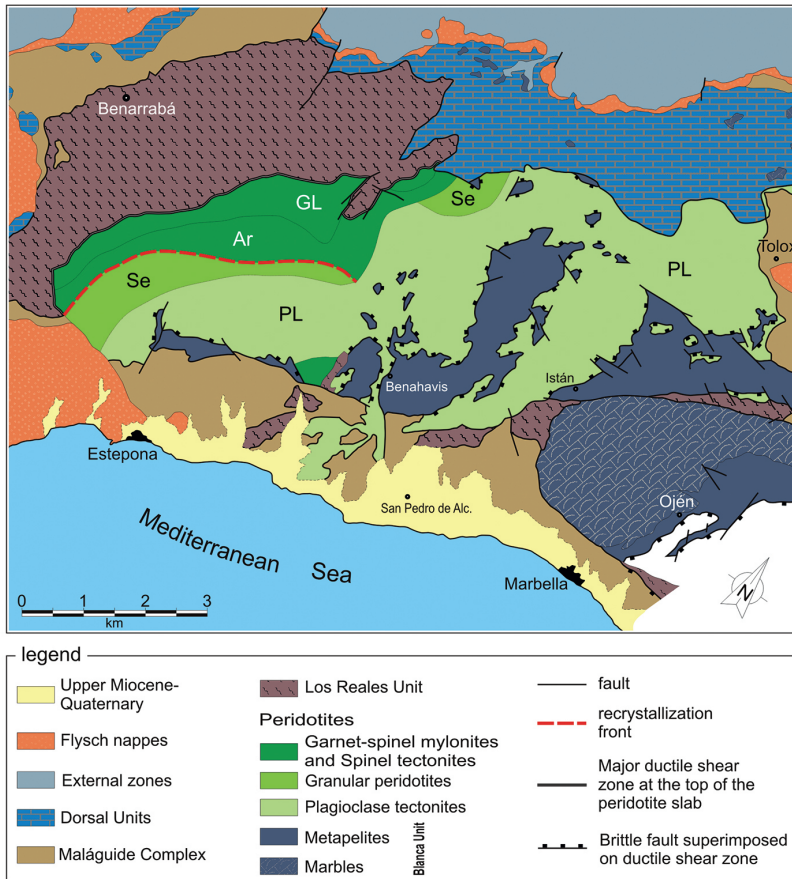
Figure 3.2. Mineral facies zoning (Obata, 1980) combined with the tectonometamorphic zoning (Van der Wal and Visser, 1993) of the Ronda ultramafic massif. GL: garnet lherzolite facies; Ar: Ariegite subfacies of the spinel lerzolite facies; Se: Seiland subfacies of the spinel lherzolite facies; PL: plagioclase lherzolite facies. The geological map of the surrounding areas is simplified from Soto (1986).

to NW, whereas closer to the southern contact with the Blanca unit it dips to SE. These orientations define a smooth antiformal structure (Hidas et al., 2013). In the eastern part of the massif, the strike of the foliation is more variable, although there is a maximum in the NW-SE direction.

Obata (1980) firstly reported the coexistence in the Ronda massif of the four types of mineral facies defined by O'Hara (1967) for upper mantle lherzolites. These include: (1) garnet lherzolite facies, (2) subfacies Agierite of the spinel lherzolite facies, (3) subfacies Seiland of the spinel lherzolite facies, and (4) plagioclase lherzolite facies. Later, Van der Val and Vissers (1993, 1996) defined a different zoning based on structural criteria, although somehow correlated with the Obata's one. According to these authors, there are three tectonometamorphic domains in the westernmost part of the Ronda massif, which from the top

(northwestern contact) to the bottom (south-southeastern contact) include: (1) garnet-spinel mylonites and spinel tectonites, (2) granular peridotites and (3) plagioclase tectonites. These igneous and structural zoning will be described more in detail in Chapter 4.

3.3   The Ojén ultramafic massif

The Ojén ultramafic massif is the second largest ultramafic body (~70 km^2) among those cropping out in the Serranía de Ronda. This massif covers most of the area of Sierra Alpujata, west to the Ojén village (Fig. 3.3), and is composed of 90-95% peridotites and 5-10% mafic layers and leucogranites. The most abundant rocks
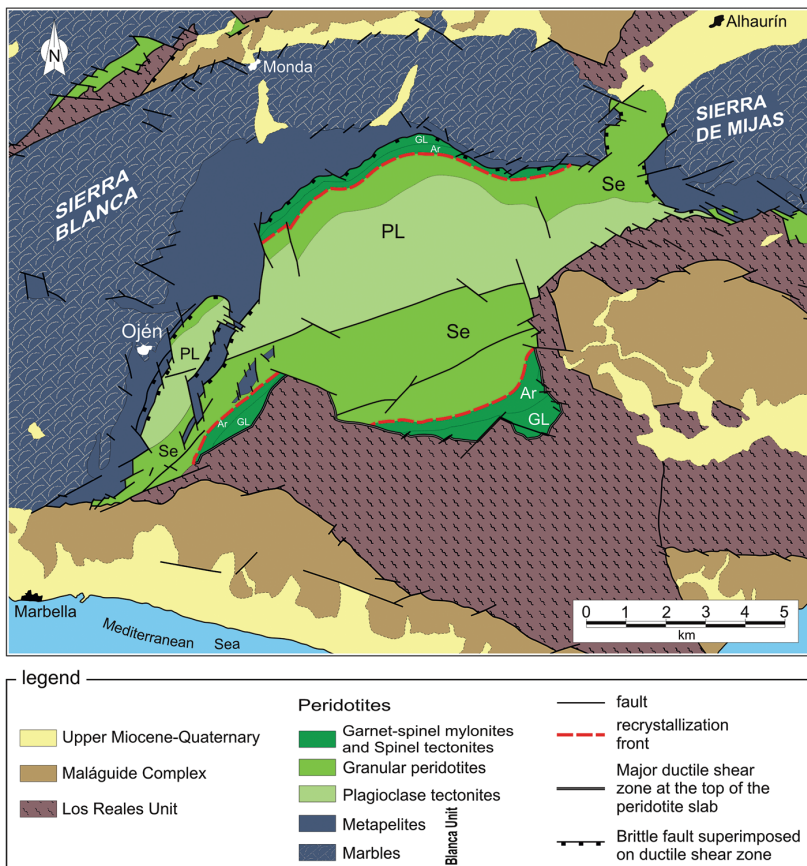
Figure 3.3. Zoning of the Ojén ultramafic massif (Gervilla, 1990) based on the distribution of mineral facies and tectonometamorphic domains as defined in the Ronda Ultramafic Massif by Obata (1980) and Van der Wal and Visser (1993), respectively. GL: garnet lherzolite facies; Ar: Ariegite subfacies of the spinel lerzolite facies; Se: Seiland subfacies of the spinel lherzolite facies; PL: plagioclase lherzolite facies. The geological map of the surrounding areas is simplified from Tubía, 1988).

in this massif are lherzolites and harzburgites with lesser amounts of dunites, although the proportion of dunites is higher than in the nearby Ronda massif. Dunites mostly crop out in the central part of the massif as tabular bodies, a few centimeters up to tens of meters thick, and locally grade to lherzolites through a transitional zone of harzburgite. Close to the contact with crustal rocks, the Ojén peridotites have mylonitic and cataclastic structures that are observable at the micro, meso and macroscales (Tubía 1988).

The ultramafic rocks of the Ojén massif have higher degrees of serpentinization than those of the Ronda massif, due to the presence of meso-scale cracks in the central part of the massif. The circulation of fluids through this penetrative fracture network produced intensive hydrothermal alteration and the formation of deposits of talc, asbestos and vermiculites (Rode et al., 1980a, b y c; Luque del Villar et al., 1985). In places, this hydrothermal alteration was linked to the intrusion of plagiogranite dykes.

The foliation in the massif strikes N30-80E and dips to the south, with the highest dips in the proximities of the northern contact. Besides foliation, peridotites also exhibit isoclinal folds (i.e., sheath-folds) striking N40E with vergence towards NW. In the central part of the massif, these isoclinal folds are more open than in the north where the sheath-folds predominate (Gervilla, 1990). According to Gervilla et al. (2002), the three tectonometamorphic domains defined in the Ronda ultramafic massif are also preserved in the Ojén massif. In particular, the central part of this massif consists of plagioclase tectonites, which are bounded to the north and south by granular peridotites and spinel tectonites (± garnet-spinel mylonites) (Fig. 3.3).

3.4   The Carratraca ultramafic massif

The Carratraca ultramafic massif is the smallest of the three main ultramafic massifs of the Serranía de Ronda (~60 km^2). The massif is located north to the Ojén massif, close to the Carratraca village, and includes peridotites cropping out in Sierra de las Aguas and Los Jarales areas (Fig. 3.4). The Carratraca massif is exclusively made up of garnet and spinel lherzolites, which are strongly serpentinized due to the development of a penetrative network of fractures and faults. The foliation strikes between N60E and N140E with a general dip towards the north (Soto and Gervilla, 1991). Granular peridotites constitute the core of the ultramafic body, whereas garnet-spinel mylonites and spinel tectonites crop out in the external areas of the massif (Fig. 3.4).
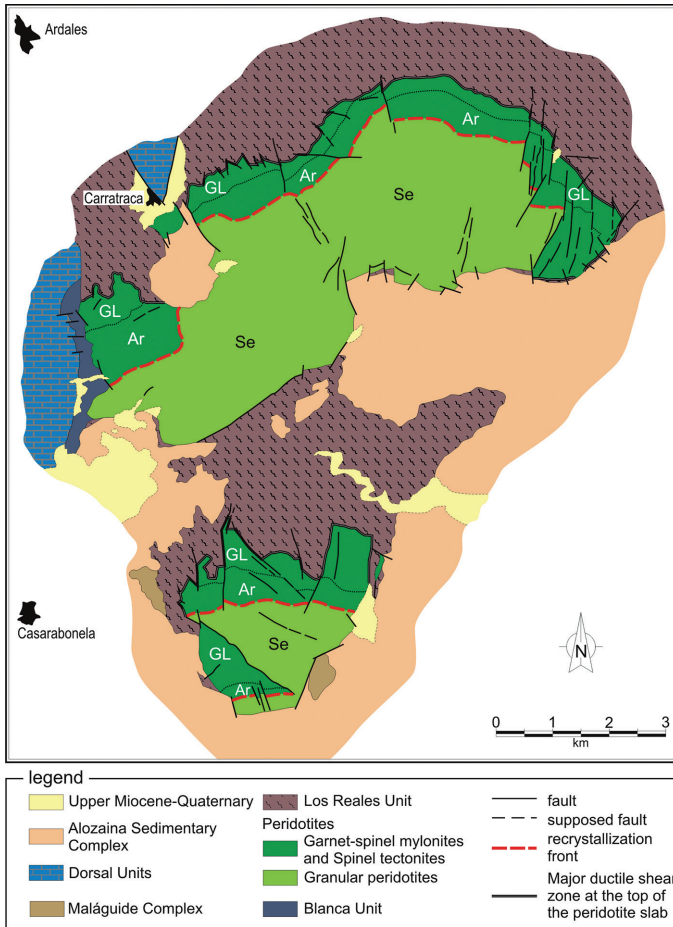
**Figure 3.4.** Geological map of the Carratraca ultramafic massif and surrounding areas (from Soto and Gervilla, 1991). Zoning of the ultramafic massifs are based on the distribution of mineral facies and tectonometamorphic domains as defined in the Ronda Ultramafic Massif by Obata (1980) and Van der Wal and Visser (1993), respectively. GL: garnet lherzolite facies; Ar: Ariegite subfacies of the spinel lerzolite facies; Se: Seiland subfacies of the spinel lherzolite facies.

References

Acosta, A. (1997). Estudio de los fenómenos de fusión cortical y generación de granitoides asociados a las peridotitas de Ronda. Ph. D. Thesis, University of Granada. Spain.

Cuevas, J., Esteban, J.J. and Tubía, J.M. (2006). Tectonic implications of the granite dyke swarm in the Ronda peridotites (Betic Cordilleras, Southern Spain). *Journal of the Geological Society of London* 163, 631–640.

Darot, M. (1973). Cinèmatique de l'extrusion, à partir du manteau, des péridotites de la –sierra Bermeja (Serranía de Ronda, Espagne). *Comptes Rendus de l'Académie des Sciences de Paris* 278, 1673-1676.

Esteban, J.J., Cuevas, J., Tubía, J.M., Liati, A., Seward, D. and Gebauer, D. (2007). Timing and origin of zircon-bearing chlorite schists in the Ronda peridotites (Betic Cordilleras, Southern Spain). *Lithos* 99, 121–135.

Esteban, J.J., Cuevas, J., Tubía, J.M., Sergeev, S. and Larionov, A. (2010). A revised aquitanian age for the emplacement of the Ronda peridotites (Betic Cordilleras, Southern Spain). *Geological Magazine* 148, 183–187.

Frey, F.A., Suen, C.J. and Stockman, H.W. (1985). The Ronda high temperature peridotite: geochemistry and petrogenesis. *Geochimica et Cosmochimica Acta* 49, 2469-2491.

Garrido, C.J. (1995). Estudio geoquímico de las capas máficas del Macizo Ultrmáfico de Ronda. Ph. D. Thesis, University of Granada.

Garrido, C.J. and Bodinier, J.L. (1999). Diversity of mafic rocks in the Ronda peridotite: evidence for pervasive melt/rock reaction during heating of subcontinental lithosphere by upwelling asthenosphere. *Journal of Petrology* 40, 729-754.

Gervilla, F. (1990). Mineralizaciones magmáticas ligadas a la evolución de las rocas ultramáficas de la Serranía de Ronda (Málaga, España). Ph. D. Thesis, University of Granada. Spain.

Gervilla, F. and Leblanc, M. (1990). Magmatic ores in high-temperature Alpine-type lherzolite massifs (Ronda, Spain) and Beni Bousera, Morocco). *Economic Geology* 85, 112-132.

González-Jiménez, J.M., Marchesi, C., Griffin, W.L., Gervilla, F., Belousova, E.A., Garrido, C.J., Romero, R., Talavera, C., Leisen, M., O'Reilly, S.Y., Barra, F. and Martin, L. (2017). Zircon recycling and crystallization during formation of chromite- and Ni-arsenide ores in the subcontinental lithospheric mantle (Serranía de Ronda, Spain). *Ore Geology Reviews* 90, 193-209.

Gutiérrez-Narbona, R. (1999). Implicaciones metalogénicas (cromo y elementos del grupo del platino) de los magmas/fluidos residuales de un proceso de percolación a gran escala en los macizos ultramáficos de Ronda y Ojén (Béticas, Sur de España). Ph. D. Thesis, University of Granada. Spain.

Hernández- Pacheco, A. (1967). Estudio petrofráfico y geoquímico del macizo ultramáfico de Ojén (Málaga). *Estudios Geológicos* XXIII, 85-143.

Hidas, K., Booth-Rea, G., Garrido, C.J., Martínez-Martínez, J.M., Padrón-Navarta, J.A., Konc, Z., Giaconia, F., Frets, E., Marchesi, C., 2013. Backarc basin inversion and subcontinental mantle emplacement in the crust: kilometre-scale folding and shearing at the base of the proto-Alborán lithospheric mantle (Betic Cordillera,southern Spain). *Journal of the Geological Society* 170, 47–55.

Jabaloy, A., Gómez-Pugnaire, M.T., Padrón-Navarta, J.A., López Sánchez-Vizcaíno, V. and Garrido, C.J. (2015). Subduction- and exhumation-related structures preserved in metaserpentinites and associated metasediments from the Nevado-Filábride complex (Betic Cordillera, SE Spain). *Tectonophysics* 644–645, 40–57.

Leblanc, M., Gervilla, F. and Jedwab, J. (1990). Noble metals segregation and fractionation in magmatic ores from Ronda and Beni Bousera lherzolite massifs (Spain, Morocco). *Mineralogy and Petrology* 42, 233-248.

Lenoir, X., Garrido, C.J., Bodinier, J.-L., Dautria, J.-M. y Gervilla, F. (2001). The recrystallization front of the Ronda peridotite: Evidence for melting and thermal erosion of subcontinental lithospheric mantle beneath the Alborán basin. *Journal of Petrology,* 42 (1), 141-158.

López Sánchez-Vizcaíno, V., Trommsdorff, V., Gómez-Pugnaire, M.T., Garrido, C.J., Müntener, O., Connolly, J.A.D. (2005). Petrology of titanian clinohumite and olivine at the high-pressure breakdown of antigorite serpentinite to chlorite harzburgite (Almirez Massif, S. Spain). *Contributions to Mineralogy and Petrology* 149, 627–646.

Luque del Villar, F.J., Rodas, M., Velasco, F. and Galan, E. (1985). Mineralogía y génesis de los yacimientos de vermiculita del macizo de Ojén (Serranía de Ronda, Málaga). *Boletín de la Sociedad Española de Mineralogía* 8, 229-238.

Michard, A., Feinberg, H., Elazzab, D., Bouybaouene, M.L. and Saddiqi O. (1992). A serpentinite ridge in a collisional paleomargin setting: the Beni Malek massif, External Rif, Morocco. *Earth and Planetary Science Letters* 113, 435-442.

Obata, M. (1977). Petrology and petrogenesis of the Ronda high-temperature peridotite intrusion, Southern Spain. Ph.D. Thesis, Massachusetts Institute of Technology. USA.

Obata, M. (1980). The Ronda peridotite: Garnet-, spinel-, and plagioclase-lherzolite facies and the P-T trajectories of a high-temperature mantle intrusión. *Journal of Petrology* 21, 533-572.

O'Hara, M.J. (1967). Mineral facies in ultrabasic rocks. In: Wyllie P.J. (ed.), *Ultramafic and Related Rocks*. New York: Wiley & Sons, 7-18.

Padrón-Navarta, J.A., López Sánchez-Vizcaíno, V., Garrido, C.J. and Gómez-Pugnaire, M.T. (2011). Metamorphic record of high-pressure dehydration of antigorite serpentinite to chlorite harzburgite in a subduction setting (Cerro del Almirez, Nevado–Filábride Complex, Southern Spain). *Journal of Petrology* 52, 2047–2078.

Pereira, M.D., Shaw, D.M., Acosta, A., 2003. Mobile trace elements and fluid-dominated processes in the Ronda peridotite, Southern Spain. *Canadian Mineralogist* 41,617–625.

Priem, H.N.A.K., Boelryjk, N.A.I.M., Hebeda, E.H., Oen, I.S., Verdurmen, T.E.A. and Verschure, R.H. (1979). Isotopic dating of the emplacemeent of the ultramafic masses in the Serranía de Ronda, Southern Spain. *Contributions to Mineralogy and Petrology* 70, 103-109.

Puga, E. (1990). The Betic ophiolite association (Southeastern Spain). *Ophioliti* 15, 97-117.

Remaïdi, M. (1993). Etude petrologique et goechimique d'une association peridotites refractaires-pyroxenites dans le massif de Ronda (Spagne). Ph. D. Thesis, University of Montpellier. France.

Rodas, M., Galán, E. y La Iglesia, A. (1980a). Mineralogía y mineralogénesis de los depósitos de talco de la Serranía de Ronda (Málaga). Parte I: Geología. *Boletín Geológico y Minero de España* 91 (3), 18-31.

Rodas, M., Galán, E. y La Iglesia, A. (1980a). Mineralogía y mineralogénesis de los depósitos de talco de la Serranía de Ronda (Málaga). Parte II: Mineralogía. *Boletín Geológico y Minero de España* 91 (4), 42-59.

Rodas, M., Galán, E. y La Iglesia, A. (1980a). Mineralogía y mineralogénesis de los depósitos de talco de la Serranía de Ronda (Málaga). Parte III: Mineralogénesis. *Boletín Geológico y Minero de España* 91 (5), 27-32.

Sánchez-Rodriguez, L., Gebauer, D., 2000. Mesozoic formation of pyroxenites and gabbros in the Ronda area (southern Spain), followed by Early Miocene subduction metamorphism and emplacement into the middle crust: U-Pb sensitive high- resolution ion microprobe dating of zircón. *Tectonophysics* 316 (1–2), 19–44.

Soto, J.I. and Gervilla, F. (1991). Los macizos ultramáficos de la Sierra de las Aguas y Sierra de la Robla como una ventana extensional (Béticas occidentales). *Geogaceta* 9, 21-23.

Suen, C.J. and Frey, F.A. (1987). Origin of the mafic and ultramafic rocks in the Ronda peridotite. *Earth and Planetary Science Letters* 85, 183-202.

Targuisti, K. (1994). Petrología y geoquímica de los macizos ultramáficos de Ojén (Andalucía) y Beni Bousera (Rif septentrional, Marruecos). Ph. D. Thesis, University of Granada. Spain.

Trommsdorff, V., López Sánchez-Vizcaíno, V., Gómez-Pugnaire, M.T. and Müntener, O. (1998). High pressure breakdown of antigorite to spinifex-textured olivine and orthopyroxene, SE Spain. *Contributions to Mineralogy and Petrology* 132, 139–148.

Tubía, J.M. (1988). Estructura de los Alpujárrides occidentales, Cinemática y condiciones de emplazamiento de las peridotitas de Ronda. *Boletín Geológico y Minero de España, Special Publication* 99, 1-124.

Van der Wal, D. (1993). Deformation processes in mantle peridotites. Ph. D. Thesis, University of Utrech. The Netherlands.

Van der Wal, D. and Bodinier, J.L. (1996). Origin of the recrystallization front in the Ronda peridotite by km-scale pervasive porous flow. *Contributions to Mineralogy and Petrology* 122, 387-405.

Van der Val, D. and Vissers, R.L.M. (1993). Uplift and emplacement of upper mantle rocks in the western Mediterranean. *Geology* 21, 1119-1122.

Van der Val, D. and Vissers, R.L.M. (1996). Structural petrology of the Ronda peridotite SW Spain: deformation history. *Journal of Petrology* 37, 23-43.

Chapter 4
Petrologic, metamorphic and geochemical zoning of the ultramafic massifs

4.1   Petrologic and metamorphic zoning

In the 70's of the past 20th century, a group of researchers (Dickey, 1970; Obata, 1977, 1980) firstly recognized a kilometric-scale petrological zoning in the ultramafic massif of Ronda. Dickey (1970) linked this petrological zoning to the magmatic differentiation of the massif within the upper mantle, suggesting that peridotites represent the residua after variable degrees of partial melting, and mafic layers are the product of crystallization of the extracted partial melts. Later, a series of works carried out by Darot (1973), Obata (1977, 1980) and Schubert (1977) highlighted that the ultramafic massifs of the Serranía de Ronda experienced recrystallization processes related to metamorphism, which partly modified and obliterated previous magmatic mineral assemblages.

   Taking in consideration the previous observations, Obata (1977, 1980) mapped the largest Ronda massif, classifying the mineral assemblages of the ultramafic and mafic rocks into four metamorphic facies on the basis of the four components of the CMAS system (CaO-MgO-Al_2O_3-SiO_2): $CaAl_2SiO_6$ (Ca-Tschermak pyroxene, CaTs), SiO_2 (quartz, Q), $CaMgSi_2O_6$ (diopside) and Mg_2SiO_4 (forsterite, Fo). Applying this approach, Obata represented phase relationships on the Fo-Q-CaTs plane using diopside as projection point and distinguished the following facies and subfacies (Fig. 3.2):

1.- ***Garnet lherzolite facies*** characterized by the presence of pyrope-type garnet in lherzolites, and defined in the Fo-Q-CaTs system by the equilibrium between forsterite, pyrope and enstatite.
2.- ***Spinel lherzolite facies*** determined by the coexistence of spinel and olivine in the ultramafic rocks. Two subfacies are distinguished in this facies based on the stable mineral paragenesis in the mafic layers: 2.1) *Subfacies Ariegite* where pyrope-type garnet is stable, and 2.2) *Subfacies Seiland* where spinel is stable instead of garnet.
3.- ***Plagioclase lherzolite facies*** marked by the stability of the forsterite-anorthite pair in both lherzolites and mafic rocks.

The Obata's metamorphic zoning originally described for the Ronda massif was also observed later in the other ultramafic massifs of Ojén and Carratraca (Gervilla, 1990; Soto and Gervilla, 1991; Targuisti, 1994) (Fig. 3.3 and 3.4). More recent petrological, structural and geochemical research (Van der Wal and Vissers 1993, 1996; Van der Wal and Bodinier 1996; Garrido and Bodinier 1999; Lenoir et al. 2001; Vauchez and Garrido 2001; Gervilla et al., 2002; Precigout et al. 2007; Bodinier et al. 2008) has revealed the existence of a distinct zoning in the western part of the Ronda ultramafic massif, which broadly corresponds to Obata's four peridotite facies. This petrological zoning includes from the top to the bottom of the mantle section (Fig. 4.1):

1.- ***Spinel (± garnet) tectonite domain.*** This domain, which includes the Obata's garnet lherzolite facies and the Agierite subfacies of spinel lherzolites, is located in the northern and western portions of the Ronda and Carratraca massif and in the northern and southern areas of the Ojen massif (Fig. 3.2, 3.3 and 3.4). This domain consists of foliated spinel tectonites bounded by garnet-spinel mylonites in direct contact with the crustal units. The garnet-spinel mylonites have been interpreted either as younger structures formed by high-pressure shearing of older spinel tectonite domain (Van der Vall and Vissers, 1996), or as originated contemporaneously with spinel tectonites by increasing strain localization and cooling at the top of the massifs (Precigout et al., 2007; Garrido et al., 2011). As a whole, this domain was interpreted
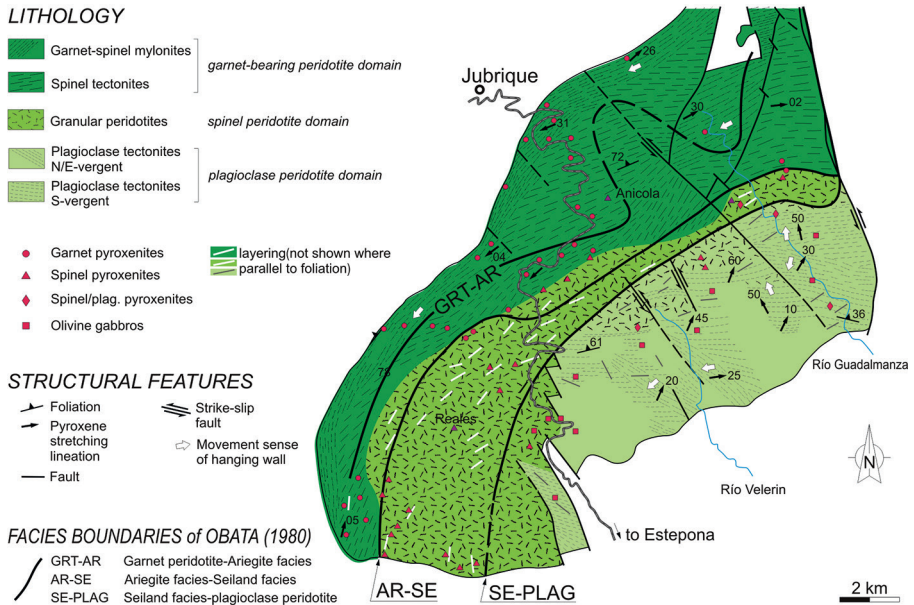
Figure 4.1. Petro-structural zoning of the western part of the Ronda Ultramafic Massif (modified from Van der Wal and Visser, 1996). The map also includes the boundaries of the mineral facies zones defined by Obata, 1980).

as a portion of subcontinental lithospheric mantle (SCLM) as old as 1.3 Ga (Reisberg and Lorand, 1995), which had experienced decompression, cooling and strain localization related to extension (from ~1150 ºC and 2.7 GPa to 900 ºC and 1.9 GPa; Precigout et al., 2007; Garrido et al., 2011). Exhumation associated with extension led to the final emplacement of the SCLM in an extremely attenuated shallow continental lithosphere in the Miocene (Garrido et al., 2011; Hidas et al., 2013). Substantial thinning of SCLM is corroborated by the presence of graphitized diamonds in garnet pyroxenites (Davies et al., 1993).

2.- *Granular peridotite domain.* This domain, which broadly coincides with Obata's Seiland subfacies, is located in the central parts of the three massifs of Ronda, Ojén and Carratraca (Fig. 3.2, 3.3 and 3.4) and consists of granular spinel peridotites and minor spinel pyroxenites. A narrow (ca. 200-400 m wide) and continuous (ca. 20 km long in the Ronda massif) transitional zone, referred to as the recrystallization front (Van der Wal and Vissers 1993, 1996; Van der Wal and Bodinier 1996; Lenoir et al., 2001), separates the spinel tectonites from the granular peridotite domain (Fig. 3.2, 3.3, 3.4 and 4.1). Granular peridotites formed by annealing, recrystallization and partial melting at >1250 ºC and 1.5 GPa of pre-existing spinel tectonites, triggered by thermal erosion of SCLM due to upwelling of the asthenosphere shortly before the crustal emplacement of the ultramafic massifs (Lenoir et al., 2001). In this scenario, the recrystallization front is interpreted as the thermal boundary above partially molten granular peridotites. Different subtypes of granular peridotites are identified at different distance from the recrystallization front (Van der Wal and Bodinier, 1996): 2.1) the *coarse-granular subdomain* (from a few meters up to 2 km thick) is located just below the recrystallization front and mainly consists of coarse-grained, olivine-rich lherzolites and harzburgites; 2.2), the *fine granular subdomain* is located in the central area and shows decreasing grain size related to dissolution processes, and 2.3) *layered-granular subdomain* corresponding to peridotites located relatively far from the recrystallization front and characterized by symmetrical layering of olivine-rich lherzolites, harzburgites and dunites, alternating with fertile plagioclase-bearing lherzolites (Fig. 4.2).

3.- *Plagioclase tectonite domain.* This domain, which occupies most of the core of the Ronda and Ojén massifs but is missing in Carratraca, corresponds to Obata's plagioclase lherzolite facies (Fig. 3.2, 3.3 and 3.4). This domain is compositionally similar to the upper granular peridotite domain, although harzburgites and dunites are relatively more abundant. The presence of plagioclase replacing spinel in strongly foliated peridotites is the distinctive characteristic of this domain, which formed at expenses of the pre-existing granular spinel peridotites. This transformation records late, low-pressure cooling (at 800-900 ºC and 0.5-0.7 GPa; Obata, 1980) associated with strain localization in subsolidus shear zones shortly before and during the final emplacement of the ultramafic massifs into the crust (Van der Wal and Vissers, 1993, 1996; Hidas et al., 2013).
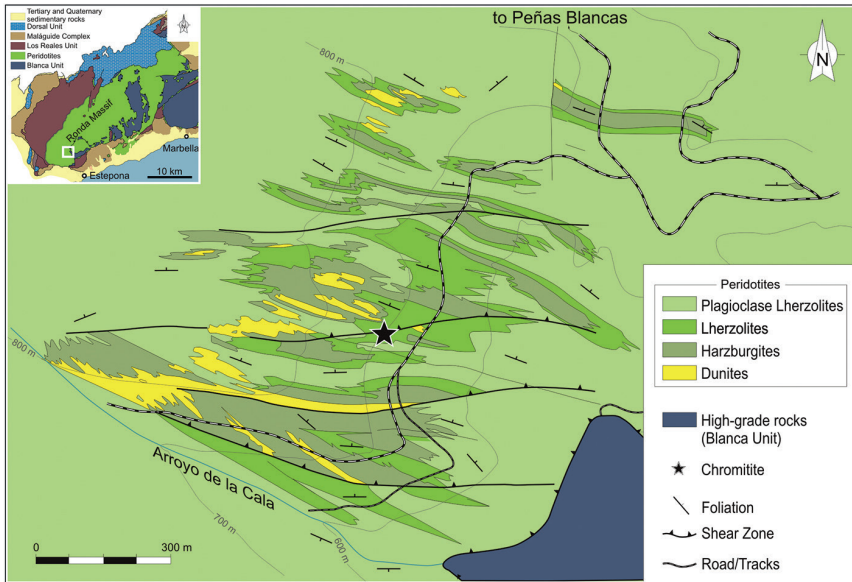
Figure 4.2. Distribution of dunite bodies enveloped by harzburgite and lherzolite within plagioclase lherzolite in the Arroyo de la Cala area. This area is located in the south-western part of the Ronda Ultramafic Massif, at the transition zone between granular peridotite and plagioclase tectonite domains, and include a small occurrence of chromitite.

4.2 Mafic layers

Suen and Frey (1987) conducted the first comprehensive mineralogical and petrological study on the mafic layers from the Ronda massif. These authors identified three main mineral assemblages in these rocks: 1) garnet pyroxenites (Cpx + Grt ± Opx ± Pl ± Qtz ± Spl), 2) spinel pyroxenites (Cpx + Opx + Spl ± Pl), and 3) olivine gabbros (Cpx + Ol + Pl + Opx + Spl). As previously reported by Dickey (1970) and Obata (1980), Suen and Frey (1987) also observed that mafic layers are typically parallel or sub-parallel to the peridotite foliation except for rare isoclinal folds. However, contrary to Dickey (1970), these authors concluded that mafic rocks in Ronda are not the products of crystallization of primary melts of peridotites, but are cumulates precipitated at > 1.9 GPa and different temperatures. In particular, Suen and Frey (1987) proposed that temperature was higher in the eastern portion of the massif, where olivine gabbros are dominant, than in the northwestern area where mafic layers are mostly garnet pyroxenites.

More than ten years later, Garrido and Bodinier (1999) published a new detailed field, petrological and geochemical investigation on the mafic layers of the Ronda massif. In this study, the mafic rocks were classified into four groups based on their current mineral assemblage, structure at the outcrop scale, texture, mineral composition, and the peridotite domain in which they crop out.

A) ***Garnet mafic granulites*** *(A1: Cpx + Grt + Pl ± Rut ± Qtz ± Amp ± Gph)* ***and garnet pyroxenites*** *(A2: Cpx + Grt ± Opx ± Rut ± Amp ± Pl ± Phl)*

crop out exclusively in the spinel tectonite domain. Most often the group A mafic rocks constitute layers up to 5 m thick oriented parallel to the tectonite foliation and are in places isoclinally folded and/or boudinaged. Rarely, near the recrystallization front, they constitute part of "*composite layers*" with rocks of groups B and D (see below). Their mineral composition and texture are of metamorphic origin and they show evidence of substantial plastic deformation.

B) *Spinel websterites and rare spinel-garnet websterites (Opx + Cpx + Sp ± Grt ± Pl ± Ol)* crop out mainly along the recrystallization front and sporadically in the coarse-granular peridotite domain. These layers, although generally hosted in non-foliated peridotites, are parallel to the foliation and layering in the spinel tectonite domain. Rarely, they form *composite layers* with groups A and D. These rocks are strongly deformed in the field and in places isoclinally folded and boudinaged. On the contrary, their microstructures are undeformed and characterized by large (up to 3 cm) Cpx and coarse clusters of Cpx + Opx + Sp + Pl after garnet. This indicates that group B formed at the expense of former group A by a process involving grain growth, annealing and chemical changes probably during the magmatic event related to the development of the recrystallization front.

C) *Spinel websterites (Opx + Cpx + Sp ± Pl ± Ol ± Amp ± Ilm)* **and olivine-spinel websterites** *(Opx + Ol ± Cpx ± Sp ± Pl ± Amp ± Ilm)* were classified as olivine gabbros in previous studies (Obata, 1980; Suen and Frey, 1987). As plagioclase is of metamorphic origin, Garrido and Bodinier (1999) classified these rocks as spinel websterites. They mostly crop out in the layered-granular peridotite domain and plagioclase tectonite domain as swarms of straight layers or elongated lenses hosted by harzburgites and dunites. They are undeformed in the field except for some rare open folds. Variations in the olivine/pyroxene ratio at different scales allow defining a poor to well-developed modal banding. These rocks have transitional contacts with enclosing peridotites and show evidence of secondary growth of clinopyroxene after olivine. These features support that group C pyroxenites formed by replacement of peridotites via pyroxene-forming melt-rock reactions.

D) *Clinopyroxenites, websterites and olivine websterites (D1: Cpx + Opx ± Ol), spinel websterites (D2: Opx + Cpx + Sp ± Ol ± Pl) and scarce orthopyroxenites (D3: Opx + Cpx ± Ol)*. They mostly crop out in the plagioclase tectonite, fine- and layered-granular peridotite domains as deformed layers oriented parallel to the foliation in the spinel tectonite domain. Contrary to their field occurrence, their microstructures are mostly undeformed and coarse-grained. Along the recrystallization front, they form *composite layers* together with rocks of groups A and B. Asymmetrical mineralogical and compositional zoning of garnet-bearing rocks (type A) or their breakdown products (type B) on one side, and group D rock on the other side, defines these layers. The transition from group A to group D in the *composite layers* is sharp and irregular and is marked by the disappearance of garnet and plagioclase, a substantial increase in pyroxene grain size and the development of undeformed microstructure (from few millimeters up to 4 cm). In some *composite layers*, 1-20 cm "xenoliths"

of deformed garnet-bearing rocks are embedded in the undeformed coarse-grained type D websterites. This indicates that group D rocks in the *composite layers* locally replaced group A rocks after the deformation event recorded in spinel tectonites. Rarely, group D pyroxenites occur also in the spinel tectonite domain as intrusive websterite dykes (D1) up to 10 cm thick crosscutting the tectonite foliation (Marchesi et al., 2012).

Garrido and Bodinier (1999) interpreted the diversity of mafic rocks in the Ronda massif in terms of a multi-stage evolution related to successive melt-rock reactions. In this model, **Group A** rocks are old mafic layers originally isolated in the lithospheric mantle. **Group B** derived by magmatic replacement of group A in an open system probably during the thermal climax of the magmatic event that originated the recrystallization front and the coarse-granular peridotite domain. Group B was formed by partial melting of group A and/or melt-producing reactions between group A and tholeiitic partial melts of the host peridotite that circulated pervasively by porous flow through the granular peridotite domain. **Group C** formed after the development of the recrystallization front by metasomatic replacement of peridotites related to melt-consuming reactions at temperatures close to the peridotite solidus. During this stage, interstitial melt became saturated in pyroxene and dissolved olivine from the host peridotite producing clinopyroxene, orthopyroxene and spinel; this process led to the formation of secondary lherzolites or websterites depending on the local melt/rock ratio (pervasive or channeled porous flow). The decreasing Mg# of olivine with increasing refertilization (i.e., modal abundance of pyroxene) indicates that the percolating melt underwent substantial fractional crystallization and olivine dissolution was limited (Bodinier et al., 2008). **Group D** was generated in a similar stage of group C but is probably somewhat later; its relatively young nature is also confirmed by its occurrence as discordant dyke in the spinel tectonite domain (Marchesi et al., 2012). These rocks were formed by replacement of older groups A, B and C when volatile-rich small melt fractions with calcalkaline-boninitic affinity percolated though the massif in the waning stages of the melt porous flow. These melts had low viscosity and crystallization temperature and were so able to percolate beyond the permeability barrier for basaltic melts represented by the recrystallization front, and crystallize in the relatively cold lithosphere represented by the spinel tectonite domain.

4.3. Geochemistry of the ultramafic and mafic rocks

4.3.1 *Distribution of lithophile elements*

The Ronda massif was the subject of pioneering studies on the isotopic composition and heterogeneity of mantle rocks. Reisberg and Zindler (1986) and Reisberg et al. (1989) documented that the Ronda massif shows nearly the entire range of Nd and Sr isotopic ratios observed in oceanic mantle-derived rocks. This heterogeneity was detected at different scales, from ~ 1 meter to tens of kilometers. Reisberg and Zindler (1986) interpreted these variations in terms of a two-stage process: 1) an episode of depletion in incompatible elements related to partial melting, followed by 2) a relatively recent (< 200

Ma) light rare earth element (LREE)-enrichment due to interaction of melting residues with exotic fluid. This interaction was spatially localized and is particularly evident in the northeastern portion of the massif.

Based on the work of Van der Wal and Vissers (1993, 1996) and Van der Wal and Bodinier (1996), Lenoir et al (2001) defined three textural groups of peridotites in Ronda: 1) deformed porphyroclastic peridotites, representing the predominant textural type in the spinel tectonite domain, 2) transitional peridotites, which mark the recrystallization front and are located in a narrow band (few hundred meters thick) between the spinel tectonite and the granular peridotite domains, and 3) coarse-granular peridotites distinguished by very coarse and annealed microstructures that exclusively crop out in the granular domain. Porphyroclastic tectonites are extremely variable in terms of fertility as indicated by the variation in CaO/MgO (0.02-0.08) and span from refractory harzburgites to very fertile lherzolite; on the other hand the transitional peridotites are dominated by mildly fertile lherzolites (CaO/MgO = 0.06-0.08) and the granular peridotites by refractory harzburgites (CaO/MgO = 0.02-0.04). In terms of REE contents (Fig. 4.3), porphyroclastic tectonites and transitional peridotites show similar patterns that are generally LREE-depleted for lherzolites and less LREE-depleted or LREE-enriched for harzburgites; on average, transitional peridotites have slightly higher MREE-HREE contents and lower LREE/MREE than porphyroclastic tectonites. The granular peridotites have lower REE abundances than lherzolites from the two other textural facies.

Lenoir et al. (2001) interpreted the lower fertility of the granular peridotites as evidence of a partial melting event at low degrees (< 5%) contemporaneous to the occurrence of melt-consuming melt-rock reactions
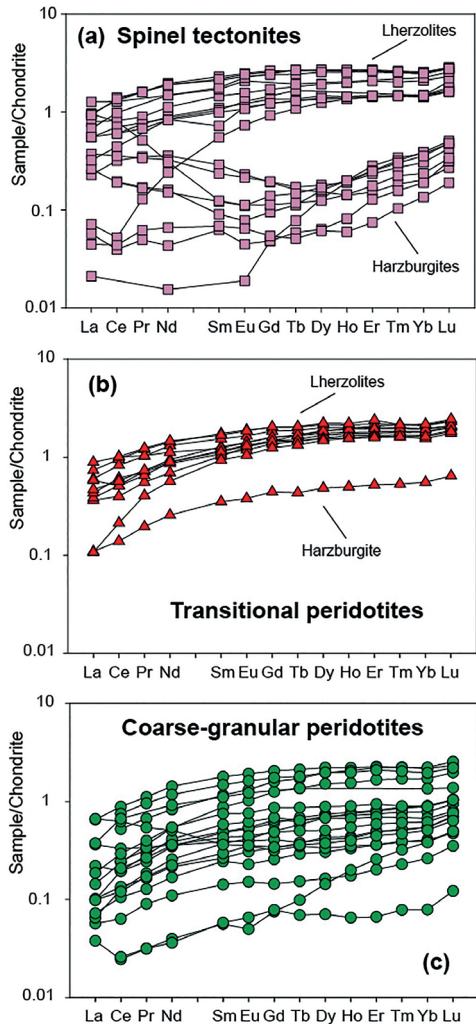
Figure 4.3. Chondrite-normalized rare earth element patterns of spinel tectonites (a), transitional peridotites from the recrystallization front (b), and coarse-granular peridotites (c) from the Ronda peridotite massif. Normalizing values from Sun and McDonough (1989). Data from Van der Wal and Bodinier (1996) and Lenoir et al. (2001).

at the recrystallization front. These reactions led to precipitation of secondary clinopyroxene and increased the average fertility of the transitional peridotites compared to the other facies. These authors concluded that the recrystallization front was an isotherm close to the anhydrous peridotite solidus ($\sim$ 1250 ºC – 1.5 GPa) and formed during the lithospheric erosion by upwelling convective asthenosphere documented in the Late Oligocene-Early Miocene evolution of the Alboran basin.

Similar to peridotites, also mafic rocks from the Ronda massif have different compositions in terms of lithophile elements (Garrido and Bodinier 1999). **Group A garnet pyroxenites** have variable Mg# [100 x MgO / (MgO + FeO$_T$)] (55-80) that is negatively correlated with Ti# [200 x TiO$_2$ / (TiO$_2$ + Al$_2$O$_3$)]. Their clinopyroxene has intermediate TiO$_2$, low Cr$_2$O$_3$ and the highest Al$_2$O$_3$ and Na$_2$O contents among the Ronda mafic rocks. In terms of trace elements (Fig. 4.4), **Group A** has strongly fractionated REE patterns with high contents of HREE and depleted LREE compositions. Some of these rocks have also positive anomalies of Ba, Sr and Eu supporting they were originally low pressure (< 1 GPa) crustal cumulates of plagioclase, clinopyroxene and olivine (Morishita et al., 2003). Locally, partial melting of these layers refertilized enclosing lherzolites and transferred their crustal-derived signature to peridotites (Marchesi et al., 2013). **Group B spinel websterites** have higher Mg# (77-90) and Cr# [100 x Cr$_2$O$_3$ / (Cr$_2$O$_3$ + Al$_2$O$_3$)] than group A, and their clinopyroxene is Al$_2$O$_3$-MgO-Cr$_2$O$_3$ rich but rather poor in Na$_2$O. Group B
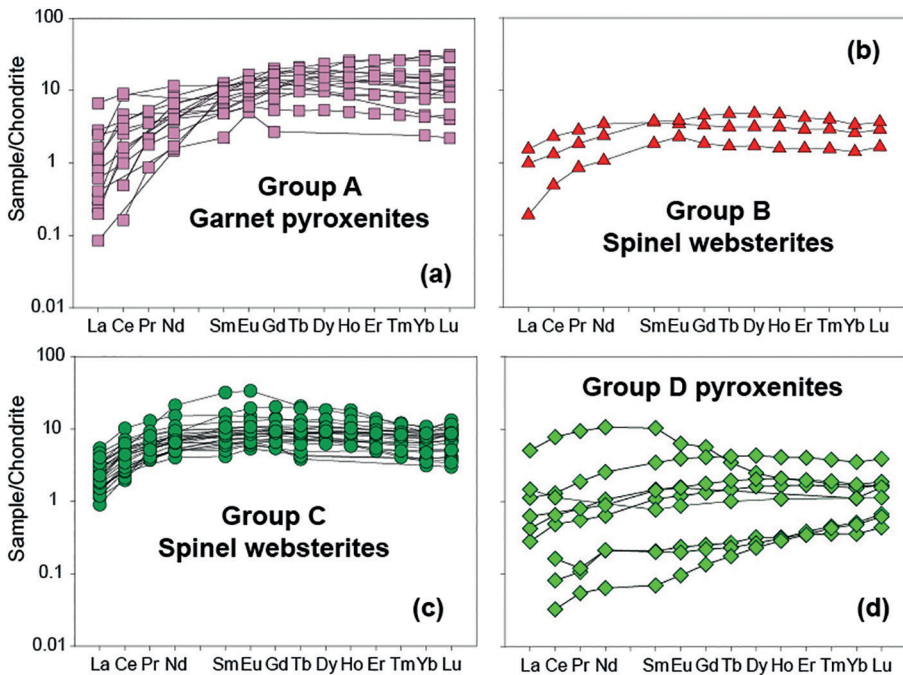
Figure 4.4. Chondrite-normalized rare earth element patterns of Group A garnet pyroxenites (a), Group B spinel websterites (b), Group C spinel websterites (c), and Group D pyroxenites (d) from the Ronda peridotite massif. Normalizing values from Sun and McDonough (1989). Data from Garrido and Bodinier (1999), Morishita et al. (2003) and Bodinier et al. (2008).

rocks have REE patterns similar to group A, but they are less fractionated and with a slight positive Eu anomaly. **Group C spinel websterites** have high Mg# (77-87) and high Ti# at a given Mg#, with clinopyroxene rich in MgO and especially in TiO_2. Group C is typically characterized by convex upward patterns depleted in LREE and HREE relative to MREE; despite the abundance of plagioclase their REE patterns do not show positive anomaly in Eu which confirms the sub-solidus origin of this phase. **Group D pyroxenites** have high Mg# (85-94) and especially high Cr# (3-25). Their clinopyroxene is very low in Al_2O_3 ant TiO_2 and very high in MgO and Cr_2O_3. Pyroxenites of Group D yield REE patterns with low contents of HREE as well as variable LREE/HREE and LREE/MREE ratios similar to boninitic-like melts. This subduction-related signature is particularly evident in clinopyroxene of rare dykes that crosscut spinel tectonites (Marchesi et al., 2012).

4.3.2 *Distribution of noble metals in peridotites and mafic rocks*

Similar to other upper mantle rocks worldwide, the ultramafic and mafic rocks of the Serranía de Ronda contain appreciable amounts of noble metals, including platinum-group elements (namely PGE: Os, Ir, Ru, Rh, Pt and Pd), Re and Au. Different authors (Gueddari et al. 1996; Gutiérrez-Narbona, 1999; Lorand et al., 2000; Becker et al., 2006; Marchesi et al., 2014) have studied the imprint on noble metals of the lithospheric erosion (i.e., asthenospherization). These studies analyzed whole-rock samples of peridotites and pyroxenites from all the different domains and subdomains of the Ronda ultramafic massif. Irrespective of their location, lherzolites show a more restricted window of variation of the bulk-rock PGE contents (13.5-57.8 ppb; n = 25) than harzburgites (7.5-39.3; n = 10), dunites (8.9-65.8; n = 6) and pyroxenites (1.5-55.4; n = 14). The PGE concentrations in lherzolites are close to or slightly below the PUM values, as typical of refertilized lherzolites or lherzolites slightly depleted by low-degrees of partial melting (Fig. 4.5). This homogeneity contrasts with the variable distribution of PGE in refractory harzburgites and dunites, which show both depletion and enrichment in Pt and Pd. Harzburgites from the coarse-granular domain are depleted in Pt and Pd due to dissolution of sulfides by interaction with asthenospheric melts undersaturated in sulfur. In contrast, harzburgites from the fine and layered granular subdomains, which contain secondary clinopyroxene, show enrichment in Pt and Pd at values above the PUM (Fig. 4.5). This enrichment evidences the effective transport of the most incompatible noble metals by melts pooled below the recrystallization front. Interestingly, this enrichment in Pt and Pd is accompanied by gold and LREE endowment, which was interpreted by Gutiérrez-Narbona (1999) as due to percolation of volatile-rich small volume melts (< 0.1% volume) through, and out from, the recrystallization front. These processes are also preserved in dunites. Clinopyroxene-free dunites from the layered-granular subdomain are poor in noble metals, expect Ru, relative to PUM (Fig. 4.5) due to sulfide dissolution and precipitation of laurite (RuS_2) by melt-rock reaction (Gutiérrez-Narbona, 1999). In contrast, dunites containing secondary clinopyroxene have Rh, Pt, and Pd contents above the PUM values, pointing to metal enrichment via clinopyroxene-forming reaction. Interestingly, all dunites are depleted in gold relative to PUM (Fig. 4.5).
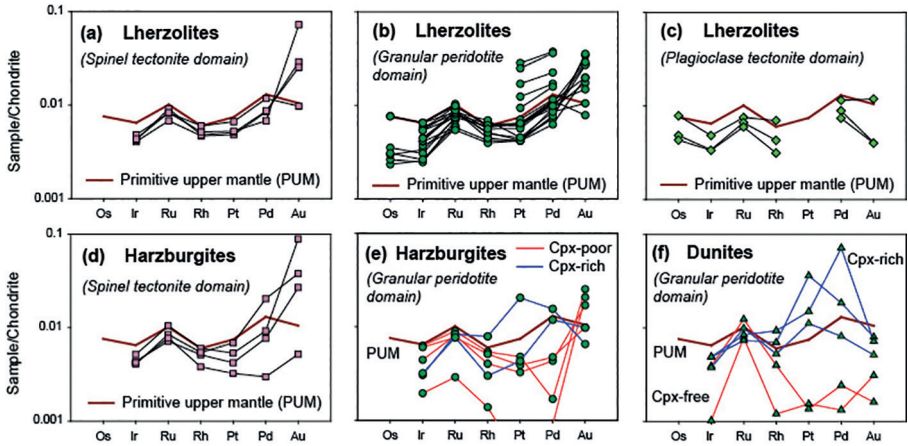
Figure 4.5. Chondrite-normalized patterns of noble metals in peridotites from the spinel tectonite domain (a: lherzolites, d: harzburgites), granular peridotite domain (b: lherzolites, e: harzburgites, f: dunites), and plagioclase tectonite domain (c: lherzolites) from the Ronda peridotite massif. Normalizing values from Naldrett and Duke (1980). Primitive upper mantle (PUM) values (dark red line) from Becker et al. (2006) and Fisher-Gödde et al. (2011). Data from Gutiérrez-Narbona (1999), Lorand et al. (2000), Becker et al. (2006) and Marchesi et al. (2014).
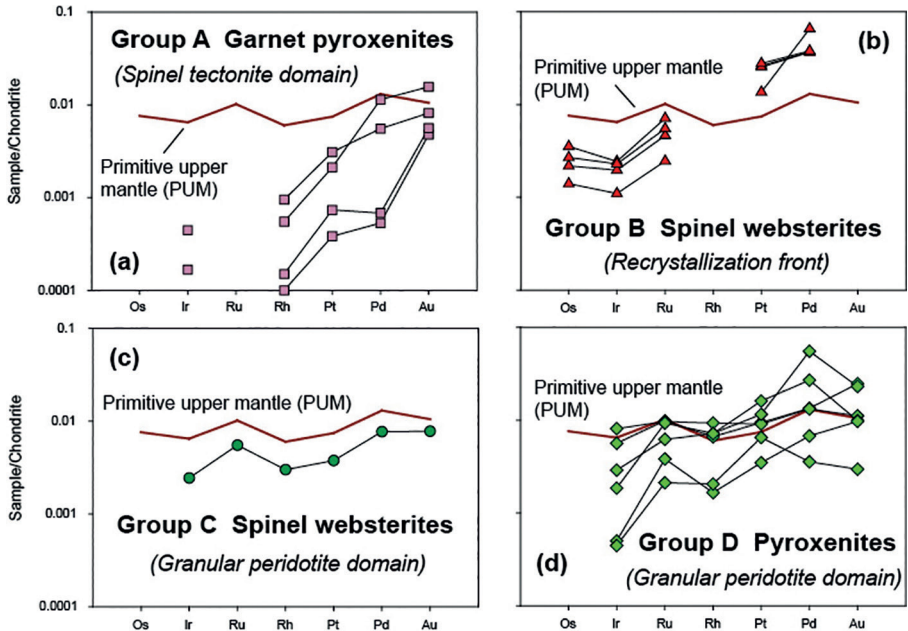
Figure 4.6. Chondrite-normalized patterns of noble metals in Group A garnet pyroxenites (a), Group B spinel websterites (b), Group C spinel websterites (c), and Group D pyroxenites (d) from the Ronda peridotite massif. Normalizing values from Naldrett and Duke (1980). Primitive upper mantle (PUM) values (dark red line) from Becker et al. (2006) and Fisher-Gödde et al. (2011). Data from Gutiérrez-Narbona (1999) and Marchesi et al. (2014).

These variations in noble metals, which are products of the superposition in time and space of the different magmatic processes associated with lithospheric erosion, are also observed in the mafic layers. Type-A garnet pyroxenites from the spinel (± garnet) tectonite domain are significantly depleted in noble metals (PGE+Au < 11.1 ppb) relative to Type-C (15.02 ppb), Type-D (11.2-54.5 ppb) and Type-B pyroxenites (51.2 to 55.4 ppb) (Fig. 4.6). In general, pyroxenites show depletion of the Ir-subgroup PGE (IPGE: Os, Ir and Ru) relative to Pt-subgroup PGE (PPGE: Rh, Pt, Pd) and Au (Fig. 4.6). The values of PPGE in pyroxenites are close to or above PUM and increased by precipitation of metasomatic platinum-group minerals (PGM) rich in Pt and Pd and semimetals (As or Te) (Fig. 4.6; Gutiérrez-Narbona, 1999).

References

Becker, H., Horan, M.F., Walker, R.J., Gao, S., Lorand, J.-P. and Rudnick, R.L. (2006). Highly siderophile element composition of the Earth's primitive upper mantle: Constraints from new data on peridotite massifs and xenoliths. *Geochimica et Cosmochimica Acta* 70, 4528-4550.

Bodinier, J.L., Garrido, C.J., Chanefo, I., Bruguier, O. and Gervilla, F., 2008. Origin of pyroxenite–peridotite veined mantle by refertilization reactions: evidence from the Ronda peridotite (Southern Spain). *Journal of Petrology* 49, 999–1025.

Darot, M. (1973). Cinèmatique de l'extrusion, à partir du manteau, des péridotites de la –sierra Bermeja (Serranía de Ronda, Espagne). *Comptes Rendus de l'Académie des Sciences de Paris* 278, 1673-1676.

Davies, G.R., Nixon, P.H., Pearson, D.G. and Obata, M. (1993). Tectonic implications of graphitized diamonds from the Ronda, peridotite massif, southern Spain. *Geology* 21, 471–474.

Dickey, J.S.Jr. (1970). Partial fusion products in Alpine-type peridotites: Serranía de Ronda and other examples. *Mieralogical Society of America Special paper* 3, 33-49.

Fischer-Gödde, M., Becker, H. and Wombacher, F. (2011). Rhodium, gold and other highly siderophile elements in orogenic peridotites and peridotite xenoliths. *Chemical Geology* 280, 365-383.

Garrido, C.J. and Bodinier, J.L. (1999). Diversity of mafic rocks in the Ronda peridotite: evidence for pervasive melt/rock reaction during heating of subcontinental lithosphere by upwelling asthenosphere. *Journal of Petrology* 40, 729-754.

Garrido, C.J., Gueydan, F., Booth-Rea, G., Precigout, J., Hidas, K., Padron-Navarta, J.A. and Marchesi, C. (2011). Garnet lherzolite and garnet-spinel mylonite in the Ronda peridotite: vestiges of Oligocene backarc mantle lithospheric extension in the western Mediterranean. *Geology* 39, 927–930.

Gervilla, F. (1990). Mineralizaciones magmáticas ligadas a la evolución de las rocas ultramáficas de la Serranía de Ronda (Málaga, España). Ph. D. Thesis, University of Granada.

Gervilla, F., Gutiérrez-Narbona, R. y Fenoll Hach-Alí, P. (2002). The origin of different types of magmatic mineralizations from small-volume melts in the lherzolite massifs from the Serranía de Ronda (Málaga, Spain). *Boletín de la Sociedad Española de Mineralogía* 25, 79-96.

Gueddari, K., Piboule, M. and Amossé, J. (1996). Differentiation of platinum-group elements (PGE) and of gold during partial melting of peridotites in the lherzolitic massifs of the Betico-Rifean range (Ronda and Beni Bousera). *Chemical Geology* 134, 181-197.

Gutiérrez-Narbona, R. (1999). Implicaciones metalogénicas (cromo y elementos del grupo del platino) de los magmas/fluidos residuales de un proceso de percolación a gran escala en los macizos ultramáficos de Ronda y Ojén (Béticas, Sur de España). Ph. D. Thesis, University of Granada.

Hidas, K., Booth-Rea, G., Garrido, C.J., Martínez-Martínez, J.M., Padrón-Navarta, J.A., Konc, Z., Giaconia, F., Frets, E. and Marchesi, C. (2013). Backarc basin inversion and subcontinental mantle emplacement in the crust: kilometre-scale folding and shearing at the base of the proto-Alborán lithospheric mantle (Betic Cordillera,southern Spain). *Journal of the Geological Society* 170, 47–55.

Lenoir, X., Garrido, C.J., Bodinier, J.-L., Dautria, J.-M. y Gervilla, F. (2001). The recrystallization front of the Ronda peridotite: Evidence for melting and thermal erosion of subcontinental lithospheric mantle beneath the Alborán basin. *Journal of Petrology,* 42 (1), 141-158.

Lorand, J.-P., Schmidt, G., Palme, H. and Kratz, K.-L. (2000). Highly siderophile element geochemistry of the Earth's mantle: new data for the Lanzo (Italy) and Ronda (Spain) orogenic peridotite bodies. *Lithos* 53, 149-164.

Marchesi, C., Dale, C.W., Garrido, C.J., Pearson, D.G., Bosch, D., Bodinier, J.-L., Gervilla, F. and Hidas, K. (2014). Fractionation of highly siderophile elements in refertilized mantle: implications for the Os isotope composition of basalts. *Earth ad Planetary Science Letters* 400, 33–44.

Marchesi, C., Garrido, C.J., Bosch, D., Bodinier, J.-L., Gervilla, F. and Hidas, K. (2013). Mantle refertilization by melts of crustal-derived garnet pyroxenite: evidence from the Ronda peridotite massif, southern Spain. *Earth and Planetary Science Letters* 362, 66–75.

Marchesi, C., Garrido, C.J., Bosch, D., Bodinier, J.-L., Hidas, K., Padrón-Navarta, J.A. and Gervilla, F. (2012). A late oligocene suprasubduction setting in the westernmost mediterranean revealed by intrusive pyroxenite dikes in the ronda peridotite (Southern Spain). *Journal of Geology* 120, 237–247.

Morishita, T., Arai, S., Gervilla, F. and Green, D.H. (2003). Closed-system recycling of crustal materials in the alpine- type peridotite. *Geochimica et Cosmochimica Acta* 67, 303–310.

Naldrett, A.J. and Duke, J.M. (1980). Pt metals in magmatic sulfide ores: the occurrence of these metals is discussed in relation to the formation and importance of these ores. *Science* 208, 1417-1424.

Precigout, J., Gueydan, F., Gapais, D., Garrido, C. J. and Essaifi, A. (2007). Strain localisation in the subcontinental mantle-a ductile alternative to the brittle mantle. *Tectonophysics* 445, 318-336.

Obata, M. (1977). Petrology and petrogenesis of the Ronda high-temperature peridotite intrusion, Southern Spain. Ph.D. Thesis, Massachusetts Institute of Technology.

Obata, M. (1980). The Ronda peridotite: Garnet-, spinel-, and plagioclase-lherzolite facies and the P-T trajectories of a high-temperature mantle intrusión. *Journal of Petrology* 21, 533-572.

Reisberg, L. and Lorand, J.-P. (1995). Longevity of sub-continental mantle lithosphere from osmium isotope systematics in orogenic peridotite massifs. *Nature* 376, 159–162.

Reisberg, L. and Zindler, A. (1986-1987). Extreme isotopic variations in the upper mantle: evidence from Ronda. *Earth and Planetary Science Letters* 81, 29-45.

Reisberg, L. C., Zindler, A. and Jagoutz, E. (1989). Futher Sr and Nd isotopic results from peridotites of the Ronda Ultramafic Complex. *Earth and Planetary Science Letters* 96, 161-180.

Schubert, W. (1977). Reacktionen in alpinotypen Peridotit masiv von Ronda (Spanien)-und seinen partiellen. Schmelzprodukten. *Contributions to Mineralogy and Petrology* 62, 205-220.

Soto, J.I. and Gervilla, F. (1991). Los macizos ultramáficos de la Sierra de las Aguas y Sierra de la Robla como una ventana extensional (Béticas occidentales). *Geogaceta* 9, 21-23.

Suen, C.J. and Frey, F.A. (1987). Origin of the mafic and ultramafic rocks in the Ronda peridotite. *Earth and Planetary Science Letters* 85, 183-202.

Sun, S.-S. and McDonough, W.F. (1989). Chemical and isotopic systematics of oceanic basalts: implications for mantle composition and processes. In: Saunders, A.D., Norry, M.J. (Eds.), Magmatism in the Ocean Basins. *Geological Society of London Special Publications* 42, 313-345.

Targuisti, K. (1994). Petrología y geoquímica de los Macizos Ultramáficos de Ojén (Andalucía) y Beni Bousera (Rif Septentrional, Marruecos). Tesis Doctoral, Universidad de Granada.

Van der Wal, D. and Bodinier, J.L. (1996). Origin of the recrystallization front in the Ronda peridotite by km-scale pervasive porous flow. *Contributions to Mineralogy and Petrology* 122, 387-405

Van der Val, D. and Vissers, R.L.M. (1993). Uplift and emplacement of upper mantle rocks in the western Mediterranean. *Geology* 21, 1119-1122,

Van der Val, D. and Vissers, R.L.M. (1996). Structural petrology of the Ronda peridotite SW Spain: deformation history. *Journal of Petrology* 37, 23-43.

Vauchez, A. and Garrido, C. J. (2001). Seismic properties of an asthenospherized lithospheric mantle: constraints from lattice preferred orientations in peridotite from the Ronda massif. *Earth and Planetary Science Letters* 192, 235-249.

Chapter 5
Age and evolution of the ultramafic massifs

5.1 Late Oligocene/ Early Miocene crustal emplacement of old Proterozoic subcontinental lithospheric mantle

Reisberg et al. (1991) carried out a pioneer geochronological study on the ultramafic rocks of the Serranía de Ronda performing Re-Os dating of whole-rock samples of peridotites from the three facies identified by Obata (1980). These results yielded an errorchron[1] age of 1.17 ± 0.12 Ga (initial $^{187}Os/^{186}Os = 0.996 \pm 0.005$ and MSWD $=2.13$). Further confirmation of a tectonothermal event within the interval of ~1.2 to 1.3 Ga in the Ronda massif came from Sm-Nd errorchron on clinopyroxene recovered from river sediments throughout the massif (Reisberg et al., 1989), and whole-rock Os model ages of peridotites and garnet pyroxenites (Reisberg et al., 1991; Reisberg and Lorand, 1995). In the near Beni Bousera ultramafic massif (northern Morocco), Re-Os model ages of garnet pyroxenite layers converge to 1.2-1.3 Ga and the Sm-Nd model age of a strongly depleted peridotite is ~1.3 Ga. More recently, Marchesi et al. (2010) analyzed the Re-Os isotopic compositions of individual sulfides from the different structural domains of Ronda, which also yield Os model ages (Re-depletion or T_{RD} ages) clustering at 1.2-1.4 Ga, in addition to other age peaks at 1.6-1.8 and 0.7-0.8 Ga (Fig. 5.1). Similarly, individual sulfides hosted in peridotites from all the different domains of the Ojén massif yield ages around 1.2 Ga, with younger peaks at 0.2 and 0.6 Ga (Fig. 5.1; González-Jiménez et al., 2013). The well-documented age of 1.2-1.4 Ga is interpreted as the time when the ultramafic massifs left the convecting mantle and were incorporated into the sub-continental lithosphere.

Interestingly, the age peak at ~1.6-1.8 Ga identified by Marchesi et al. (2010) in individual sulfides from the Ronda peridotites is consistent with the U-Pb age of 1783 ± 37 Ma determined for an inherited zircon core in a garnet pyroxenite from the spinel tectonite domain (Sánchez-Rodríguez and Gebauer, 2000). Other

---

[1] errorchron (or pseudoisochron) is a term used for a set of data points which are not colinear, that is, unlike in a true isochron isotope ratios do not fall on a line representing a single age. It can be recognized as a valid dating method only if the points for which the line was calculated have greater scatter than indicated by the standard deviation.
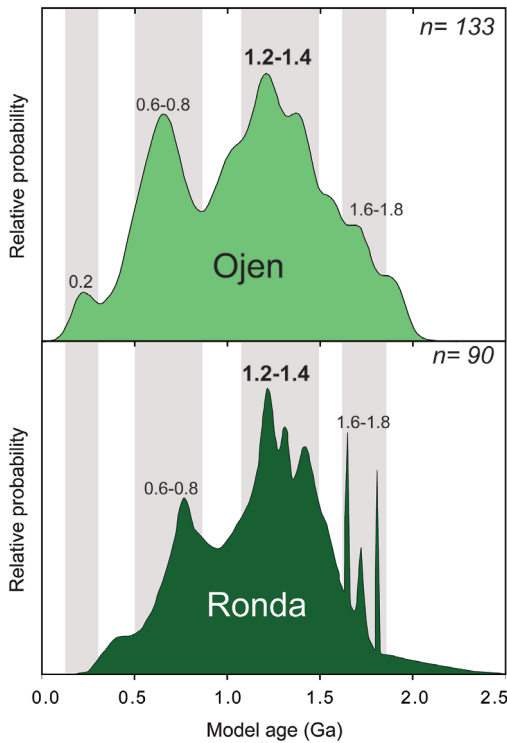
Figure 5.1. Cumulative probability plots of Re-depletion ages (T_{RD}) for mantle sulfides in the Ojén (top) and Ronda (bottom) massifs. See text for references and further details.

zircons separated from HT/ultra-HP garnet pyroxenites yield much younger ages of 178 ± 6 Ma, 143 ± 16 Ma and 131 ± 3 Ma. Peripheral domains of some of these zircons yield even younger ages clustering at 22.8 ± 1.8 Ma (Sánchez-Rodríguez and Gebauer, 2000). This dating confirmed a similar age of 21.5 ± 1.8 Ma reported by Zindler et al. (1983) for a Sm-Nd isochron using whole-rock and mineral separates of clinopyroxene and plagioclase of garnet pyroxenites from Ronda. These Late Oligocene–Early Miocene ages are within the error of the 22 ± 4 Ma age determined by a Rb-Sr isochron (Priem et al., 1979) and 18.8 ± 4.9 Ma U-Pb ages (Sánchez-Rodríguez and Gebauer, 2000) obtained for cordierite-bearing, late alkali granites intruding the Ronda peridotite. The latter age defines the time of the anatexis associated with the emplacement of the ultramafic massif into the crust. More recently, a series of studies (Esteban et al., 2004, 2007, 2010) on large populations of zircons and apatites (including U-Pb ages and fission-track analysis) have provided a precise age estimation of the time of hot emplacement (22.36 ± 0.62 to 21.8 ± 0.5 Ma) and cooling (19.2 ± 1.1 Ma) of the anatectic acid dykes.

5.2   Structure of the tectonometamorphic domains

Most structural studies have been focused on the largest Ronda massif, where the oldest deformational structures were preserved in preserved in the garnet-spinel mylonite and the underlying spinel-tectonite domain (Van der Wal and Vissers 1996; Precigout et al. 2007; Soustelle et al. 2009). These include compositional layering (S_0) of the garnet pyroxenites, and high-temperature ductile peridotite foliation (S_1) with a NE-SW trending stretching lineation (L_1) defined by elongated orthopyroxene in garnet-spinel mylonite and spinel aggregates in spinel-tectonite (Darot 1973; Balanyá et al. 1997; Precigout et al. 2007; Soustelle et al. 2009). The S_1 foliation is subparallel to the S_0 compositional layering and dips generally

70-80° to the WNW (Van der Wal and Vissers 1996; Soustelle et al. 2009). In the most intensely foliated spinel tectonites, the S_0 compositional layering exhibits boudins and meter-scale isoclinal folds with axial planes parallel to the S_1 foliation (Gervilla, 1990; Van der Wal and Vissers 1996; Garrido and Bodinier 1999). The S_1 spinel-tectonite foliation progressively disappears at the recrystallization front due to the partial melting and subsequent crystal annealing that promoted the formation of undeformed granular spinel peridotite at expenses of the spinel tectonite peridotites (Van der Wal and Bodinier 1996; Van der Wal and Vissers 1996; Lenoir et al. 2001). The S_0 compositional layering is represented by spinel pyroxenite in the granular spinel peridotite domain (Seiland facies of Obata 1980) and by plagioclase-spinel pyroxenite in the plagioclase-tectonite domain (Garrido and Bodinier 1999; Bodinier et al. 2008).

The lower part of the granular spinel peridotite domain and the plagioclase-tectonite domain are characterized by two newly developed structures, in addition to S_0. These structures are not observed elsewhere in the higher levels of the lithospheric mantle column and they are: (i) a higher-temperature peridotite foliation S_2 (hereafter referred as high-temperature structure), and (ii) a lower-temperature and/or higher stress (hereafter referred as low-temperature structure) mylonitic to ultramylonitic foliation (S_m) developed in shear zones that cut the high-temperature structures (Hidas et al., 2013a). At the transition of granular spinel peridotite to plagioclase-tectonite domains, the S_0 compositional layering rotates gradually clockwise, at the base of the massif having a dip of 40-60º to the ENE. The first occurrence of the new high-temperature S_2 foliation is found close to the recrystallization front, where plagioclase-free spinel lherzolite shows foliation dipping 60-80° to the N that crosscuts the spinel pyroxenite S_0. Further to the SSE in the plagioclase-tectonite domain, the S_2 foliation becomes increasingly penetrative in porphyroclastic lherzolite that shows plagioclase rims around spinel and it is weaker in more refractory peridotite that lacks plagioclase. In both cases the S_2 foliation crosscuts S_0 compositional layering and former isoclinal folds, and shows a quite uniform dip of 50-70° to the NNE with stretching lineation (L_2) trending NE-SW in the foliation plane (Hidas et al., 2013a). The rotation of the S_0 compositional layering and its crosscutting relationship with high-temperature S_2 foliation is consistent with a km-scale fold structure (Fig. 5.2.). This single fold has only two major limbs and a high-temperature axial plane foliation (S_2), which is well developed in the reverse limb. The fold axial surface dips 50° to the N (average orientation of the S_2 foliation) and the fold axis plunges approximately 45° to the NE (intersection between the layering in both limbs and between the S_2 foliation and the layering). Because the Ronda peridotite is a coherent lithospheric mantle section (Obata 1980; Van der Wal and Vissers 1996) that is also continuous with its overlying crustal envelope (Tubía 1994; Balanyá et al. 1997; Argles et al. 1999; Platt et al. 2003), the polarity in the northern side of the massif is upwards. It follows that the km-scale fold at the base of the mantle section is a non-cylindrical, moderately plunging, moderately inclined, downward facing synform (i.e., anticline).

The youngest low-temperature structure is marked by the development of mylonitic-ultramylonitic microstructures in ductile shear zones that first occur as
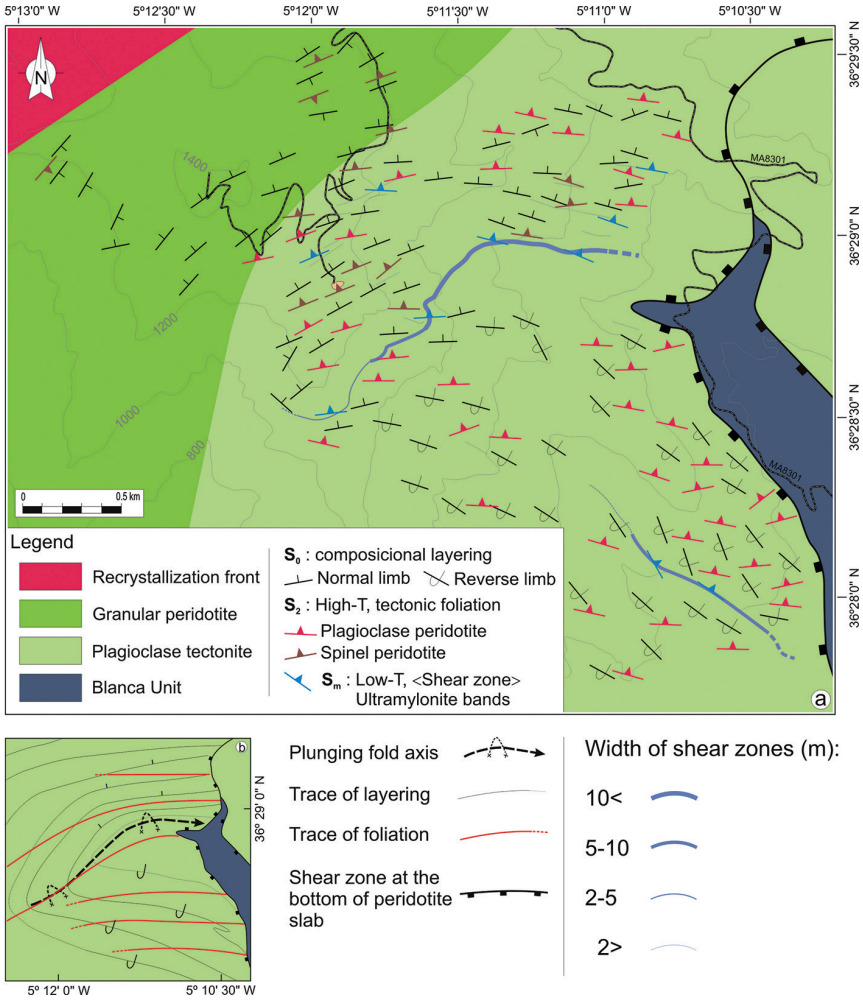
Figure 5.2. (a) Structural map of the transition from the granular peridotite to the plagioclase tectonite domains of the Ronda ultramafic massif. (b) Interpretative map of the large scale folding of the S_0 compositional layering with the S_2 axial plane foliation, which developed during the emplacement of the massif in the crust. Simplified from Hidas et al. (2013a).

thin (<10 cm) and discontinuous bands at the base of the granular spinel peridotite domain and as much wider shear zones (up to 50 m width) in the plagioclase-tectonite domain (Fig. 4.2 and 5.2). The strike of the low-T S_m mylonitic foliation is subparallel to that of the high-T S_2 foliation but it dips more gently, 30-50º to the NNE. Elongated orthopyroxene porphyroclasts and spinel denote a NE-SW trending lineation L_m, subparallel to the high-T L_2 lineation of plagioclase tectonite. Microstructure of the low-temperature mylonites implies top-to-SW sense of shear in accordance with the sigmoidal character of S_2 foliation in the shear zones (Hidas et al., 2013a). It should be noted that fold axis is subparallel to the trace of the

stretching L_2 lineation in the S_2 peridotite foliation plane, which was also observed in other orogenic peridotites (e.g., Nicolas and Boudier 1975; Boudier 1978). In fact, the parallelism between fold axis and mineral lineation is a common feature in rocks deformed by folding associated to shearing (e.g. Bell 1978 and references therein), where the fold is formed initially by flattening but the increase of simple shear component progressively rotates fold axis within its own axial plane until it lays parallel to lineation (cf. sheath fold). In the Ronda massif, high-temperature (S_2-L_2) and low-temperature (S_m-L_m) structures show alike orientation, which indicates that they must record similar kinematics. Therefore, low-temperature shear zones are interpreted to be formed synkinematic to the folding by increasing strain localization upon cooling at the brittle-ductile transition of peridotite (Hidas et al., 2013a,b, 2016).

5.3   Evolution of the ultramafic massifs in the SCLM and intracrustal emplacement

5.3.1   P-T-time path

The identification of undeformed graphite pseudomorphs after diamond in garnet pyroxenites from Ronda suggest that these massifs came from depths >140 km (Davies et al., 1993). Uplift and thinning from a thick, diamond facies lithosphere to a thinner, graphite facies lithosphere most likely occurred during Tethyan extension in the Mesozoic, although this later high-temperature equilibration in the graphite facies transformed diamond to graphite and obliterated any further structural and geochemical record of this event (Davies et al., 1993; Van der Wal and Vissers, 1993) (thick dark arrow in Fig. 5.3).

     The oldest structures preserved at the top of the massif in the garnet-spinel mylonite and spinel-tectonite domains include peridotite protomylonite that occasionally contain, in pressure shadows around and as inclusions in garnet porphyroclasts, a coarse-grained, four-phase garnet lherzolite assemblage consisting of olivine + orthopyroxene + clinopyroxene + garnet (Garrido et al., 2011). Geothermobarometric calculations for this prekinematic assemblage yield minimum equilibrium conditions of 2.4-2.7 GPa and 1020-1100 °C, demonstrating that the Ronda massif equilibrated at ca. 85 km depth (grey field-1 in Fig. 5.3). This prekinematic structure is interpreted to correspond to the oldest vestiges of the Proterozoic lithospheric mantle (Garrido et al., 2011 and references therein), which was formed before subsequent shearing at 800-900 °C and 1.95-2.00 GPa as preserved in synkinematic garnet and spinel assemblages that overprinted the aforementioned garnet lherzolite assemblage (Precigout et al., 2007; Garrido et al., 2011) (grey field-2 in Fig. 5.3). The synkinematic garnet and spinel assemblages preserved in the garnet-spinel mylonite domain formed at the early stages of lithosphere extension during backarc extension in the western Mediterranean, and they have been interpreted either as younger structure formed by high-pressure shearing of an older spinel tectonite domain (Van der Wal and
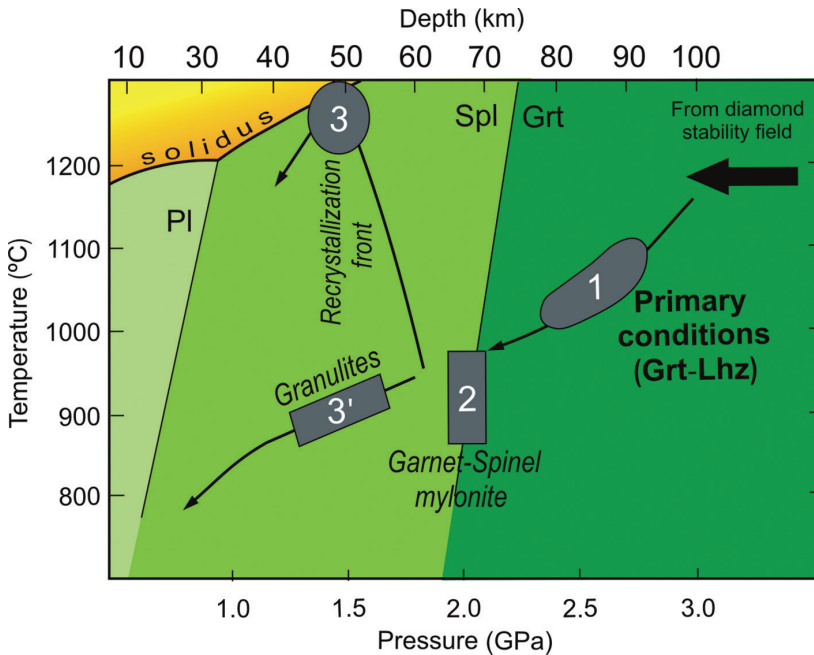
Figure 5.3. Pressure-temperature (P-T) path estimated for the exhumation of the ultramafic massifs of the Serranía de Ronda. The primary P-T conditions in the garnet-lherzolite facies stability field is indicated by the grey-field and is followed by garnet-spinel mylonites (grey-field 2). Upon exhumation, the felsic granulites from the Los Reales unit (grey-field 3') overlying the peridotites followed a continuous decreasing P-T path whereas the peridotites of the inner part of the massif were thermally eroded giving rise to the development of the recrystallization front (grey-field 3) coeval with the formation of the granular peridotites, followed by the development of the plagioclase tectonites during the crustal emplacement of the massifs. Modified from Garrido et al. (2011).

Vissers 1996), or as formed coevally with spinel tectonites by increasing strain localization and cooling at the top of the massif (Precigout et al. 2007; Garrido et al. 2011).

The granular spinel peridotite domain was formed subsequently by annealing of the spinel tectonites during thermal erosion and partial melting (>1250 °C, 1.5 GPa) (Fig. 5.3) above the upwelling asthenosphere, at the base of the extremely attenuated lithospheric section (Van der Wal and Bodinier 1996; Van der Wal and Vissers 1996; Lenoir et al. 2001; Vauchez and Garrido 2001; Bodinier et al. 2008; Soustelle et al. 2009). As noted in Chapter 4, the transition from the spinel tectonite to the granular spinel peridotite domain is nowadays marked by the recrystallization front representing the former isotherm overlying partially molten granular peridotites (Van der Wal and Bodinier 1996; Lenoir et al. 2001). On the other hand, the youngest deformational structures are exposed at the base of the mantle section in the plagioclase-tectonite domain, which overprints the granular spinel peridotites, and record evolutional stages of the massif under progressive cooling

(800-900°C) and decompression (0.5-0.7 GPa, Obata 1980) prior to the intracrustal emplacement (Fig. 5.3). The latest ductile events are recorded at the transition from granular spinel peridotite to plagioclase-tectonite domains in the form of low-temperature shear zones (F. 4.2), synkinematic to the development of foliation in plagioclase-tectonites as discussed earlier. Strain localization in pyroxenite and peridotite lithologies is interpreted as due to the phase transformation reaction from spinel to plagioclase facies associated with cooling and decompression (Hidas et al., 2013b), and the infiltration of hydrous fluids resulting in dissolution-precipitation creep (Hidas et al., 2016), respectively. Both types of low-temperature shear zones record low pressure (<0.8 GPa) and temperature (750-1000 °C) conditions (Hidas et al., 2013b, 2016).

5.3.2   The record of intra-crustal emplacement in the plagioclase-tectonite domain

The plagioclase-tectonite domain has been interpreted to represent (1) either an asthenospheric mantle diapir upwelled at the base of a thinned continental lithosphere during mantle extrusion in a transform-fault context (Tubía, 1994) or triggered by sublithospheric delamination (Tubía et al. 2004), (2) or ductile extensional shear zones affecting partially molten lithosphere prior to its intracrustal emplacement (Van der Wal and Vissers 1996). However, the km-scale fold structure of this domain (Hidas et al., 2013a) is not consistent with these models: decoupling between older mantle structures (S_0 and S_1 planes and coupled L_1 lineation) and newly developed ones (S_2 and S_m foliations and coupled L_2 and L_m lineations) is at odds to the penetrative foliation-lineation relationship expected in a mantle diapir, and the large-scale gradual rotation of the S_0 compositional layering cannot be accounted solely by shearing. According to the latest model, folding initiated during decompression and cooling of the massif from spinel to plagioclase lherzolite facies in the deep, hottest part of the partially molten mantle domain below the recrystallization front (Fig. 5.4; Hidas et al., 2013a). Paleo-orientation of the present day structures, inferred from restoring the Miocene tectonic tilting and vertical axis clockwise paleomagnetic rotation of the massif (Villasante-Marcos et al., 2003), indicates a subhorizontal inclined anticline and a top-to-the-S sense of shear for the synkinematic shear zones (Hidas et al., 2013a). The low-temperature shear zones were formed upon cooling near the brittle-ductile peridotite transition mainly in the reverse limb of the fold (Fig. 5.4). Folding further developed along a low-angle basal thrust-zone that continuously juxtaposed hot peridotite over colder metamorphic units during decompression, leading to intracrustal emplacement of the massif (Hidas et al., 2013a). This scenario resulted in a geometry where peridotites were conductively cooled from above and progressively cooled in the basal plagioclase-tectonites with the hottest domain preserved in the center of the massif. This atop-and-below cooling would also account for the preservation of the metastable high-pressure garnet-spinel mylonites and the freezing of the recrystallization front in the core of the massif.
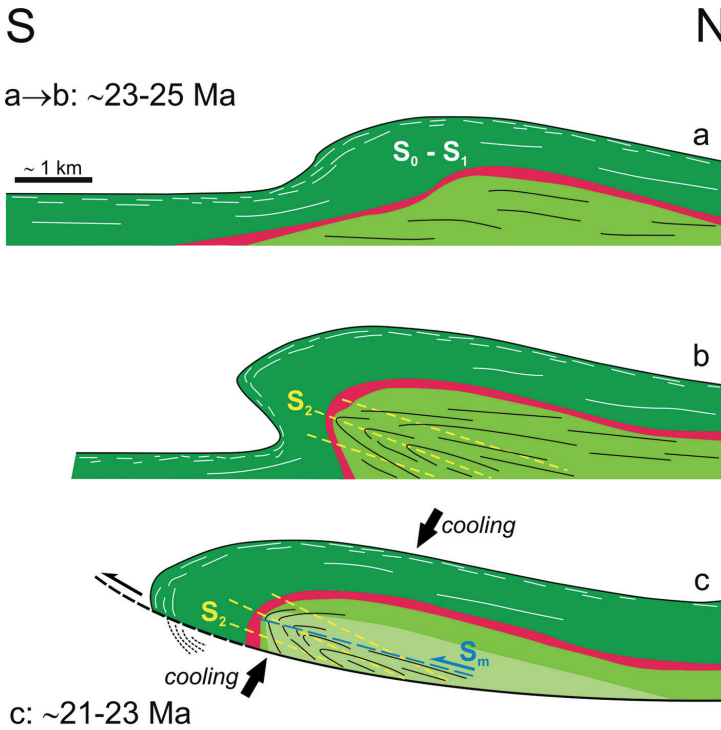
Figure 5.4. Proposed scenario in north–south cross-sections for the Oligo-Miocene evolution and intracrustal emplacement of the Ronda ultramafic massif. Keys: S_0: compositional layering; S_1: spinel tectonite foliation; S_2: plagioclase tectonite foliation; S_m: low-temperature shear zone foliation. See text for further details. Simplified from Hidas et al. (2013a).

5.4 Geodynamic model

The geodynamic significance of the formation event of shallow plagioclase tectonite discussed above relies on the interpretation of the age and nature of the processes that led to the internal tectono-magmatic zoning so characteristic of the Betic and Rif orogenic peridotites (Frets et al., 2014; Garrido et al., 2001, 2011; Hidas et al., 2013a, 2015; Obata, 1980; Précigout et al., 2007, 2013; Van der Wal and Vissers,

1996). Previous studies have suggested a Hercynian (Acosta-Vigil et al., 2014; Sanz de Galdeano and Ruiz Cruz, 2016), Cenozoic-Mesozoic (Michard et al., 1997; van Hinsbergen et al., 2014) or an Alpine (Hidas et al., 2013a; Johanesen et al., 2014; Platt et al., 2003a, 2003b, 2006, 2013; Van der Wal and Vissers, 1996) age for the late tectono-magmatic evolution and intra-crustal emplacement of the Betic-Rif peridotites.

The systematic existence of Mesozoic U-Pb zircon ages in Ronda UHP and HP garnet pyroxenite does not support a Hercynian age for the emplacement of the peridotite in the crust (Sánchez-Rodriguez and Gebauer, 2000). In contrasts, a hyper-extended margin setting for the intrusion of gabbroic rocks in Betic mantle peridotites is in good agreement with the Jurassic extensional event that pervasively affected ALKAPECA terrains (i.e. the Alboran, Kabylides, Peloritani, and Calabria domains) in the western Mediterranean due to the opening of the Piemonte-Ligurian Ocean (Michard et al., 1997; van Hinsbergen et al., 2014). However, a Jurassic age and a passive margin tectonic setting do not account, among other observations, for: (1) the late Miocene thermochronological ages recorded in zircons rims (U-Pb) and garnets (Lu-Hf) in garnet pyroxenites from the Betic-Rif peridotites (Pearson and Nowell, 2004; Sánchez-Rodriguez and Gebauer, 2000), (2) the pervasive Miocene resetting of U-Pb zircon and monazite ages in overlying Los Reales crustal section (Sánchez-Rodriguez and Gebauer, 2000; Pearson and Nowell, 2004; Platt et al., 2013; Massonne, 2014), (3) the supra-subduction radiogenic signature of late pyroxenite intrusive dykes in the Ronda peridotite (Marchesi et al., 2012), and (4) the arc tholeiitic affinity of late mantle-derived, gabbroic dykes intruding in the Ronda and Ojén plagioclase tectonites (Hidas et al., 2016). These data are more consistent with a supra-subduction back-arc setting for the Paleocene Alpine evolution of the Alborán domain due to slab rollback in the westernmost Mediterranean (Royden, 1993; Faccenna et al., 2004; Jolivet et al., 2009; Garrido et al., 2011; Mancilla et al., 2015).

The Alpine history of the Ronda peridotite is therefore interpreted as strong thinning of continental lithosphere (Garrido et al., 2011), induced by slab rollback or delamination, in a backarc basin situated several hundred kilometers eastward of their present emplacement (i.e., south of the current Balearic Islands) and developed upon the previous Alpujárride-Maláguide orogenic wedge (Booth-Rea et al., 2007). Hidas et al. (2013a) propose that after thinning and extension in a back-arc setting recorded in the Ronda spinel tectonite domain and the recrystallization front (Lenoir et al., 2001; Soustelle et al., 2009; Garrido et al., 2011), the final Miocene exhumation of Ronda peridotite is associated with early folding and later but probably synkinematic shearing of the SCLM in a contractive geodynamic setting recorded in the low-pressure plagioclase tectonite domain of the Ronda peridotite. The reconstructed fold initiated under upper mantle conditions in the spinel stability field within the hottest part of the peridotite body, at that time represented by the granular spinel peridotites formed earlier by partial melting of spinel tectonites (Hidas et al., 2013a). Major folding was accounted at the base of the massif under lower crustal conditions and it is now preserved in plagioclase tectonites. Close to the ductile-brittle transition, folding was also accompanied by strain localization along S_m shear zones in the hotter limb recording the same kinematics as the S_2 plagioclase tectonites (Hidas et al.,

2013b, 2016). The proposed folding further developed along a gentle basal thrust zone that continuously juxtaposed hot peridotite to cooler metamorphic units (Hidas et al., 2013a). This model can also answer the pivotal question on the preservation of the metastable garnet-spinel mylonites and that of the recrystallization front in the Ronda peridotite, both have frozen in because of their exposition to cooler overlying metamorphic units (Hidas et al., 2013a).

In the above proposed model, the formation of the Ronda's garnet-spinel mylonite domain fits well with the strong isothermal decompression recorded in the overlying Alpujárride crustal envelope during Paleogene extension (Balanyá et al., 1997; Argles et al. 1999; Platt et al., 2003; Barich et al., 2014). Lu-Hf cooling ages in clinopyroxene-garnet pairs, with blocking temperature of ca. 800 °C, in garnet pyroxenite in the similar Beni Bousera garnet-spinel mylonite domain yields ages of 24 ± 3 Ma (Pearson and Nowell, 2004). This closure age implies that garnet-spinel mylonites formed in the Oligocene by decompression and cooling from garnet lherzolite facies primary conditions. Cooling and freezing of garnet-spinel equilibrium in mylonites at the top of the mantle lithospheric section, as well as the pressure gap between primary conditions in peridotites (2.4–2.7 GPa) and the overlying crustal granulites (1.5 GPa) (Haissen et al., 2004), may be explained by excision of thickened lower mafic crust (almost absent in Alpujárrides units) and the juxtaposition of the lithospheric mantle with cooler middle crust (Garrido et al., 2011). Alternatively, garnet-spinel mylonites could be the locus of subcrustal strain localization associated with early uplift and thinning of the Alborán domain lithospheric mantle (Argles et al., 1999). Further extension during Late Oligocene to Early Miocene induced melting at the base of extremely attenuated subcontinental lithospheric mantle (Lenoir et al., 2001). This stage was likely coeval with the intrusion of arc tholeiitic dikes in the Maláguide complex on top of the crustal envelop (Duggen et al., 2004).

The peridotite structures at the base of the Ronda mantle section in the youngest tectonometamorphic domains indicate southward kinematics, which can be linked to an inversion from a backarc extension during slab rollback to a contractional basin during Late Oligocene-Early Miocene collision of the Alborán orogenic wedge with the Maghrebian Passive Margin. The orogenic shortening and southward thrusting very likely initiated the ductile fold allowing the early Miocene intracrustal emplacement of the Ronda massif (Hidas et al., 2013a). Thus, the 21-23 Ma intracrustal emplacement (Priem et al. 1979; Esteban et al. 2011) occurred after the collision with the Maghrebian Passive Margin (ca. 23-25 Ma; Booth-Rea et al. 2005), providing a common origin for the peridotite bodies in the Betic-Rif and in the Kabylies in Algeria (Caby et al. 2001; Bruguier et al. 2009). Lonergan (1993) also proposed initial south-directed migration of the Alborán Domain to explain the southward directed thrusting of the Maláguide-Alpujárride nappe-stack after undoing paleomagnetic rotations in the eastern Betics. During the early Miocene, the system propagated westward producing the oblique collision with the South Iberian Passive Margin and the high-pressure metamorphism of the Nevado-Filábride units between 15-17 Ma (López Sánchez-Vizcaíno et al. 2001; Platt et al. 2006). All these time constraints are in correspondence with the 25 ± 1 Ma Lu-Hf ages obtained for the formation

of overlying garnet pyroxenites in the Beni Bousera massif (Blichert-Toft et al. 1999; Pearson and Nowell 2004) as well as with the 19 ± 5 Ma U-Pb ages of crystallization of late granites that crosscut the Ronda massif (e.g., Sánchez-Rodríguez and Gebauer, 2000).

References

Argles, T. W., Platt, J. P. and Waters, D. J. (1999). Attenuation and excision of a crustal section during extensional exhumation: The Carratraca Massif, Betic Cordillera, southern Spain, *Journal of the Geological Society* 156, 149-162.

Balanya, J. C., Garcia-Duenas, V., Azañón, J. M. and Sánchez-Gomez, M. (1997). Alternating contractional and extensional events in the Alpujarride Nappes of the Alboran domain (Betics, Gibraltar arc). *Tectonics* 16, 226-238.

Bell, A. M. (1981) Vergence: an evaluation. *Journal of Structural Geology*, 3, 197-202.

Blichert-Toft, J., Albarede, F. and Kornprobst, J. (1999). Lu-Hf isotope systematics of garnet pyroxenites from Beni Bousera, Morocco: Implications for basalt origin. *Science* 283, 1303-1306.

Bodinier, J.L., Garrido, C.J., Chanefo, I., Bruguier, O. and Gervilla, F., 2008. Origin of pyroxenite–peridotite veined mantle by refertilization reactions: evidence from the Ronda peridotite (Southern Spain). *Journal of Petrology* 49, 999–1025.

Booth-Rea, G., Azañón, J. M., Martínez-Martínez, J. M., Vidal, O. and García-Dueñas, V. (2005). Contrasting structural and P-T evolution of tectonic units in the southeastern Betics: Key for understanding the exhumation of the Alboran Domain HP/LT crustal rocks (western Mediterranean). *Tectonics*, 24, 10.1029/2004tc001640.

Booth-Rea, G., Ranero, C. R., Martinez-Martinez, J. M. and Grevemeyer, I. (2007). Crustal types and Tertiary tectonic evolution of the Alboran sea, western Mediterranean. *Geochemistry Geophysics Geosystems* 8, 25, Q10005. 10.1029/2007gc001639, 2007.

Boudier, F. (1978). Structure and petrology of the Lanzo peridotite massif (Piedmont Alps). *Geological Society of America Bulletin* 89, 1574-1591.

Bruguier, O., Hammor, D., Bosch, D. and Caby, R.(2009). Miocene incorporation of peridotite into the Hercynian basement of the Maghrebides (Edough massif, NE Algeria): Implications for the geodynamic evolution of the Western Mediterranean. *Chemical Geology* 261, 171-183.

Caby, R., Hammor, D. and Delor, C. (2001). Metamorphic evolution, partial melting and Miocene exhumation of lower crust in the Edough metamorphic core complex, west Mediterranean orogen, eastern Algeria. *Tectonophysics* 342, 239-273.

Darot, M. (1973). Cinèmatique de l'extrusion, à partir du manteau, des péridotites de la –sierra Bermeja (Serranía de Ronda, Espagne). *Comptes Rendus de l'Académie des Sciences de Paris* 278, 1673-1676.

Davies, G.R., Nixon, P.H., Pearson, D.G. and Obata, M. (1993). Tectonic implications of graphitized diamonds from the Ronda, peridotite massif, southern Spain. *Geology* 21, 471–474.

Duggen, S., Hoernle, K., van den Bogaard, P. and Harris, C. (2004). Magmatic evolution of the Alboran region: The role of subduction in forming the western Mediterranean and causing the Messinian Salinity Crisis. *Earth and Planetary Science Letters*, 218, 91-108.

Esteban, J.J., Sánchez-Rodríguez, L., Seward, D., Cuevas, J. and Tubía, J.M. (2004). The late thermal history of the Ronda area, southern Spain. *Tectonophysics* 389, 81–92.

Esteban, J.J., Cuevas, J., Tubía, J.M., Liati, A., Seward, D. and Gebauer, D. (2007). Timing and origin of zircon-bearing chlorite schists in the Ronda peridotites (Betic Cordilleras, Southern Spain). *Lithos* 99, 121–135.

Esteban, J.J., Cuevas, J., Tubía, J.M., Sergeev, S. and Larionov, A. (2010). A revised aquitanian age for the emplacement of the Ronda peridotites (Betic Cordilleras, Southern Spain). *Geological*

Magazine 148, 183–187Garrido, C.J. and Bodinier, J.L. (1999). Diversity of mafic rocks in the Ronda peridotite: evidence for pervasive melt/rock reaction during heating of subcontinental lithosphere by upwelling asthenosphere. *Journal of Petrology* 40, 729-754.

Garrido, C.J., Gueydan, F., Booth-Rea, G., Precigout, J., Hidas, K., Padron-Navarta, J.A. and Marchesi, C. (2011). Garnet lherzolite and garnet-spinel mylonite in the Ronda peridotite: vestiges of Oligocene backarc mantle lithospheric extension in the western Mediterranean. *Geology* 39, 927–930.

Gervilla, F. (1990). Mineralizaciones magmáticas ligadas a la evolución de las rocas ultramáficas de la Serranía de Ronda (Málaga, España). Ph. D. Thesis, University of Granada.

González-Jiménez, J.M., Marchesi, C., Griffin, W.L., Gervilla, F., Belousova, E.A., Garrido, C.J., Romero, R., Talavera, C., Leisen, M., O'Reilly, S.Y., Barra, F. and Martin, L. (2017). Zircon recycling and crystallization during formation of chromite- and Ni-arsenide ores in the subcontinental lithospheric mantle (Serranía de Ronda, Spain). *Ore Geology Reviews* 90, 193-209.

Haissen, F., Garcia-Casco, A., Torres-Roldan, R. and Aghzer, A. (2004). Decompression reactions and P-T conditions in high-pressure granulites from Casares-Los Reales units of the Betic-Rif belt (S Spain and N Morocco). *Journal of African Earth Sciences*, 39, 375-383.

Hidas, K., Booth-Rea, G., Garrido, C.J., Martínez-Martínez, J.M., Padrón-Navarta, J.A., Konc, Z., Giaconia, F., Frets, E. and Marchesi, C. (2013a). Backarc basin inversion and subcontinental mantle emplacement in the crust: kilometre-scale folding and shearing at the base of the proto-Alborán lithospheric mantle (Betic Cordillera,southern Spain). *Journal of the Geological Society* 170, 47–55.

Hidas, K., Garrido, C. J., Tommasi, A., Padrón-Navarta, J. A., Thielmann, M., Konc, Z., Frets, E. and Marchesi, C. (2013b). Strain localization in pyroxenite by reaction-enhanced softening in the shallow subcontinental lithospheric mantle. *Journal of Petrology* 54, 1997-2031.

Hidas, K., Tommasi, A., Garrido, C.J., Padrón-Navarta, J.A., Mainprice, D. Vauchez, A., Barou, F. and Marchesi, C. (2016), Fluid-assisted strain localization in the shallow subcontinental lithospheric mantle, *Lithos*, 262, 636–650.

Lenoir, X., Garrido, C.J., Bodinier, J.-L., Dautria, J.-M. y Gervilla, F. (2001). The recrystallization front of the Ronda peridotite: Evidence for melting and thermal erosion of subcontinental lithospheric mantle beneath the Alborán basin. *Journal of Petrology,* 42 (1), 141-158.

Lonergan, L. (1993). Timing and kinematics of deformation in the Malaguide Complex, internal zone of the Betic Cordillera, southeast Spain. *Tectonics* 12.

López Sánchez-Vizcaino, V., D. Rubatto, M. T. Gómez-Pugnaire, V. Trommsdorff, and O. Müntener (2001), Middle Miocene high-pressure metamorphism and fast exhumation of the Nevado-Filabride Complex, SE Spain. *Terra Nova* 13(5), 327–332.

Marchesi, C., Griffin, W.L., Garrido, C.J., Bodinier, J.-L., O'Reilly, S.Y. and Pearson, N.J. (2010). Persistence of mantle lithospheric Re–Os signature during asthenospherization of the subcontinental lithospheric mantle: insights from in situ isotopic analysis of sulfides from the Ronda peridotite (southern Spain). *Contributions to Mineralogy and Petrology* 159, 315–330.

Nicolas, A. and Boudier, F.(1975). Kinematic interpretation of folds in Alpine-type peridotites, *Tectonophysics* 25, 233-260.

Pearson, D. G. and Nowell, G. M. (2004). Re–Os and Lu–Hf Isotope Constraints on the Origin and Age of Pyroxenites from the Beni Bousera Peridotite Massif: Implications for Mixed Peridotite–Pyroxenite Mantle Sources. *Journal of Petrology* 45, 439-455.

Platt, J. P., Argles, T. W., Carter, A., Kelley, S. P., Whitehouse, M. J. and Lonergan, L. (2003). Exhumation of the Ronda peridotite and its crustal envelope: constraints from thermal modelling of a P-T-time array. *Journal of the Geological Society* 160, 655-676.

Platt, J. P., Anczkiewicz, R., Soto, J.-I., Kelley, S. P. and Thirlwall, M. (2006). Early Miocene continental subduction and rapid exhumation in the western Mediterranean. *Geology* 34, 981-984.

Precigout, J., Gueydan, F., Gapais, D., Garrido, C. J. and Essaifi, A. (2007). Strain localisation in the subcontinental mantle-a ductile alternative to the brittle mantle. *Tectonophysics* 445, 318^336.

Priem, H.N.A.K., Boelryjk, N.A.I.M., Hebeda, E.H., Oen, I.S., Verdurmen, T.E.A. and Verschure, R.H. (1979). Isotopic dating of the emplacemeent of the ultramafic masses in the Serranía de Ronda, Southern Spain. *Contributions to Mineralogy and Petrology* 70, 103-109.

Obata, M. (1980). The Ronda peridotite: Garnet-, spinel-, and plagioclaseioclase-lherzolite facies and the P-T trajectories of a high-temperature mantle intrusión. *Journal of Petrology* 21, 533-572.

Reisberg, L. and Lorand, J.-P. (1995). Longevity of sub-continental mantle lithosphere from osmium isotope systematics in orogenic peridotite massifs. *Nature* 376, 159–162.

Reisberg, L. C., Zindler, A. and Jagoutz, E. (1989). Futher Sr and Nd isotopic results from peridotites of the Ronda Ultramafic Complex. *Earth and Planetary Science Letters* 96, 161-180.

Reisberg, L. C., Allegre, C. J. and Luck, J. M. (1991). The Re-Os Systematics of The Ronda Ultramafic Complex of Southern Spain. *Earth and Planetary Science Letters* 105, 196-213.

Sánchez-Rodriguez, L., Gebauer, D., 2000. Mesozoic formation of pyroxenites and gabbros in the Ronda area (southern Spain), followed by Early Miocene subduction metamorphism and emplacement into the middle crust: U-Pb sensitive high- resolution ion microprobe dating of zircón. Tectonophysics 316 (1–2), 19–44.

Soustelle, V., Tommasi, A., Bodinier, J.L., Garrido, C.J. and Vauchez, A. (2009), Deformation and reactive melt transport in the mantle lithosphere above a large-scale partial melting domain: The Ronda peridotite massif, southern Spain. *Journal of Petrology* 50(7), 1235–1266.

Tubía, J. M. (1994). The Ronda Peridotites (Los Reales nappe) - An example of the relationship between lithospheric thickening by oblique tectonics and late extensional deformation within the Betic Cordillera (Spain). *Tectonophysics* 238, 381-398.

Tubía, J. M., Cuevas, J. and Esteban, J. J. (2004). Tectonic evidence in the Ronda peridotites, Spain, for mantle diapirism related to delamination. *Geology* 32, 941-944.

Van der Wal, D. and Bodinier, J.L. (1996). Origin of the recrystallization front in the Ronda peridotite by km-scale pervasive porous flow. *Contributions to Mineralogy and Petrology* 122, 387-405

Van der Val, D. and Vissers, R.L.M. (1993). Uplift and emplacement of upper mantle rocks in the western Mediterranean. *Geology* 21, 1119-1122,

Van der Val, D. and Vissers, R.L.M. (1996). Structural petrology of the Ronda peridotite SW Spain: deformation history. *Journal of Petrology* 37, 23-43.

Vauchez, A. and Garrido, C. J. (2001). Seismic properties of an asthenospherized lithospheric mantle: constraints from lattice preferred orientations in peridotite from the Ronda massif. *Earth and Planetary Science Letters* 192, 235-249.

Villasante-Marcos, V., Osete, M.L., Gervilla, F. and García-Dueñas, V. (2003). Paleomagnetic study of the Ronda peridotites (Betic Cordillera, Southern Spain). *Tectonophysics* 377, 119-141

Zindler, A., Staudigel, H., Hart, S. R., Endres, R. and Goldstein, S. (1983). Nd and Sr isotopic study of a mafic layer from Ronda ultramafic complex. *Nature* 304, 226-230.

Chapter 6
Metallogeny

6.1. Types of ores

Besides to their petrological and metamorphic singularity, the ultramafic massifs of the Serranía de Ronda have also the peculiarity to host an assemblage of mineralizations of Cr, Ni, Cu and noble metals that is unique in the world and includes (Gervilla, 1990; Gervilla and Leblanc, 1990):

> *(1) Chromium-nickel (Cr-Ni) ores* made up of chromite and Ni arsenides associated with orthopyroxenite and/or cordierite dykes.
> *(2) Sulfide-graphite (S-G) ores* consisting of irregular bodies of sulfides (pyrrhotite, pentlandite, chalcopyrite and minor cubanite) containing chromite and <u>graphite</u>, which are found filling fractures and fault zones.
> *(3) Chromium (Cr) ores* that form bodies of chromitites such as pods, lenses and entwined veins or schlierens associated with clinopyroxenites, orthopyroxenites or dunites.

These three different types of ores are distributed heterogeneously within the three main massifs of the Serranía de Ronda, although spatially ordered according to their petrological-structural zoning (Fig. 6.1). Thus, the Cr-Ni and S-G ores are found in the peripheral parts of the massifs hosted in peridotites of spinel tectonite, mainly above the recrystallization front, although some small, cordierite-free, Ni arsenide-poor Cr-Ni ores occur in the granular domain and in the plagioclase-tectonite domain (Fig. 6.1). In contrast, the Cr ores are exclusively found within the plagioclase tectonite domain always below the recrystallization front (Fig. 6.1).

In addition to these magmatic ores, other mineralizations related with the partial melting of the underlying crustal metapelites and the activity of late hydrothermal fluids, such as magnetite skarns can be also found along the interface between the ultramafic rocks and their crustal envelope.

6.2.   Chromium-Nickel (Cr-Ni) ores

6.2.1.   *Localization and style of the mineralization*

The main known deposits of this type of ores include the already exploited mines of *Mina Baeza, El Lentisco*, *El Nebral* and *La Gallega* from the Ojén ultramafic massif, and those of *El Sapo*, *San Agustín* and the *Los Jarales District* (San Juan, El Inglés and Pozo Moreno) from the Carratraca ultramafic massif (Fig. 6.1). Two small-unexploited Cr-Ni ores known as the *Arroyo de la Cala* and *Barranco de las Acedías* also crop out in the Ronda ultramafic massif (Fig. 6.1).

   This type of ores represents a rather unique example of magmatic ores associated with upper mantle rocks and consists of assemblages of massive chromite and nickel arsenides ± orthopyroxene ± cordierite, which may occur as veins or layers concordant and discordant to the foliation of the host peridotites but always showing sharp contacts (Oen, 1973, Gervilla, 1990; Gervilla and Leblanc, 1980). The thickness of the individual veins and layers vary between 5 and 70 cm and extend laterally between 20 and 50 m, although locally can reach up to 100 m as observed in La Gallega and San Juan mines (Fig. 6.1). In some localities, there are leucocratic dykes of cordierite- and phlogopite-bearing plagiocasite-rich (hereafter plagioclasites) or quartz-feldspar leucogranite spatially associated with the ores, although their geometric relationships between these leucocratic rocks vary depending on their nature (see below).
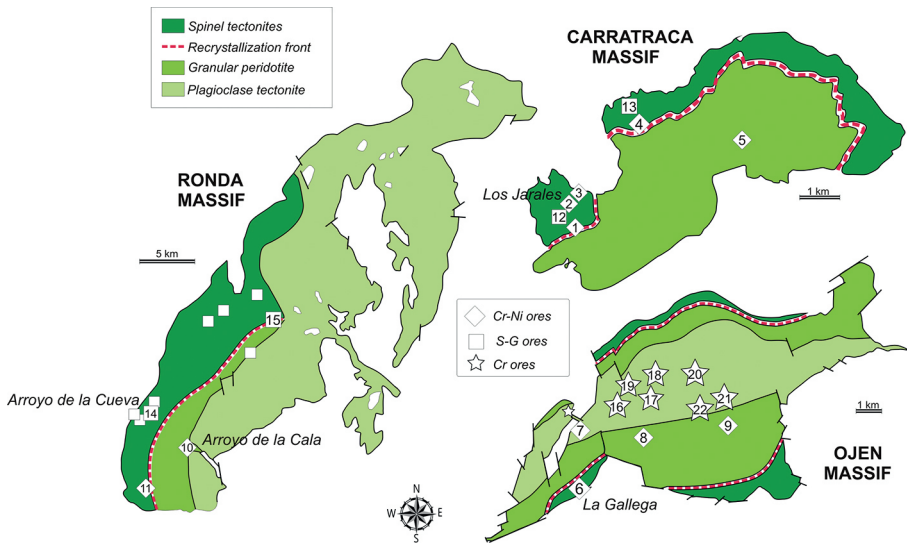
Figure 6.1.   Distribution of the different ore bodies in the ultramafic massifs of the Serranía de Ronda. Cr-Ni ores: 1: Pozo Moreno, 2: El Inglés, 3: San Juan, 4: San Agustín, 5: El Sapo, 6: La Gallega, 7: Mina Baeza, 8: el Lentisco, 9: El Nebral, 10: Arroyo de la Cala and 11: Barranco de las Acedías. S-G ores: 12: Los Pobres, 13: El Gallego, 14: Minas del Majar del Toro and 15: Mina Marbella. Cr ores: 16: Cerro del Algarrobo, 17, 18 and 19: CAB, ACA and ARC, respectively, from the Arroyo de los Caballos, 20: Cerro del Águila, 21: Pista and 22: Cañada del Lentisco.

In the area known as *Mina Baeza* (Fig. 6.1) the mineralization comprises two different types of ores: (1) a chromite-orthopyroxene vein containing up to 2 vol.% of maucherite ($Ni_{11}As_8$) (it could be considered as Cr-Ni ore type) to the north, and (2) two disseminated podiform chromitites (Cr ores) to the south. The Cr-Ni ore vein is hosted by partly serpentinized dunites and extends for 30 m with a maximum thickness of 10 cm. Mina Baeza is located in the western part of the Ojén Massif, within the plagioclase tectonite domain. The morphology and structure of the two podiform bodies will be described later, in the Cr ores section.

The *El Lentisco* and *El Nebral* occurrences consist of veins of few tens of centimeters of thickness and up to 30 m of lateral extend hosted in strongly serpentinized peridotites of the granular peridotite domain within the central graben of the Ojén ultramafic massif (Fig. 6.1). These are two cordierite-free, Ni-arsenide poor chromite deposits with predominance of maucherite over nickelite, which are accompanied by other metallic minerals such as orcelite ($Ni_{5-x}As_2$), pentlandite [$(Fe,Ni)_9S_8$], millerite (NiS), heazlewoodite (Ni_3As2) and parkerite [$Ni_3(Bi,Pb)_2S_2$] (Oen et al., 1980).

The *La Gallega* mine is located in the southwestern most part of the Ojén ultramafic massif (Fig. 6.1), near the village of Ojén. Nowadays it is an abandoned mine where relicts of several dyke-like orebodies of massive chromite + nickelite that were exploited in the 70s of the 20th Century are still preserved. These exploited orebodies were up to half a meter in thickness and >100 m long discordant to the foliation of the enclosing peridotites of the spinel tectonite domain. In some unexploited part of the mine there are relicts of the original mineralization in the form of a network of veins consisting of fine-grained mixtures of massive nickelite and chromite with an overall arsenide/chromite ratio = 0.20 (Fig. 6.2). Other metallic minerals that accompany nickelite (NiAs) include smaller amounts of löllingite ($FeAs_2$), gersdorffite (NiAsS), maucherite and westerveldite (FeAs), as well as traces of rammelsbergite ($NiAs_2$), pyrrhotite ($Fe_{1-x}S$), pentlandite, chalcopyrite ($CuFeS_2$), cubanite ($CuFe_2S_3$), native gold, molibdenite (MoS_2) and graphite. Chromite often contains abundant inclusions of phlogopite. These veins of massive chromite and Ni arsenides can be associated with either orthopyroxene (± ilmenite) or (2) cordierite (±rutile). In some parts of the mine the veins of massive chromite and Ni arsenides (usually <20cm thick) laterally grade to orthopyroxenite or cordieritite rock, and the later each one (Fig. 6.3). Thus, when the chromite-arsenide ore is hosted in orthopyroxenite, the chromitite host large inclusions of orthopyroxene while the orthopyroxenite often contain accessory chromite and interstitial Ni-arsenides. In contrast, when the chromitite-arsenide ore is associated with, or hosted by, cordieritites (>90 % volume cordierite) the chromitite may contain accessory cordierite and the cordieririte contains chromite and Ni-arsenides too. The increasing of the chromite-nickelite aggregates in the interstices of granular cordierite give rise, in first instance, to the banded chromite-nickelite/cordierite ores, and in other cases, to the formation of occluded cordieritites within the dyke-like bodies (Figure 6.3). Transitions between orthopyroxenites and cordierititic rocks are also observed and marked by an increasing of the content of large crystals (up to 2 cm) of prismatic orthopyroxene in the cordieritite. Sulfides, mainly pyrrhotite and chalcopyrite (pentlandite is rare) occur as rounded or lamella-like inclusions in nickelite, in samples with arsenide content well above the average (> 20 vol.%)
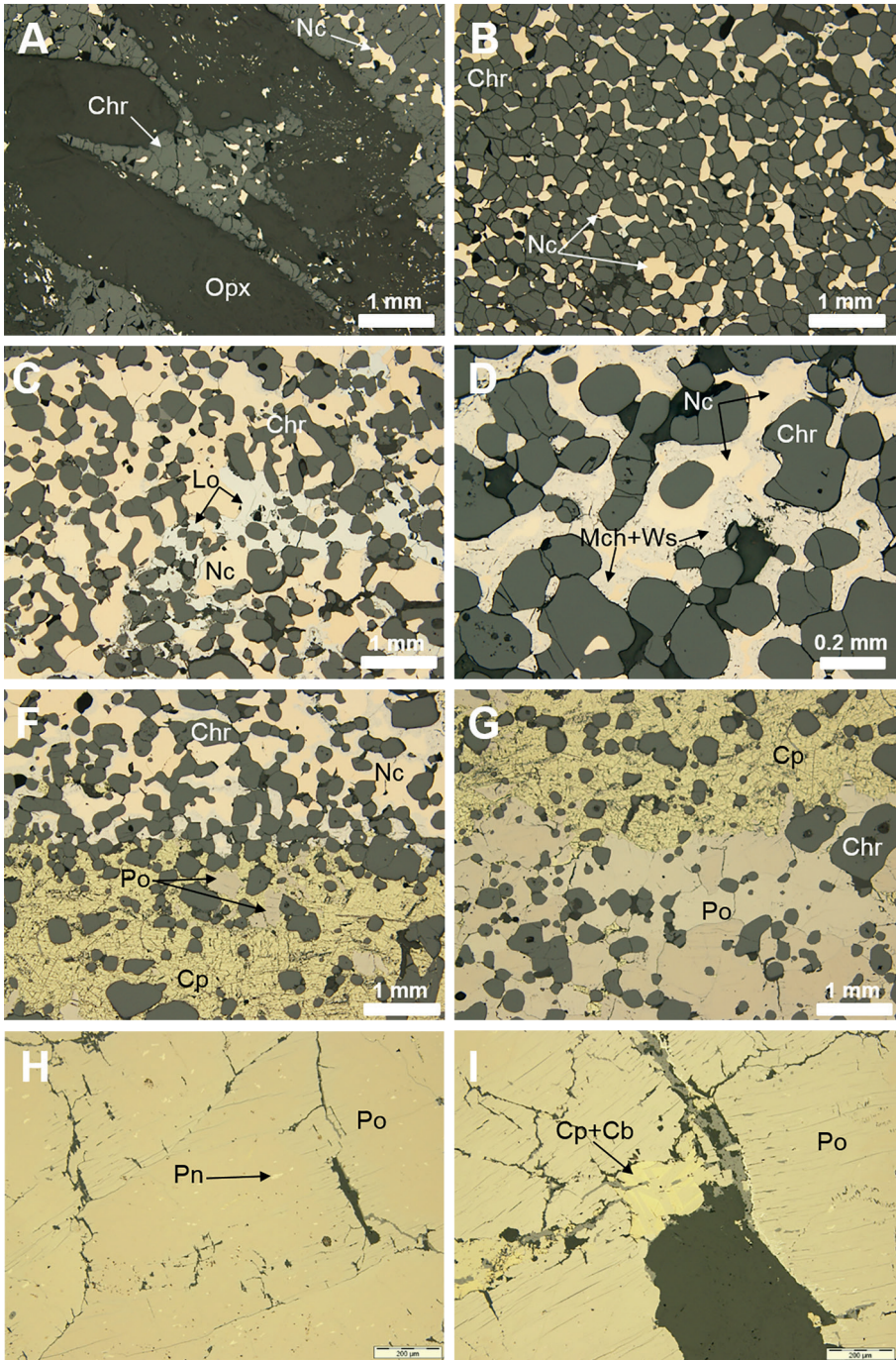
Figure 6.2. Mineral assemblages of the Cr-Ni ores at La Gallega Mine. A: prismatic orhopyroxenes with intercumulus chromite and nickelite (note the abundance of chromite and nickelite inclusions in larger orthopyroxene crystals); B: anhedral and subidiomorphic chromite cemented by nickelite;

C: chromite+nickelite ore assemblage with higher proportion of nickelite partially replaced by nickeliferous loellingite; D: intergranular nickelite partially transformed to a fine-grained intergrowth of maucherite and westerveldite; E and F: chromite-bearing sulfide layer (with sublayers of chalcopyrite and pyrrhotite) interbedded with chromite-bearing nickelite layer; G and H: internal characteristic of single sulfide veins satellite to the Cr-Ni ore veins (note the scarcity of pentlandite in the assemblage, only limined to minute, flame-like exsolutions in pyrrhotite). Keys: Opx: orthopyroxene, Chr: chromite, Nc: nickelite, Lo: loellingite, Mch: maucherite, Ws: westerveldite, Po: pyrrhotite, Pn: pentlandite, Cp: chalcopyrite and Cb: cubanite.

(Gervilla and Leblanc, 1990). Nevertheless, one of the samples contain sulfides forming separate layers of pyrrhotite-chromite and chalcopyrite-chromite of few millimeters in thickness, intercalated in the massive chromite-nickelite ore, revealing immiscibility processes between arsenide and sulfide melts. (Fig. 6.2). Furthermore, pyrrhotite and chalcopyrite with minor cubanite and traces of pentlandite fill late discordant veins (2-3 cm thick) in the host spinel tectonites of the mine galleries (Fig. 6.2). The Cr-Ni veins and the associated pyroxenite-cordierite rocks are locally cut by leucocratic dykes (i.e., plagioclasites) made up of plagioclase, cordierite, phlogopite and minor potassium feldspar and quartz, with accessory amounts of apatite and zircon.

The *El Sapo* mine is located in the central part of the Carratraca massif (Fig. 6.1) although nowadays it is not possible to observe in situ the orebodies of this mine owing the extensive mining work and collapsing of this mine. Moreover,
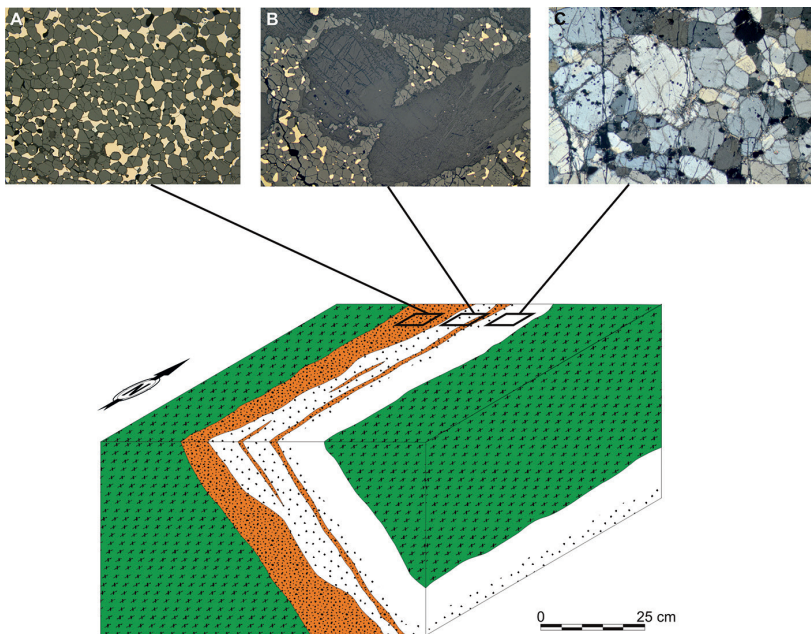
Figure 6.3. Structure of a chromite-nickelite-cordierite vein from the La Gallega Mine made up of: A: massive chromite-nickelite ore; B: chromite-nickelite ore intercumulus to anhedral (rounded) cordierite crystals; C: partly recrystallized, mosaic-like texture of the cordierite host rock.

no information is available about their morphology and size in previous mining reports and scientific works. Samples collected from the dumps show that the ore consist of fine-grained chromite (100-300 μm) with intergranular nickelite, grading to orthopyroxenite. The chromite-nickelite ore also contain minor maucherite, löllingite, and westerveldite, as well as smaller quantities of ilmenite, pyrrothite and chalcopyrite. Some of the samples contain Cr-Ni ore locally intruded by leucocratic dykes giving rise to contact aureole mainly made up of antophyllite and phlogopite.

The *San Agustin* mine comprises several galleries in the northwestern part of the Carratraca massif (Fig. 6.1). As in the El Sapo Mine, the nature of the ores can only be recognized from unweathered samples accumulated in the old dumps. Here, the proportion of chromite plus nickelite ore is < 20% volume, consisting of variably sized (50-500μm), rounded cumulus crystals of chromite with interstitial nickelite, disseminated in a cordierite rock containing small amounts of plagioclase. The ore assemblage also contains minor amounts of rutile, rammelsbergite, nickeliferous loellingite, gersdorffite, native gold and sperrylite ($PtAs_2$) (Chatzipanagiotou, 2016)

The *Los Jarales* mining district covers an area of approximately 2 km^2 in the southwestern part of the Carratraca ultramafic massif (Fig. 6.1). As noted before, this mining district groups the orebodies of San Juan, El Inglés and Pozo Moreno. The San Juan mine, is located in a strongly tectonized peridotite explaining the distinct morphology of the orebodies: "the orebodies have the shape of elliptic pockets aligned along the SW-NE direction…within these pockets, the ore occurs as almost pure, spherical nodules weighing 100-150 kilograms… the pockets show rosary-like shape both along their superficial extent and downwards" [translated from Álvarez de Linera (1851), in Orueta-Duarte (1917)]. The mineralogy and texture of the ores also exhibit distinctively different characteristic to other Cr-Ni ores of the Serranía de Ronda (Fig. 6.4): (1) the chromite-Ni arsenide ore is locally associated with clinopyroxene instead orthopyroxene; (2) cordierite is the predominant mineral of the gangue, which frequently occurs associated with plagioclase and phlogopite; (3) the assemblage of metallic minerals is similar to that found in the La Gallega mine, although, in San Juan the arsenide/chromite ratio is much higher (up to 0.4) as well as the amount of maucherite (up to 20% of the arsenides) and native gold, in contrast, the arsenide assemblage is free of löllingite and gersdorffite; (4) there is a late generation of skeletal chromite enriched in Cr and Fe, which formed in equilibrium with plagioclase (Gervilla et al., 1990). In the orebodies of the El Inglés and Pozo Moreno, the opaque assemblage is similar to that described for the case of San Agustín, although there are higher proportions of chromite+nickelite relative to cordierite, and none of the samples contain sperrylite.

The mineralization of the *Arroyo de la Cala* is a stock-work of foliated massive chromitite poor in arsenides (<1 % volume), with a sigmoidal morphology (surface projection 9 x 5 m; Fig. 6.5), hosted in a low-temperature shear zone cutting depleted dunite-harzburgite at the transition zone between granular spinel peridotite and plagioclase-tectonite domains (Fig. 4.2). The chromitite ore veins enclose lenticular bodies of cumulus orthopyroxenite and angular blocks of the country, sheared harzburgite and dunite (Fig. 6.5). The contact between the chromitite veins and the angular blocks of peridotite is usually sharp but with the cumulus orthopyroxenite is gradual. The chromitite body shows internal structures such as a vertical lineation and foliation subparallel to that of the low-temperature shear zones developed during
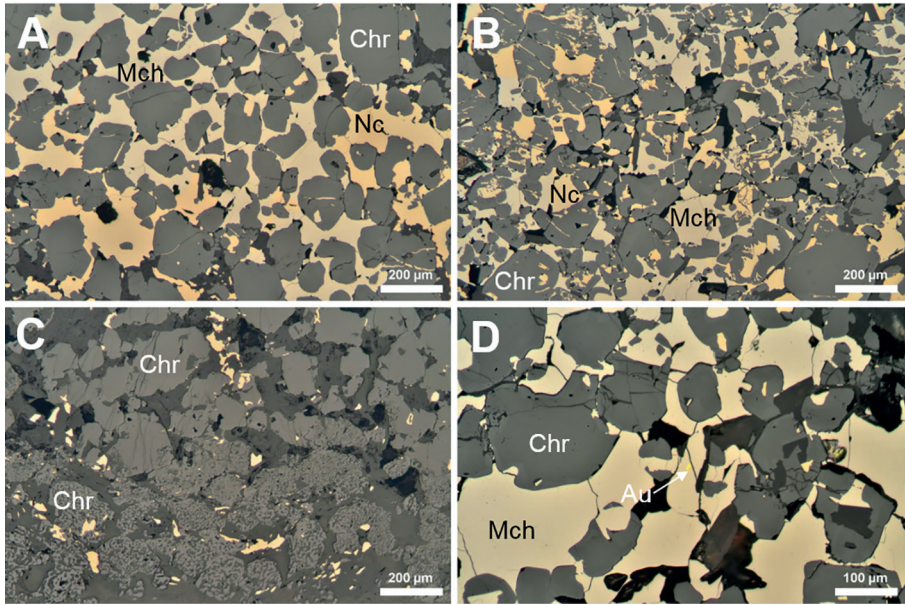
**Figure 6.4.** Mineral assemblages of the Cr-Ni ores at San Juan Mine. A: partly corroded chromite with intergranular maucherite and nickelite; B: partly corroded and fractured chromite with interstitial maucherite and nickelite; C: Recrystallized (secondary) chromite formed by reaction of pre-existing magmatic chromite with an intruding plagioclase-rich vein; D: grain of native gold included in maucherite. Keys: Chr: chromite, Nc: nickelite, Mch: maucherite, Ws: westerveldite and Au: gold.

the crustal emplacement of the massif (see Chapter 5). These structures have been interpreted to reflect the deformation of an unconsolidated ore, probably related to syntectonic magmatic crystallization (Gervilla et al., 2002).
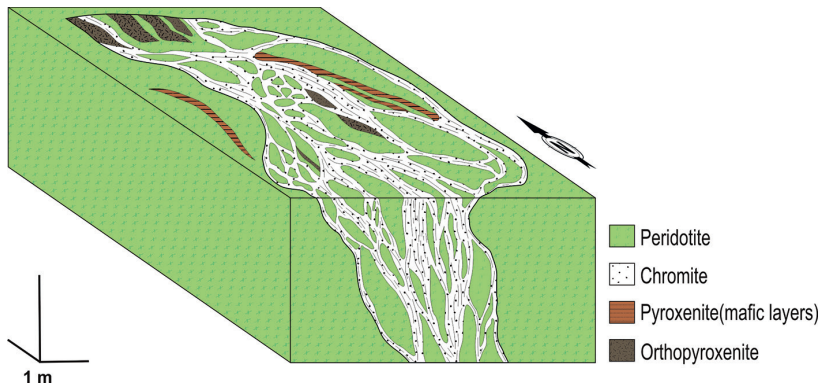
Figure 6.5. Sketch showing the mesostructure of the chromitite pod (Cr-Ni ore) cropping at the Arroyo de la Cala in the southern portion of the Ronda ultramafic massif. 12 (Modified from Gervilla and Leblanc, 1990).

The ore from the *Barranco de las Acedías* is a small dyke (15 m long and 25 cm thickness) of weathered massive chromitite with minor Ni arsenides intergrown with an orthopyroxenite that laterally grades to massive cordieritite. It crops out in the SW portion of the spinel tectonite domain of the Ronda massif. The assemblage of metallic minerals mainly consists of chromite with minor ilmenite and rutile, variable proportions of nickelite depending on the degree of alteration (it is mainly preserved as inclusions in chromite), and orthopyroxene and cordierite as gangue minerals.

6.2.2   *Chemistry of chromite and arsenides*

The chemical composition of chromite from Cr-Ni ores plots in a wide com-compositional field in the Y_{Cr} [$Y_{Cr}=Cr/(Cr+Al+V+Ti+Fe^{3+})$] versus X_{Mg} [$X_{Mg}=Mg/(Mg+Fe2+,Zn+Mn)$] diagram (Fig. 6.6) varying from $Y_{Cr} = 0.25$ and $X_{Mg} = 0.21$ in chromite-nickelite ores associated with cordierite from La Gallega to $Y_{Cr} = 0.70$ and $X_{Mg} = 0.62$ in the ore vein from Mina Baeza. Chromite shows a progressive depletion in Al and Fe^{2+}, and enrichment in Mg and Cr from ores found in the spinel tectonite domain to those hosted by granular peridotites, and especially, in ores located well below the recrystallization front in the plagioclase tectonite domain. In the former ores, there is a similar depletion in Al and Fe^{2+} from chromite associated with cordierite to that associated with orthopyroxene. Such a compositional field is rather unique but slightly overlaps the fields of chromites from podiform-like chromitites hosted in the upper mantle section of ophiolite complexes as well as stratiform chromitites from ultramafic-mafic layered complexes hosted in the continental crust (Fig. 6.6). Chromite from Cr-Ni ores has unusually high Zn and V contents (0.2-1.2 wt. % ZnO, and 0.5-2 wt. % V_2O_3) as well as significant amounts of TiO_2 (up to 0.7 wt.%). It is worth mentioning that the higher TiO_2 contents were measured in chromite crystals containing abundant micrometric exsolution lamellae of ilmenite or rutile (Gervilla and Leblanc, 1990).

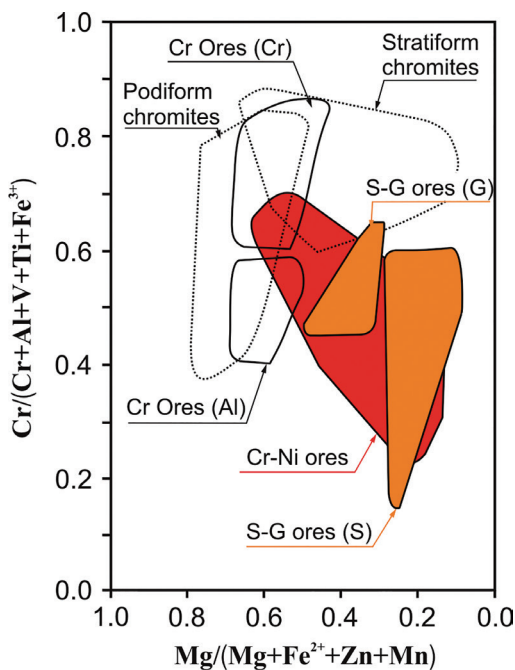**Figure 6.6.** Chemical composition of chromite from the different ore types in terms of their Y_{Cr} (=$Cr/\Sigma R^{3+}$) versus X_{Mg} (=$Mg/\Sigma R^{2+}$) ratios. The compositional fields of chromite from podiform chromitites from the ophiolitic complexes and stratiform chromitites are plotted for comparison. Data from Gervilla and Leblanc (1990), Gutiérrez-Narbona (1999) and Chatzipanagiotou (2017).

The abundance of arsenides in the Cr-Ni ores significantly decreases from La Gallega (20 vol.% on average) in the garnet mylonites of the spinel tectonite domain to Mina Baeza (< 2 vol.%) in the plagioclase tectonite domain as the Al and Fe^{2+} contents of the associated chromite do. Nevertheless, the higher amounts of arsenides (up to 40%) occur in the tectonized "pockets" of ore of the San Juan Mine. The composition of nickelite approaches its stoichiometry (NiAs) with only very minor amounts of Fe and Co. In contrast, diarsenides exhibit wide compositional variations from rammelsbergite ($NiAs_2$) to Ni- and Fe-rich safflorite ($CoAs_2$) and mainly to Ni- and Co-rich löllingite ($FeAs_2$) (Oen et al., 1971) defining a compositional field that could represent the approximate solvus position at around 625ºC in the system $CoAs_2$-$NiAs_2$-$FeAs_2$ (Gervilla and Rønsbo, 1992). When present (mainly in La Gallega), gersdorffite inherits the composition of the replaced assemblage nickeliferous lollingite+nickeline, becoming rich in Fe and, at lesser extent Co.

6.2.3   Geochemistry and mineralogy of noble metals

The analyses of whole-rock and mineral concentrates carried out by Leblanc et al., (1990) and Gervilla and Leblanc (1990) indicate that the Cr-Ni ores are much richer in Au (up 19 ppm) than in PGE (up to 1 ppm Pt + Pd). This is clearly shown in their chondrite-normalized PGE+Au patterns (Fig. 6.7a), which systematically exhibit a marked positive slope from Pt to Au. The distribution of noble metals is very heterogeneous among the different Cr-Ni orebodies and within a single ore body, depending on the modal percentage of Ni arsenides in the ore (Gervilla et al., 1996). The ore veins from the northern part of *Mina Baeza* are the poorest in noble metals,
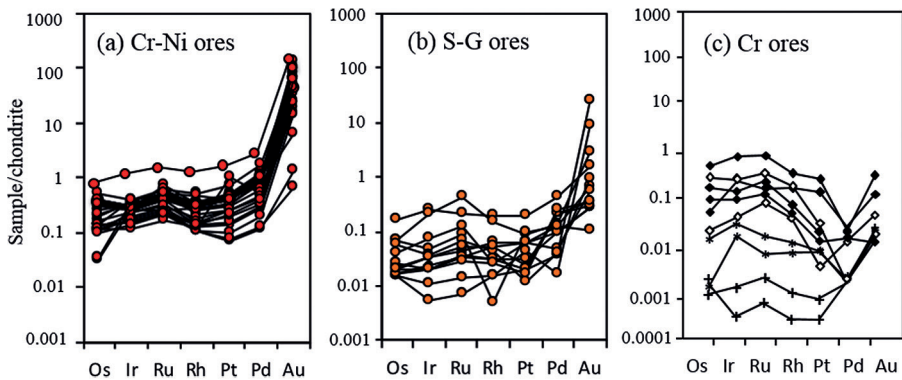
Figure 6.7. Chondrite-normalized platinum-group element patterns of Cr-Ni ores, S-G ores and Cr ores cropping out in the ultramafic massifs of the Serranía de Ronda. The data sets in (a) and (b) include samples (undifferentiated) from Arroyo de la Cala, Mina Baeza, La Gallega, San Juan and San Agustin (Cr-Ni ores) as well as from Los Pobres, El Gallego and Minas del Majar del Toro (S-G ores). Data from Gervilla and Leblanc (1990) and Chatzipanagiotou (2017). The plotted samples in (c) come from Arroyo de los Caballos (CAB: black diamonds; ACA and ARC: open diamonds), Cañada del Lentisco (asterisks) and Cerro del Algarrobo (crosses). Data from Torres-Ruiz et al. (1996) and Gutiérrez-Narbona et al. (2003). Normalizing values from Naldrett and Duke (1980).

with 304 ppb PGE and 48 ppb Au. In contrast, the Cr-Ni ores from San Juan mine form the *Los Jarales* mining district are the richest in Ni arsenides, and accordingly have the highest total contents of PGE (1.79 ppm) and Au (19 ppm). However, these relatively high bulk-rock abundances of PGE do not have mineralogical expression in the form of platinum-group minerals (PGM) except in the San Agustín Mine where minute grains of sperrilyte were detected in a sample with a positive anomaly in Pt relative to Rh and Pd, in its chondrite-normalized PGE pattern (Chatzipanagiotou, 2016). The pioneering in situ analysis of the arsenides by Gervilla et al. (2004) using EPMA and micro-pixe revealed variable contents of Ru in nickelite (up to 4 ppm) and Ni-rich löllingite (up 19 ppm) as well as Pd in nickelite (up to 7 ppm), Ni-rich löllingite (up to 30 ppm) and, mainly, in maucherite (up to 64 ppm). Recent refinement of the laser ablation technique coupled to ICP-MS allowed a better accuracy of the analysis, revealing that nickelite, maucherite and löllingite all host relatively high amounts of PGE (Piña et al. 2015). This explains the higher concentrations of noble metals in the samples containing high Ni arsenide abundances. Nickeliferous löllingite contains the most PGE (48 ppm Pt, and the other PGEs in the range of 1.0-3.4 ppm). Nickelite from *La Gallega* has contents of Pd and Au averaging 2.2 ppm and 6 ppm, respectively, while the remaining PGE are below 1 ppm. Nickelite from the San Juan ore is richer in PGE and Au than that from La Gallega (~ 0.6 ppm Os and Ir, ~ 1.7 ppm Ru, ~ 0.25 ppm Rh, ~ 1 ppm Pt, ~ 58 ppm Au). Maucherite from San Juan has similar PGE abundances to nickelite, except for Pd and Pt whose abundances are significantly higher in maucherite (25 ppm Pd, 5 ppm Pt) than in nickelite. In the case of Au, although high (10.3 ppm), its content is much lower in maucherite than in nickelite.

Unlike PGE, Au is not only detected by LA-ICP-MS in solid solution in arsenides but relatively often occur as single, irregular grains varying in size from 1 to 80 μm, in nickelite, maucherite (Fig. 6.4D) and Ni-löllingite. Its composition varies from pure Au to Au-Cu and Au-Cu-Ag alloys with minor but detectable amounts of Bi and Te (Torres-Ruiz et al., 1991; Chatzipanagiotou, 2016).

6.2.4 Geochronology

Gervilla (1990) carried out the first attempt to date the timing of formation of the Serrania de Ronda's ores using the $^{40}Ar/^{39}Ar$ geochronology applied on primary phlogopite from a plagioclasite spatially associated with the Cr-Ni ores at *La Gallega* in the Ojén ultramafic massif. This author obtained a $^{40}Ar/^{39}Ar$ plateau age of 21 ± 0.5 Ma. The LA-ICP-MS data obtained by González-Jiménez et al. (2017) from eleven idiomorphic zircons recovered from this plagioclasite yielded slightly younger concordant ages scattering between 20.1 ± 0.2 Ma and 17.9 ± 0.1 Ma, with a weighted mean $^{206}Pb/^{238}U$ of 18.5 ± 0.3 (MSWD=22, 1σ uncertainty). U-Pb ages obtained from other four idiomorphic zircons separated from the spatially associated chromitite yield concordant and discordant ages overlapping this time interval (19.8 to 21.0 Ma; mean $^{206}Pb/^{238}U$ age of 20.4 ± 0.87 Ma, MSWD = 2.4 a), supporting the hypothesis that this Cr-Ni ore was formed during the thermal climax that affected the ultramafic massifs of the Serranía de Ronda just before their crustal emplacement.

Twenty-one anhedral and partly corroded zircons recovered from the cordieritite hosting this chromitite yield much more scattered ages varying from 33.8 ± 1 Ma to 781 ± 10 Ma; these zircons are interpreted as inherited from the crustal envelope of the ultramafic massifs. Similarly, eleven rounded zircons from the cordieritite of the *Barranco de las Acedías* in the Ronda ultramafic massif, yield concordant Cambrian to Neoproterozoic ages (536.9 ± 9.5 Ma to 568 ± 10 Ma); some of these zircons also interpreted as inherited from the crustal envelope may have external rims with Aguitanian ages $(21.2 \pm 0.4$ Ma) overlapping that of the youngest zircons found in the plagioclasite and chromitite from *La Gallega* mine.

On the other hand, six zircons recovered from a sample of massive chromitite of the *Arroyo de la Cala* ore in the Ronda ultramafic massif yield both concordant and discordant ages between 2309 ± 37 Ma and 109 ± 15 Ma. Two Proterozoic ages obtained for zircons of this population (1815 ± 9 Ma and 1794 ± 17 Ma) are identical, within error, to those of zircons reported previously in the garnet pyroxenites of Ronda (1783 ± 37 Ma). Similarly, concordant Early Jurassic (192 ± 13 Ma) and Cretaceous ages (109 ± 15 Ma) obtained from the core and rim, respectively, of a single zircon from the chromitite are also consistent with the ages (180 ± 5 Ma, 178 ± 6 Ma, and 131 ± 3 Ma) already reported for magmatic zircons from corundum-bearing garnet pyroxenites in the Ronda massif.

6.3   Sulfide-Graphite (S-G) ores

6.3.1   *Localization and style of the mineralization*

More than 50 occurrences of sulfide-graphite veins have been reported from the ultramafic massifs, mainly in the Ronda and Carratraca Massifs. The main mines in the Ronda Massif are *Mina Marbella* and several mines in the *Arroyo de la Cueva* area including *Mina San Pedro*, *Mina del Majar del Toro, Mina Piña, El Robledalillo* and *La Herrumbrosa*. In the Carratraca Massif, the main mines include *El Aguila*, *El Gallego* and *Los Pobres*.

The main feature of this type of mineralization is the presence of sulfides, frequently weathered to earthy masses of Fe oxy-hydroxides, containing variable amounts of graphite nodules. These sulfide-graphite ores occur as veins, irregular lenticular bodies and stockworks related to fracture zones in the spinel-tectonite domain and more rarely in the granular domain. The thickness of the mineralization ranges widely from several centimetres to 7 m, and it extends laterally over tens of meters. These orebodies often contain xenoliths of host rocks (peridotites and pyroxenites) and rarely show brecciated textures. The contact between mineralization and host rocks is commonly sharp and peridotites are typically unaltered. Locally, in the occurrences of the *Arroyo de la Cueva* area, the contact exhibits an aureola of hydrothermal alteration consisting of talc, chlorite and muscovite in the sulfides, and amphibole and serpentine in the peridotites (Hem, 1998; Hem et al., 2001).

The mineralization consists of variable amounts of graphite, pyrrhotite, pentlandite, chalcopyrite, cubanite and chromite (Fig. 6.8). Locally, accesory ore minerals include rutile, ilmenite, magnetite, pyrite, nickelite, maucherite, cobaltite, molibdenite and

sphalerite. The orebodies range from graphite-rich (> 60 vol. %) with up to 10 vol. % disseminated chromite and traces of Fe-Ni-Cu sulfides to Cu sulfide-rich, graphite- and chromite-free sulfide ores. In most cases, graphite constitutes 10-60 vol. %, sulfides 40-60 vol. %, and silicate minerals (mostly, Na-rich phlogopite, clinopyroxene, and/ or plagioclase An$_{70-80}$) and chromite never exceed 30 and 10 vol. %, respectively. The richest graphite ore is found in *Mina Marbella* where graphite comprises more than 90 vol. % of the mineralization with only disseminated chromite and traces of Fe-Ni-Cu sulfides. At the opposite, *Arroyo de la Cueva* mines are typically grapite-free and ores
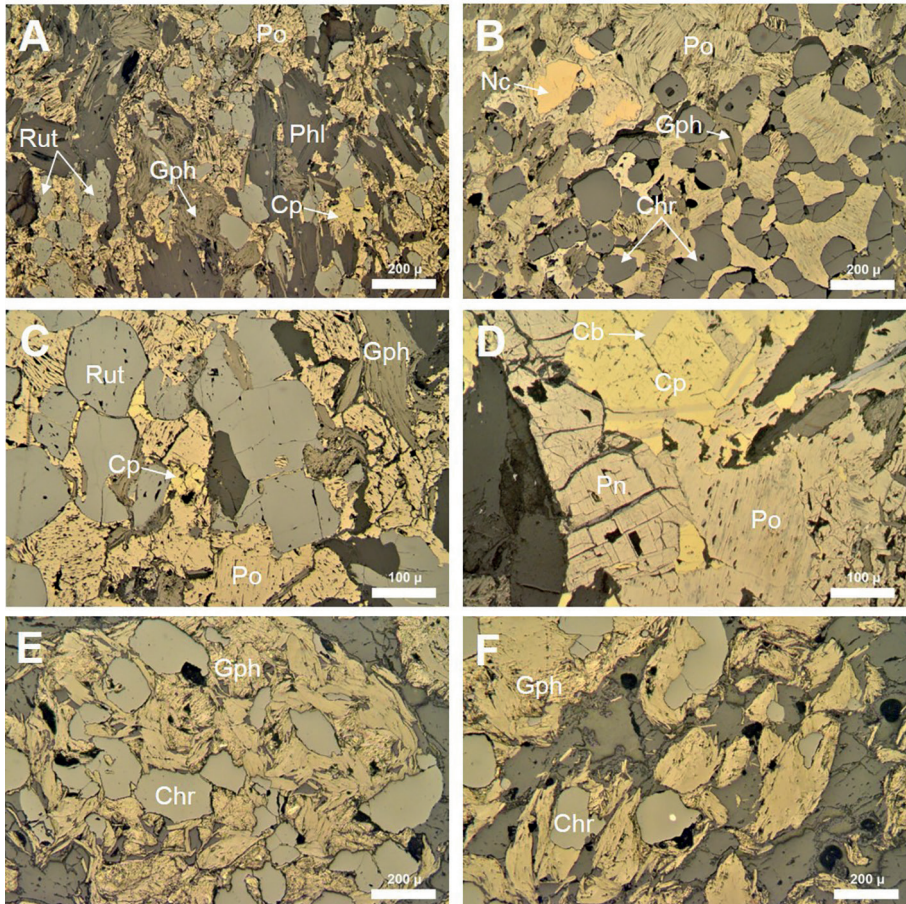
Figure 6.8. Mineral assemblages of the S-G ores at El Gallego (sulfide-rich S-G ore) and El Águila (graphite-rich S-G ore). A: sulfides (pyrrhotite, pentlandite and chalcopyrite) with graphite interstitial to rutile and phlogopite; B: pyrrhotite-rich sulfide assemblage containing some nickelite interstitial among rounded, partly corroded chromite grains; C: close up of a rutile-rich zone showing the relationships between rutile, graphite and sulfides; D: close up of a sulfide assemblage made up of pyrrhotite, pentlandite (mostly altered to violarite) and chalcopyrite intergrown with cubanite; E and F: partly corroded chromite grains associated to graphite nodules in El Águila occurrence. Keys: Phl: phlogopite, Rut: rutile, Chr: chromite, Gph: graphite, Nc: nickelite, Po: pyrrhotite, Pn: pentlandite, Cp: chalcopyrite and Cb: cubanite.

have a mineral assemblage consisting of Fe-Ni-Cu sulfides, Fe-Co-Ni sulfarsenides and diarsenides, and sphalerite (Hem, 1998; Hem et al., 2001).

Primary sulfides exhibhit the typical textures of fractional crystallization of monosulfide solid solution (mss) and later subsolidus reequilibration upon cooling. Pyrrhotite is the most abundant sulfide mineral and forms rectilinear grain boundaries and triple joints developing a mosaic texture. Typically, pyrrhotite contains pentlandite exsolution flames and, in most samples, is partially altered to Fe oxides and hydroxides along cleavage planes. Most pentlandite occurs as granular aggregates intergranualr to pyrrhotite crystals and chalcopyrite fills intergranular spaces and fractures. Locally, cubanite is intergrown with chalcopyrite and pentlandite is partially replaced by violarite ($FeNi_2S_4$). Trace amounts of sphalerite occur interstitially situated between sulfides and host numerous minute chalcopyrite inclusions. Nickelite, maucherite and cobaltite (CoAsS) are accesory minerals with the nickelite and maucherite ocurring as inclusiones within pyrrohite and cobaltite in form of subidiomorphic crystals intergrowth with pyrrhotite and chalcopyrite or enveloped by cobaltite. The latter often contain micrometric inclusions of Pd and Ni tellurides [e.g. merenskyite ($PdTe_2$) and melonite ($NiTe_2$)], as well as tellurobismuthite (Bi_2Te_3) and tsumoite (BiTe),

Graphite shows two distinctive texture types depending on the alteration degree. In strongly altered mineralizations (*Los Pobres*, *El Águila* and *Mina Marbella*), graphite occurs as variably sized (from 5-10 m and several meters) nodules and lenticular bodies hosted by limonitic masses where some relict fresh sulfides are occasionally preserved. These graphite masses usually host disseminations of irregular chromite crystals. By contrast, in unaltered mineralizations as for example *El Gallego*, graphite occurs as disseminated tabular crystals with an average size of 0.4 to 0.04 mm, locally aggregated in irregular nodules often associated with, and included in chromite grains enclosed in sulfides.

Chromite occurs in variable proportions in sulfide-graphite ores. Although in some deposits it can reach 20 vol. %, its modal content is commonly lower than 10 vol. %. Its morphology and grain size depend on minerals with which it appears associated. In orebodies with unaltered massive sulfides, chromite forms 0.2 mm-sized rounded crystals, often clustered in polygonally-textured aggregates. In altered graphite-rich orebodies, chromite occurs as 0.2-0.4 mm-sized disseminated irregular crystals with clear signs of corrosion within plagioclase and phlogopite.

6.3.2   Chemistry of chromite, arsenides and sulfides

Chromite in this type of ores exhibits extreme compositional variation between graphite-rich mineralizations typically hosted by spinel-bearing lherzolites to sulfide-rich orebodies typically hosted by garnet-bearing lherzolites. Chromite from the graphite-rich ores is richer in MgO (6-10 wt. %), with slightly higher proportions in Cr_2O_3 (35-46 wt. %) and lower proportions of ZnO (0.3-1.0 wt. %), V_2O_3 (0.3-1.0 wt. %) and TiO_2 (< 0.3 wt. %) than chromite from sulfide-rich ores (2-6 wt. % MgO, 25-37 wt. % Cr_2O_3, 1.0-1.6 wt. % ZnO, 1.0-3.1 wt. % V_2O_3, 0.2-0.8 wt. % TiO_2). These compositional differences are clearly illustrated on the Y_{Cr} versus X_{Mg} diagram where chromites from S-G ores plot roughly in the Cr-Ni ore chromite field located

above the recrystallization front (Fig. 6.6) and those from the graphite-rich ores plot in the same field as chromites from orthopyroxene-bearing Cr-Ni ores (Fig. 6.6). In constrast, chromite forming sulfide-rich ores plots in the field of the cordierite-bearing Cr-Ni ores (Fig. 6.6). In the *El Gallego* mine, chromite show similar chemical variation, which chromite from the inner parts being more enriched in Cr_2O_3 and, to a lesser extent, Fe relative to chromite from the outer parts, which contain higher amounts of V and Ti (Chatzipanagiotou, 2017).

The compositional trend exhibited by chromite in the S-G type mineralizations is analogous to that observed in the Cr-Ni type mineralizations, with an increase in Al, Fe, Zn, Ti and V from the most internal to the most peripheral mineralizations (Gervilla and Leblanc, 1990).

Pyrrhotite contains variable concentrations of Fe (58.1-63.3 wt.%), pentlandite have Fe/Ni ratios around 0.93 and is usually Co poor, except in the Arroyo de la Cueva ores where Co contents in pentlandite reach 36 wt.% (Hem et al., 2001). Chalcopyrite, cubanite and pyrite have stoichiometric compositions. Cobaltite have a composition between 50 and 90 mol.% CoAsS, 5 and 36 mol.% NiAsS and 4 and 20 FeAsS. The Co richest compositions in this mineral are reported in the Arroyo de la Cueva ores were cobaltite occurs associated with Co- and Ni-rich löllingite, alloclasite (CoAsS), arsenopyrite (FeAsS) and Co-rich pentlandite (Hem et al., 2001).

6.3.3   *Geochemistry and mineralogy of noble metals*

The chondrite-normalized PGE and Au patterns in Figure 6.7b clearly show that S-G ores are much poorer in noble metals than Cr and Cr-Ni ores respectively. PGE abundances range between 0.01 and 1 times the chondritic values, whereas Au values range from 0.1 to 1 times the chondritic values. Nevertheless, two samples from *El Gallego* have relatively high Au contents (up to 10.7 ppm Au; 185 times the chondritic values once recalculated to 100% sulfides), which are associated to positive anomalies in Pt relative to Rh and Pd (Chatzipanagiotou, 2016). The bulk PGE and Au concentrations are quite heterogeneous between the different sulfide-graphite orebodies probably reflecting the variable modal proportion of chromite, graphite, base metal sulfides, arsenides and sulfarsenides. The positive correlation between whole-rock As content and PGE and Au abudance suggest that the latter minerals, although accessory, played an important role in partitioning the noble metals (Gervilla et al., 1996). Chondrite-normalized PGE patterns show positive and negative Pt anomalies probably caused by random distribution of minute crystals of sperrylite, although they have not been detected yet. It is worth mentioning the extremely low noble metals abundance of a sulfide ore vein from *La Gallega* (203 ppb PGE and 16 ppb Au) compared to that of massive Cr-Ni ores (~1,7 ppm PGE and ~7,5 ppm Au on average) from the same mine.

Sulfides from S-G mineralization are strongly depleted in PGE relative to arsenides from Cr-Ni ores (Piña et al. 2015). Pyrrhotite contains 0.08 ppm Os and < 0.01 ppm Ir, Rh and Pd. Pentlandite contains 0.47 ppm Pd and 0.04 ppm Os, and chalcopyrite contains only 0.67 ppm Pd. In all sulfides, Pt is less than 0.01 ppm and

Ir and Rh do not exceed 0.01 ppm. These low PGE contents explain the whole rock low concentrations of the mineralizations. Although no Ni arsenides were analyzed by LA-ICP-MS in S-G ore samples from the Serranía de Ronda ultramafic massifs, in similar ores from the Beni Bousera massif (the Amasined orebody) in north Morocco, the high average PGE and Au contents of maucherite (8.29 ppm Os, 25.85 ppm Ir, 7.55 ppm Ru, 8.64 ppm Rh, 7.48 ppm Pt, 61.73 ppm Pd and 33.93 ppm Au) (Piña et al., 2013) account for the relatively high whole-rock abundance of these noble metals in the ore samples (Gervilla et al., 1996).

6.3.4 S and C isotopes

Few unpublished analysis of a sample from *El Gallego* showed S isotopic composition of pyrrhotite and pentlandite varying from $\delta^{32}S = -1‰$ to $\delta^{32}S = +4‰$, typical of magmatic sulfides. In contrast, a deeper survey on C isotopic composition of graphite was performed by Crespo et al. (2006) who showed that this mineral exhibited light carbon isotopic signatures, varying from $\delta^{13}C = -15‰$ to $\delta^{13}C = -21‰$. Nevertheless, some graphite nodules show large core to rim isotopic zoning varying from $\delta^{13}C = -3.3‰$ to $\delta^{13}C = -15.2‰$. The cores have well defined cubic morphologies and were interpreted as probable pseudomorphs after diamonds. Crespo et al. (2006) interpreted the light carbon isotopic signatures of graphite from S-G ores as an indication of their derivation from kerogen-rich crustal material subducted into de mantle.

6.4 Chromite (Cr) ores

6.4.1 Localization and style of the mineralization

This type of ore comprises occurrences of massive chromite (i.e., chromitite) that exhibit morphologies, chemical compositions and mineralogy of solid inclusions similar to podiform chromitites hosted in the mantle section of ophiolitic complexes, although they are much smaller (< 30 cm thickness and < 5 m long). These occurrences include seven orebodies hosted within the plagioclase tectonite domain of the Ojén ultramafic massif in the localization of the *Cerro del Águila* (CDA), *Arroyo de los Caballos* (ARC, ACA and CAB), *Cerro del Algarrobo* (CD), *Cañada del Lentisco* (L) and *Pista* (PIS) (Fig. 6.1; Gervilla, 1990; Torres-Ruíz et al., 1996; Gutiérrez-Narbona, 1999; Gutiérrez-Narbona et al., 2003).

The chromitite occurrence of the *Cerro del Águila* (CDA; Fig. 6.1) is an anastomosing network of thin chromitite veins (< 2cm) and Cr-rich clinopyroxenite (< 5 cm) within dunite. Chromite in these chromitite veins contains tiny inclusions (< 100 μm) of silicates (pargasite, clinopyroxene, mica, olivine and serpentine), base-metal sulfides, arsenides and sulfarsenides, as well as noble metals (see below).

Two of the three chromitite occurrences known in the *Arroyo de los Caballos* (ARC and ACA) are also intimately related with mafic layers hosted by dunites, although these are Cr-rich orthopyroxenites instead clinopyroxenites (i.e., Group D pyroxenites of Garrido and Bodinier, 1999). The ARC occurrence consists of thin

(1-7 cm thick) chromitite veins located just in the contact between an orthopyroxenite layer and their host dunite, whereas ACA is a thin chromite vein (1-3 cm thick) at the contact between within two orthopyroxenite layers hosted in dunite. In these two chromitite occurrences, chromite invades and replaces orthopyroxenite and locally dunite (Fig. 6.9). Thus, the matrix silicates are either orthopyroxene or olivine depending if the chromitite replace orthopyroxenite or dunite, respectively. Chromitites of the two occurrences lack of clinopyroxene whereas amphibole (tremolite) has a late hydrothermal origin. Chromite forming both chromitite occurrences contains abundant inclusions of base metal opaque minerals, including sulfides, arsenides, sulfarsenides and PGM, which may be found as solid inclusions within chromite crystals or fractures affecting them as well as in the interstitial silicate matrix among chromite grains (Gutiérrez-Narbona, 1999; Gutiérrez-Narbona et al., 2013). In ARC chromitites, the BMS included in chromite are single grains of pentlandite (< 200 µm), which may also be found filling pores and open fractures of chromite. Interestingly, these isolated grains of pentlandite concentrate in the antinodular texture at the contact between orthopyroxenite and chromitite while the more massive chromitite adjacent to dunite are devoid of BMS. In the ACA chromitite, there are also grains of pentlandite partly replaced by heazlewoodite coexisting with subordinate maucherite, parkerite and PGM.

The CAB occurrence is a larger podiform-like chromitite body (25 cm thick and 1.25 m long) included in clinopyroxene- and orthopyroxene-bearing dunite (Fig. 6.9 and 6.10). Interestingly, the chromite body encloses lenses of dunite and has peripheral veins of massive chromitite penetrating the host dunite, suggesting that it was possibly formed shortly after the solidification of the dunite host (Fig. 6.9 and 6.10). The chromitite also shows pull-apart fractures resulting from plastic deformation of the host. The mineral inclusions in the chromitite include silicates (pargasite, phlogopite, orthopyroxene, and lesser amounts of clinopyroxene, olivine and serpentine) and frequent tiny (< 100 µm) opaque minerals, including pentlandite and PGM, found associated with these silicates (Torres-Ruiz et al., 1996; Gutiérrez-Narbona, 1999; Gutiérrez-Narbona et al., 2013).

The *Cerro del Algarrobo* chromitite orebody consists of a small schlieren of disseminate chromite, veins and irregular pods (less than 5 cm thick) hosted in a hectometric dunite body. The dunite hosting these chromitites contain disseminations of pyroxenes, which were interpreted as the record of the impregnation/crystallization of basaltic melts that migrated by porous flow through these refractory peridotites (Gutiérrez-Narbona, 1998). This dunite body was exploited in the past 20th Century and nowadays remains as an abandoned open pit so-called in Spanish as the "Cantera de Dunitas" (CD). In this occurrence, the chromite crystals exhibit subhedral morphologies and often have corroded outlines and internal deformation structures. Highly magnesian olivine (Fo = 92.9; Gutiérrez-Narbona et al., 2003) is the only matrix silicate, which is also found as inclusions in chromite together with orthopyroxene, pargasite and phlogopite. The CD chromitites have a greater abundance of Ni-rich opaque minerals than the other chromitite occurrences reported above. These metallic minerals are located in a crack-seal developed in the chromite crystals as well as in the interstices among chromite grains. The opaque mineralogy recognized by Gutiérrez-Narbona et al (2003) includes: Ni- and Cu-rich BMS
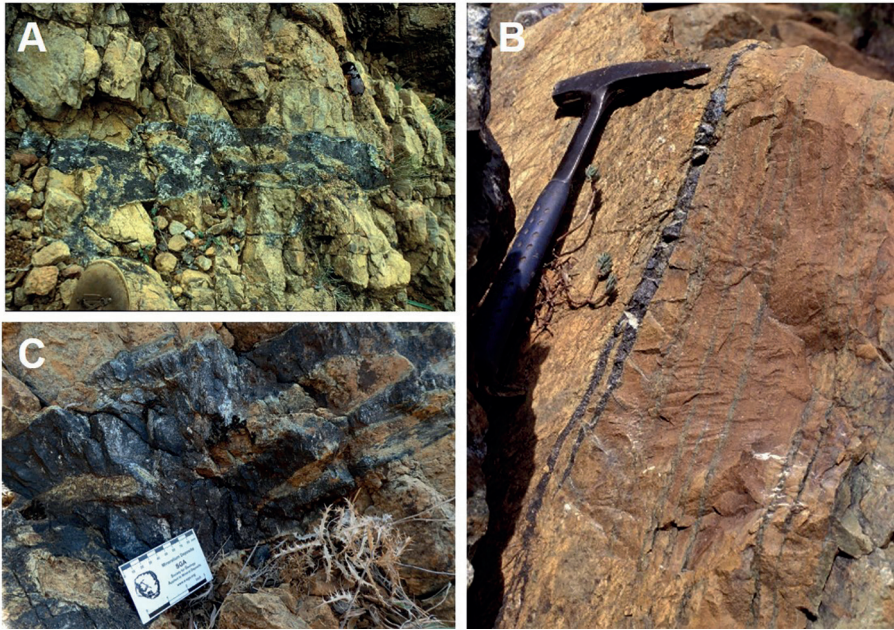
Figure 6.9. Field photographs showing the vein-like morphology of the Cr ores cropping at the Arroyo de los Caballos in the Ojén ultramafic massif. A and C: CAB; B: ACA.

(millerite, goldlevskite, chalcopyrite), Ni-rich arsenides (maucherite, nickelite, orcelite, westerveldite), the Ni-rich sulfarsenide gersdorffite and parkerite. These base-metal minerals are heterogeneously distributed at the hand scale and are almost lacking from the most massive chromitite samples, although maucherite (± nickelite ± orcelite) associated with the BMS millerite and chalcopyrite may represent up to 1 % volume of the interstices in chromitite schlierens within dunite. It's worth noting that no PGM were found in the studied chromitite samples, but a single laurite grain.

The chromitite occurrence at *Cañada del Lentisco* (L) consists of an anastomosing stock-work and schlieren of chromitite (< 5 cm thick) within a strongly serpentinized dunite. They are made up of large chromite crystal (several millimeters across) exhibiting anhedral shapes hosting inclusions of serpentine and strongly altered clinopyroxene, olivine, and mica. The opaque minerals found inside chromite include nickelite, rare pentlandite and one PGM.

The chromitite occurrence *Pista* (PIS) is a single vein of massive chromitite of up to 7 cm in thickness within strongly serpentinized dunite. This chromitite vein is also made up of aggregates of anhedral chromite crystals of up 3 mm across. Similarly to what we have described above for the *Cerro del Algarrobo* occurrence, the silicates found as solid inclusions in this chromitite are strongly altered. Gutiérrez-Narbona (1999) reported only few tiny grains of pentlandite partly replaced by heazlewoodite and millerite originated during the serpentinization process of the host dunite.
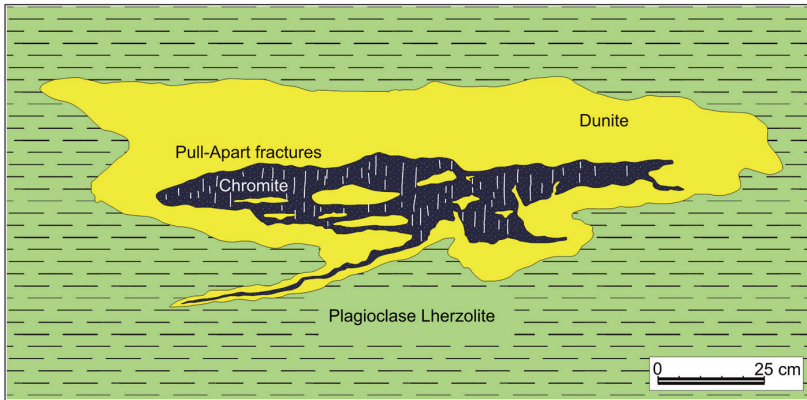
Figure 6.10. Sketch illustrating the morphology and field relationships with host rocks of the CAB chromitite pod cropping in the lowermost part of the Arroyo de los Caballos in the Ójén ultramafic massif (Modified from Gervilla and Leblanc, 1990).

6.4.2 Chemistry of chromite

The chromitite bodies of the Ojén ultramafic massif can be classified into two groups according to the Y_{Cr} [Y_{Cr}=Cr/(Cr+Al+V+Ti+Fe^{3+})] of their chromites: high-Cr (Y_{Cr} =0.60–0.84) and high-Al (Y_{Cr}=0.40–0.57) chromitites (Fig. 6.6). In terms of Y_{Cr} versus X_{Mg} diagram, the compositional field of these Cr ore type chromites is quite similar to that of chromites of most podiform ophiolite chromitites worldwide, although the Cr ores from the Ojén massif are slightly richer in Fe.

The high-Cr group is associated with Cr-rich orthopyroxenite (in ARC and ACA) or contains abundant inclusions of orthopyroxene (in CD); the chromitite occurrence PIS also fit within this group. Chromite of this group has a relatively narrow range of variation in X_{Mg} (0.42–0.64) and a large range of TiO_2 (0.19–0.63 wt.%).

The high-Al chromitites are associated with Cr-rich clinopyroxenites (in CDA) or have clinopyroxene and olivine as the predominant silicate inclusions (in CAB and L). These ore bodies have chromite with similar X_{Mg} (0.50–0.66) and even more variable TiO2 (0.19–0.89 wt.%) compared to chromite of the high-Cr group.

In both types of chromitites, chromite is poor in Zn, V and Ti with values ranging from 0.39 to 0.19 wt. % TiO_2, 0.41 to 0.13 wt. % V_2O_3, and up to 0.37 wt. % ZnO.

6.4.3 Geochemistry and mineralogy of noble metals

Torres-Ruiz et al. (1996) and later Gutiérrez-Narbona et al. (2003) analyzed the contents of the six platinum-group elements (PGE, Os, Ir, Ru, Rh, Pt, Pd) plus Au in whole-rock samples collected from all the chromitite occurrences from the Ojén ultramafic massif. Their results indicate that as a whole, bulk-rock PGE contents in these Cr ores span more than three orders of magnitude (3.8-1912 ppb) irrespective of the chemical composition of the chromite or the modal abundance of base-metal

sulfides or arsenides. Thus, the total absolute concentrations of PGE vary greatly from one occurrence to another, increasing from chromitites of the Cerro del Algarrobo (3.8-6.3 ppb) to those of Cañada del Lentisco (35-85 ppb), Cerro del Águila (271-699 ppb) and Arroyo de los Caballos (ACA = 139 ppb, ARC = 718ppb and CAB = 432-1912 ppb). Most chromitites show similar chondrite-normalized PGE patters with convex-upward, or nearly flat, segment from Os to Rh (between 0.1 and 100 times the chondritic values), and variable depletion in Pt and Pd (Fig. 6.7c). Overall these chromitites exhibit a remarkably positive slope of Pd and Au. These general trends are very similar to those shown by chromitites hosted in the mantle section of ophiolitic complexes, although the average of PGE is relatively higher, and the negative slope Ru-Rh-Pt-Pd is less steeped.

Consistently with these relatively high contents of noble metals, the chromitite occurrences contain a number of grains of PGM and Au. The PGM population comprises specific phases of all the six PGE, and on the basis of both textural and paragenetic evidence, the PGM population can be divided into two groups (Torrez-Ruíz et al., 1996; Gutiérrez-Narbona et al., 2003): (1) those grains included in chromite that were originated during the magmatic stage of formation of the chromitite and, (2) grains that are located in fractures and interstitial matrix, which were either originally formed in the magmatic stage and were altered during post-magmatic alteration processes, or directly precipitated during these latter secondary alteration processes.

The most abundant primary PGM are members of the solid solution laurite (RuS_2)-erlichmanite (OsS_2), singularly enriched in As and Ir, together with PGE sulfarsenides exhibiting compositions intermediate between irarsite (IrAsS), ruarsite (RuAsS), osarsite (OsAsS) and hollingworthite (RhAsS) end-members. Other magmatic PGM reported in these chromitites include the Pt arsenide sperrylite ($PtAs_2$), malanite [$Cu(Pt, Ir)_2S_4$], Pt-Fe alloys (Pt-Fe, Pt_3Fe), Pt-Os alloy, stibiopalladinite, and some undefined minerals including sulfides [$(Ni,Fe,Cu)_2(Ir,Rh)S_3$, (Pt,Rh,Ir,Cu)S, and PdS], arsenide [(Pd,Ni)As] and bismuthide (PdBi). The secondary mineralogy includes those grains of native Ru or Pt-Fe formed during serpentinization along pull-apart fractures in chromite as a result of desulfurization of laurite and Pt-bearing sulfides.

6.4.4   Geochronology

González-Jiménez et al. (2013) carried out LA-MC-ICPMS analysis to measure in situ the Re-Os isotopic composition of 180 grains (members of the solid solution laurite–erlichmanite, Os-rich platarsite, an Os–Pt alloy, and two-phase aggregates of laurite with smaller grains of irarsite or pentlandite) and 100 base-metal mineral grains (including maucherite, pentlandite, heazlewoodite and godlevskite) from all chromitite bodies except La Cañada del Lentisco. PGM in chromitite have initial $^{187}Os/^{188}Os$ ratios ranging from 0.1181 to 0.1760 and $^{187}Re/^{188}Os$ ratios below 0.031, whereas the base-metal minerals show smaller variations in $^{187}Os/^{188}Os$ ratios (0.1217–0.1234) and greater ranges in $^{187}Re/^{188}Os$ (0.001–0.121) than coexisting PGM (Fig. 6.11). These values are similar to those described in other mantle-hosted chromitites from ophiolite complexes and, as a whole, yield a distribution of T_{RD} model ages clustering at ~0.3 Ga and show a series of older minor peaks recording magmatic events back ~ 1.4 Ga (Fig. 6.11).
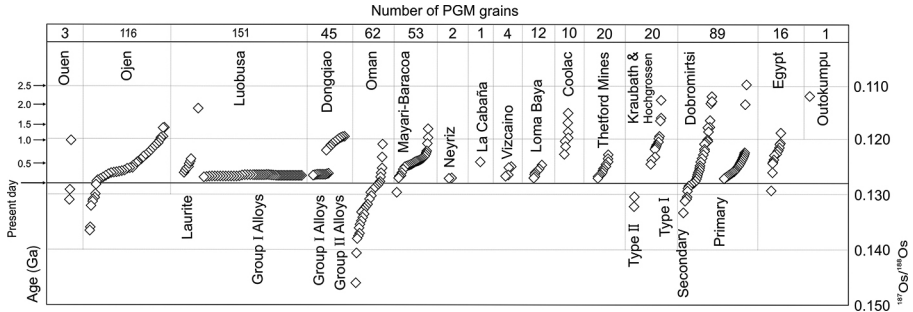
Figure 6.11. $^{187}Os/^{188}Os$ isotopic ratios and corresponding T_{RD} model ages for PGM analyzed *in situ* in chromitites from ophiolite-type ultramafic complexes (modified from O'Driscoll and González-Jiménez, 2016).

6.5   Metallic ores at the peridotite slab-crustal envelope interface

6.5.1   Skarn-type magnetite deposits

As noted in Chapter 1, magnetite has been mined intermittently in the Serranía de Ronda since the middle of the 19th Century till mid 20th Century. The most important mining operations focused on the *El Peñoncillo Mine* (also known as *La Concepción Mine*) in Ojén, near de city of Marbella (Leine, 1967; Westerhof, 1975), although some other small-scale mining exploitations developed in the *Mina San Manuel* (North of Estepona) and *El Robledal* and *La Víbora mines* (south of Ronda) (Orueta, 1917). The marbles underlying the Serranía de Ronda peridotites always hosts magnetite ore, although each deposit exhibits its own, characteristic mineral assemblage.

At *El Peñoncillo*, magnetite is associated with small amounts of pyrrhotite, pyrite and locally fassaite-type pyroxene, forming irregular, banded lenses in amphibolites within dolomitic marbles. According to Westerhof (1975), this deposit cannot be classified as skarn but formed during regional metamorphism due to oxidation of silicates caused by progressive increase of oxygen fugacity linked to synmetamorphic changes of pressure, temperature and partial pressure of water. Iron concentration took place by the combined effect of metamorphism and alteration of silicates and low-temperature hydrothermal alteration related with the intrusion of basic sills and dykes.

The iron mineralization at *San Manuel* is located within a tectonic slice imbricated into peridotite along the lower thrust contact of the Ronda ultramafic massif. Magnetite forms both massive and disseminated bodies within a lithologic sequence consisting, from bottom to top, of migmatites, prograde magnesian skarn containing olivine, calcite and diopside, and dolomitic marble replaced downwards by retrograde magnesian skarn composed of chlorite, serpentine and brucite. Magnetite displays different types of zoning in which magnetite, magnesioferrite and magnetite containing abundant, crystallographically oriented,

minute inclusions of spinel arrange in different patterns, depending on the host assemblage. Other metallic minerals include very minor pyrite and chalcopyrite randomly disseminated in the groundmass of the semi-massive magnetite or in the metasomatized carbonatic rock.

At *El Robledal* and *La Víbora* mines, the ore assemblage is largely dominated by intermediate members of the magnesioferrite-magnetite solid solution series occurring associated with different types of borates, ludwigite ($M_2Fe^{3+}BO_5$), szaibelyite [$MgBO_2(OH)$] and kotoite ($Mg_3B_2O_6$), together with brucite [$Mg(OH)_2$]. The orebody is located too within a tectonic slice of the marble-bearing, underlying metapelitic sequence (the Blanca Unit) pinched by the basal thrust contact of the Ronda peridotites and the partly metamorphosed carbonates of the Nieves Unit (Mazzoli et al., 2014). According to Ares (2017) the iron ore at *El Robledal* whose zoning is made up of massive ludwigite+magnesioferrite to the south, toward the contact with the Ronda peridotites and forming disseminations and vein fillings (1-50 cm in thickness) of magnesioferrite, magnetite, brucite, kotoite and szaiblyite within the calcite marbles of the Blanca Unit to the north. Phase and textural relationships suggest that ludwigite could start crystallizing slightly above 600ºC replacing lizardite, followed by magnesioferrite and later by kotoite at 450-350ºC. Magnetite, szaibelyite and brucite formed as a consequence of the destabilization of the earlier assemblage.

Despite systematic mining of this type of iron ore in the area and the abundance of scientific studies dealing with the Serranía de Ronda ultramafic massifs and their metamorphic aureoles, little has been done to understand the genesis of such deposits (apart from the research by Westerhof, 1975). Many questions arise from the preliminary studies carried out in the San Manuel, El Robledal and La Vibora mines such as the origin of iron and boron, the meaning of the complex mineral zonings observed in some magnetites, the nature of mineralizing fluids, the formation mechanism of Mg-rich assemblages in Mg-poor, calcite marbles and, above all, the role played by the peridotites in these peculiar iron ore forming systems.

6.5.2 Scheelite deposits

Orueta (1917) reported for the first time the presence of isolated scheelite crystals in soils developed on migmatite-gneisses of the Blanca Unit north of Estepona. Later, in the twenties of the past 20th Century this mineral was exploited in two mines, Mina Conchita and Mina Lucía, where it occurs within dolomitic marbles, forming part of a complex mineral assemblage including mainly native bismuth, bismuthinite (Bi_2S_3), joseite [$Bi_4(S,Te)_3$], members of the tetradymite-telluromismuthite (Bi_2Te_2S-Bi_2Te_2Te) series, aleksite ($Bi_2PbTe_2S_2$), minor pyrrhotite, pyrite, arsenopyrite and graphite, with calcite, dolomite, chondrodite, forsterite and diopsite as the main gangue minerals (Romero Silva et al., 2012). These authors suggest a skarn-related, metasomatic origin for this deposit, linked with the anatexis of the gneisses underlying the Ronda peridotite slab but a more detailed scientific research is needed to understand the genesis of this unusual ore assemblage.

References

Alvarez de Linera, A. (1951). Descripción del criadero de níquel de Carratraca. Málaga. Imprenta del Comercio.

Ares, G. (2017). La Mina El Cañuelo (Cordillera Bética occidental): ¿Un ejemplo de skarn de Fe y B no convencional? Master Thesis, University of Zaragoza. Spain.

Chatzipanagiotou, C. (2017). The San Agustín chromite-Ni arsenide and El Gallego Fe-Ni-Cu sulfide-graphite deposits, Carratraca ultramafic massif, southern Spain: mineralogy and geochemistry. Master Thesis, University of Geneva. Switzerland.

Crespo, E., Luque, F.J., Rodas, M., Wada, H. and Gervilla, F. (2006). Graphite-sulfide veins in Ronda and Beni Bousera orogenic lherzolites (Spain and Morocco) and the origin of Carbon in mantle-derived rocks. *Gondwana Research* 9, 279-290.

Gervilla, F. (1990). Mineralizaciones magmáticas ligadas a la evolución de las rocas ultramáficas de la Serranía de Ronda (Málaga, España). Ph. D. Thesis, University of Granada. Spain.

Gervilla, F., Cabri, L.J., Kojonen, K., Oberthür, T., Weiser, T.W., Johanson, B., Sie, S.H., Campbell, J.L., Teesdale, W.J. and Laflamme, J.H.G. (2004). Platinum-group element distribution in some ore deposits: results of EPMA and micro-PIXE analyses. *Microchimica Acta* 147, 163-173.

Gervilla, F., Fenoll Hach-Alí, P.; Torres-Ruiz, J. and Leblanc, M. (1990). Peculiaridades de las mineralizaciones de la Mina San Juan (Los Jarales, Carratraca) en el contexto de los depósitos de cromita-arseniuros de niquel de los macizos ultramáficos bético-rifeños. *Boletín de la Sociedad Española de Mineralogía* 12-2, 209-224.

Gervilla, F., Gutiérrez-Narbona, R. y Fenoll Hach-Alí, P. (2002). The origin of different types of magmatic mineralizations from small-volume melts in the lherzolite massifs from the Serranía de Ronda (Málaga, Spain). *Boletín de la Sociedad Española de Mineralogía* 25, 79-96.

Gervilla, F. and Leblanc, M. (1990). Magmatic ores in high-temperature Alpine-type lherzolite massifs (Ronda, Spain) and Beni Bousera, Morocco). *Economic Geology* 85, 112-132.

Gervilla, F., Leblanc, M., Torres-Ruiz, J. and Fenoll Hach-Alí, P. (1996). Immiscibility between arsenide and sulfide melts: a mechanism for the concentration of noble metals. *The Canadian Mineralogist*, 34, 485-502.

Gervilla, F. y Rønsbo, J. (1992). New Data on (Ni,Fe,Co) diarsenides and sulpharsenides in chromite-niccolite ores from Málaga province, south Spain. *Neues Jahrbuch für Mineralogie Monatshefte* H.5, 193-206.

González-Jiménez, J.M., Marchesi, C., Griffin, W.L., Gervilla, F., Belousova, E.A., Garrido, C.J., Romero, R., Talavera, C., Leisen, M., O'Reilly, S.Y., Barra, F. and Martin, L. (2017). Zircon recycling and crystallization during formation of chromite- and Ni-arsenide ores in the subcontinental lithospheric mantle (Serranía de Ronda, Spain). *Ore Geology Reviews* 90, 193-209.

González-Jiménez, J.M., Marchesi, C., Griffin, W.L., Gutiérrez-Narbona, R., Lorand, J.P., O'Reilly, S.Y., Garrido, C.J., Gervilla, F., Pearson, N.J. and Hidas, K. (2013). Transfer of Os isotopic signatures from peridotite to chromitite in the subcontinental mantle: insights from in situ analysis of platinum-group and base-metal minerals (Ojén peridotite massif, southern Spain). *Lithos* 164-167, 74-85.

Gutiérrez-Narbona, R. (1999). Implicaciones metalogénicas (cromo y elementos del grupo del platino) de los magmas/fluidos residuales de un proceso de percolación a gran escala en los macizos ultramáficos de Ronda y Ojén (Béticas, Sur de España). Ph. D. Thesis, University of Granada. Spain.

Gutiérrez-Narbona, R., Lorand, J.P., Gervilla, F. and Gros, M. (2003). New data on base metal mineralogy and platinum-group minerals in the Ojén chromitites (Serranía de Ronda, Betic Cordillera, Southern Spain). *Neues Jahrbuch für Mineralogie Abhandlungen* 179 (2), 143-173.

Hem, S.R. (1998). The ore mineralogy of the Arroyo de la Cueva deposits, Ronda massif, Southwest Spain. Master Thesis. University of Copenhagen. Denmark.

Hem, S.R., Makovicky, E. and Gervilla, F. (2001). Compositional trends in Fe, Co and Ni sulfarsenides and their crystal chemical implications: results from the Arroyo de la Cueva deposits, Ronda Peridotite, South Spain. *The Canadian Mineralogist,* 39 (3), 831-854.

Leblanc, M., Gervilla, F. and Jedwab, J. (1990). Noble metals segregation and fractionation in magmatic ores from Ronda and Beni Bousera lherzolite massifs (Spain, Morocco). *Mineralogy and Petrology* 42 (1-4), 133-248.

Leine, L. (1967). Geology of a magnetite deposit of the Mg-Skarn type near Marbella, Spain. *Economic Geology* 62, 926-931.

Mazzoli, S., Martín-Algarra, A., Reddy, S.M., Sánchez-Vizcaíno, V.L., Fedele, L. and Noviello, A. (2014). The evolution of the footwall to the Ronda subcontinental mantle peridotites: insights from the Nieves Unit (western Betic Cordillera). *Journal of the Geological Society* 170(3), 385-402.

Oen, I.S. (1973). A peculiar type of Ce-Ni mineralization; cordierite-chromite-niccolite ores of Málaga, Spain, and their possible origin by liquid unmixing. *Economic Geology* 68, 831-842.

Oen, I.S., Burke, E.A.J., Kieft, C. and Westerhof, A.B. (1971). Ni arsenides, Ni-rich löllingite and (Fe-Co)-rich gersdorffite in Cr-Ni ores from Málaga province, Spain. *Neues Jahrbuch für Mineralogie Abhandlungen* 115 (2), 123-139.

Oen, I.S., Kieft, C., Burke, E.A.J. and Westerhof, A.B. (1980). Orcelite and associated minerals in the Ni-Fe-As-S system in chromitites and orthopyroxenites of Nebral, Málaga, Spain. *Bulletin de Mineralogie* 103, 198-208.

Orueta-Duarte, D. (1917). Estudio geológico y petrográfico de la Serranía de Ronda. *Memorias del Instituto Geológico y Minero de España* 32, 571 pp.

Piña, R., Gervilla, F., Barnes, S.-J, Ortega, L. and Lunar, R. (2013). Partition Coefficients of Platinum Group and Chalcophile Elements Between Arsenide and Sulfide Phases as Determined in the Beni Bousera Cr-Ni Mineralization (North Morocco). *Economic Geology* 108, 935-951.

Piña, R., Gervilla, F., Barnes, S.-J, Ortega, L. and Lunar, R. (2015). Liquid immiscibility between arsenide and sulfide melts: evidence from LA-ICP-MS study in magmatic deposits from Serranía de Ronda (Spain). *Mineralium Deposita* 50, 265-279.

Romero Silva, J.C., Martos Martín, J. and Navarro García, J.M. (2012). La Mina Conchita de Estepona (Málaga). Un raro yacimiento de metales complejos en Sierra Bermeja. *Takurunna* 2, 9-39.

Torres-Ruiz, J., Garuti, G., Gazzoti, M., Gervilla, F. and Fenoll Hach-Alí, P. (1996). Platinum-group minerals in chromitites from the Ojén lherzolite massif (Serranía de Ronda, Betic Cordillera, Southern Spain). *Mineralogy and Petrology*, 56, 25-50.

Torres-Ruiz, J., Gervilla, F. and Leblanc, M. (1991). Mineralogía y comportamiento geoquímico del oro en los macizos lherzolíticos bético-rifeños (España-Marruecos). *Estudios Geológicos* 47, 281-293.

Westerhof, A.B. (1975). Genesis of magnetite ore near Marbella, Southern Spain: Formation by oxidation of silicates in polymetamorphic gedrite-bearing and other rocks. *GUA papers of geology*. Amsterdam. 216 pp.

Chapter 7
Genesis of ores hosted in the ultramafic rocks

7.1 Keys for a magmatic origin of the ores

In the ultramafic massif of the Serranía de Ronda, Cr-Ni ores rich in noble metals (~ 2 ppm PGE and 15 ppm Au) and S-G ores poor in noble metals (<800 ppb PGE and 230 ppb Au) are mainly located above the recrystallization front in the spinel (± garnet) tectonite domain. In contrast, Cr ores (up to 2 ppm PGE and 9 ppb Au) always occur in refractory peridotites within the plagioclase tectonite domain. This spatial distribution of the different types of ores according to the zoning of the ultramafic massifs was already observed since early scientific works, although interpreted in different ways. Thus, pioneering works dated at the 70s of the 20th Century linked the origin of arsenide ores to hydrothermal processes, suggesting that the assemblage of chromite and Ni arsenides in the Cr-Ni ores of the Serranía de Ronda ultramafic massifs resulted from hydrothermal deposition of arsenides on a pre-existing magmatic chromite-orthopyroxene ore (Instituto Geológico y Minero de España, 1978).

An almost contemporaneous model proposed by Oen (1973) suggested a magmatic origin of the Cr-Ni ores. In the model proposed by Oen (1973) the ores formed via fractional crystallization of a mafic parental melt, which would evolve within the system Mg_2SiO_4-$MgAl_2O_4$-$MgCr_2O_4$-SiO_2 (Irvine, 1967) by the syn-crystallization of orthopyroxene and chromite, followed by cotectic crystallization of orthopyroxene+cordierite and chromite. This author hypothesized that a sudden change in the ore-forming system (it could be the addition of an Al_2O_3-rich component) should be enough to modify phase relations to those shown in Fig. 7.1a. At this stage, the parental melt (L) should have a composition within the two-liquids region of Fig. 7.1a, which unmixed into an orthpyroxene-rich liquid (L1) and a cordierite-rich liquid (L2). The latter (L2) could crystallize separately forming cordierite and the former (L1) could form cordierite-orthopyroxene. Assuming some CaO in the melt L2 would form cordierite-plagioclase and L1 cordierite-clinopyroxene, as is observed in the San Juan ores. Fig. 7.1b further hypothesizes on the possible coexistence of a third chromite-rich liquid (L3) in the system. Oen (1973) argues that As (and eventually S) should partition towards this chromite-rich liquid (L3), which became saturated in S and As due to the strong consumption of FeO by the crystallizing chromite as well
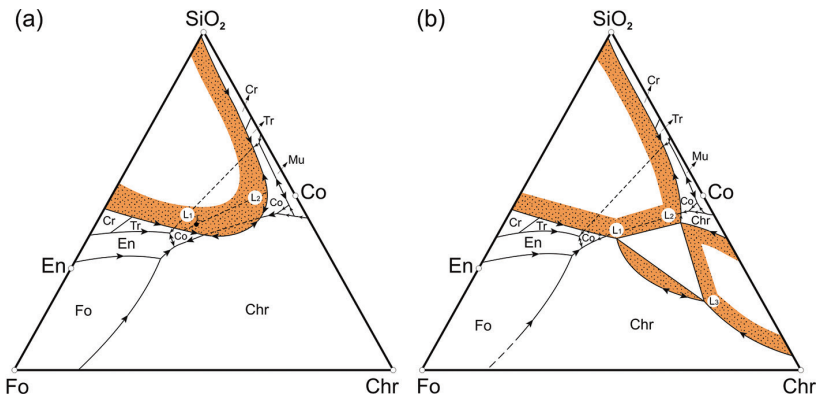
Figure 7.1. Phase relations in the system forsterite-quartz-chromite suggested by Oen (1973) to explain the formation of the chromite-orthopyroxene-cordierite assemblages forming the Cr-Ni ores of the ultramafic massif of the Serranía de Ronda. Keys: Fo: forsterite, Chr: chromite, En: enstatite, Co: cordierite, Tr: trydiminte, Cr: crystobalite, Mu: mullite.

as the SiO_2 enrichment triggered in the residual melt. As and S saturation promoted segregation of an immiscible melt which fractionate later by the crystallization of Ni arsenides intergranular to chromite and leaving a S-rich residual melt. The segregation and separate crystallization under appropriate conditions of all these liquids would give rise to the formation of the different ore assemblages observed in Cr-Ni ores. This model seems to fit with the observed textural, mineralogical and chemical evidences observed in the Cr-Ni apparently indicating the magmatic crystallization of the Ni-arsenides and chromite, i.e., 1) intimate association of chromite and Ni arsenides in cumulate-textured ores with Cr-Ni layers grading to silicate layers; 2) syncrystallization textures such as arsenide and chromite inclusions along the borders of the cumulus crystals of orthopyroxene, and arsenide and orthopyroxene inclusions in chromite; 3) the presence of Ni- and Co-rich loellingite (Oen et al., 1971; Gervilla and Rønsbo, 1992) indicating crystallization at high temperatures (>625ºC) and also the presence of multiphased lamelar sulfide inclusions in nickelite attesting to the former existence of a high-temperature (>800ºC) monosulfide solid solution-NiAs mixed phase; and 4) platinum-group element contents in arsenides similar to those from platiniferous sulfide-rich horizons in stratiform magmatic complexes, suggesting an early magmatic segregation of an As-rich, platinum-group element-collecting phase (Gervilla and Leblanc, 1990). What was unexplained in Oen's model is why this cotectic crystallization of orthopyroxene and chromite evolved to the formation of monomineralic cordierite rocks in equilibrium with chromite. Moreover, in a first instance the mineral assemblage characterizing the Cr-Ni ores (Al-rich chromite with Y_{Cr}=0.25 associated with Ni arsenides, orthopyroxe and cordierite) can hardly be envisaged as magmatic as derived from "usual" mantle-derived basaltic melts. Thus some questions arise when one attempt to interpret the magmatic origin of these ores: 1) what mantle processes could produce the melts with such high Al contents?, 2) how these melts could become sufficiently enriched in arsenic to form ores with up to 50 vol.% Ni arsenides.

Almost two decades later, Gervilla (1990) and Gervilla and Leblanc, (1990) linked the formation of the Cr-Ni ores to the fractionation of an immiscible As-S-Fe-Ni-Cu-rich liquid eventually segregated at high temperature after the crystallization of chromite, orthopyroxene and/or cordierite from a highly differentiated mafic melt. They related the origin of this parental mafic melt to the partial melting of a SCLM already metasomatized with As, which was deduced from the presence of anomalous As contents in some peridotites from the Serranía de Ronda (Gervilla and Leblanc, 1990) and accessory Ni arsenides in mafic layers from the equivalent Beni Bousera ultramafic massif (Lorand, 1987). In this model, the mafic melts originated from a SCLM strongly metasomatized with As should have experienced extreme fractionation when migrating from the lower, partially molten zone of the mantle upwards while precipitating the different types of ores, thus explaining the spatial relationships between ore types and zoning of the host peridotites (Gervilla, 1990; Gervilla and Leblanc, 1990). Strong fractionation resulting in highly fractionated mafic-ultramafic melts could be eventually achieved if one consider that these corresponded to very small fraction of melts migrating through the cooling upper mantle (Gervilla et al., 2002). However, these models did not provide conclusive evidence on the origin of the As that metasomatized this volume of SCLM, on the nature of the parental mafic melts nor on the timing of ore formation within the framework of the mantle evolution of these ultramafic rocks and their subsequent crustal emplacement. More recent petrological, structural, geochemical and geochronological data provided new evidences on the evolution of the SCLM before and during its intra-crustal emplacement and the timing of the ore-types formation, suggesting a genesis of the ores related with interaction between this portion of the SCLM and the adjacent continental crust during the emplacement of the former (see below).

7.2   Genesis of the Cr-Ni and S-G ores by contamination of the SCLM with crustal components

As noted in Chapter 5, the ultramafic massifs of the Serranía de Ronda are fragments of an old Proterozoic SCLM emplaced tectonically into the continental crust in the Early Miocene, probably during the development of a back-arc basin behind the Betic-Rifean orogenic wedge (e.g. Van der Wal and Vissers, 1993; Van der Wa and Bodinier, 1996; Garrido and Bodinier, 1999; Lenoir et al., 2001; Hidas et al., 2013; González-Jiménez et al., 2017) (Fig. 7.2). Southward to westward retreat of the Thethys oceanic slab that was consumed under this arc during the Late Oligocene-Early Miocene (~25 Ma) promoted extensive back-arc lithosphere extension, leading to extreme thinning of the Alboran crust and its underlying SCLM (Garrido et al., 2011). This attenuation of the lithospheric root promoted a km-scale upwelling of asthenosphere-derived melt that pervasively infiltrated and partially melted the thinned SCLM (Van der Wall and Bodinier, 1996; Garrido and Bodinier, 1999; Lenoir et al., 2001; Marchesi et al., 2012). In this scenario, the rapid uplift of the peridotites (ascent rates of 0.4 cm/year; Platt et al., 1998) caused cooling of the shallowest portion of the upper mantle preventing the upward migration of the partial melts above the recrystallization front
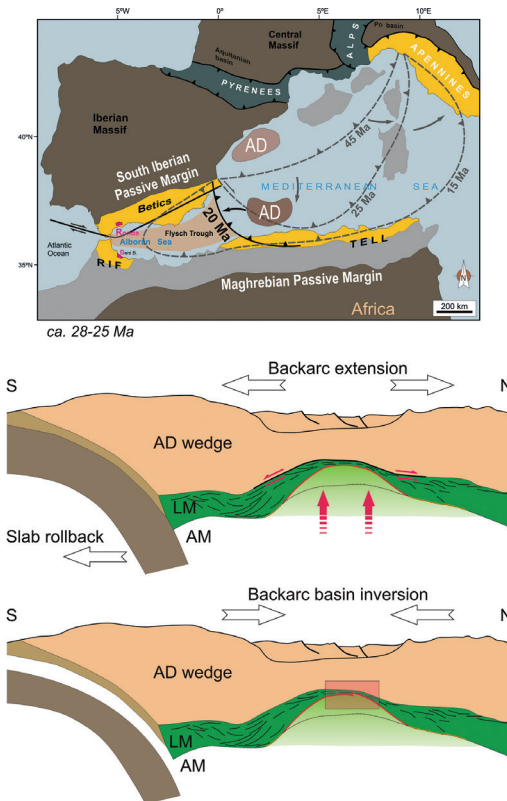
Figure 7.2. Tectonic evolution of the Western Mediterranean realm during the Cenozoic (modified from Hidas et al., 2013).

(Van der Wal and Vissers, 1993), corresponding to an isotherm close to the dry peridotite solidus (Lenoir et al., 2001). Thus, when upward migrating partial melts reached the recrystallization front they reacted with the host peridotite to form clinopyroxene ± spinel at expenses of orthopyroxene (or olivine) while segregated small-volume of residual, volatile-rich melts. These small fractions of residual melt migrated away the recrystallization front experiencing fractionation (as a result of the crystallization of interstitial clinopyroxene), or they were injected into opening fractures giving rise to intrusive, Cr-rich pyroxenite dykes (Garrido, 1995; Marchesi et al., 2012). The residual melts generated by these processes became progressively richer in SiO_2, Al_2O_3, TiO_2, V_2O_3 and FeO, and concentrate the volatile components (H_2O, F, Cl and C) as well as As, S and chalcophile elements (including PGE and Au) from which the Cr-Ni ores, S-G ores and later the Cr ores were formed (Gervilla et al., 2002). This model requires anomalous As contents in the SCLM prior to the infiltration of the asthenosphere-derived melts as well as an efficient mechanism to concentrate As in the small-volume, residual melts up to reaching their saturation and the subsequent segregation of arsenide or, more probably, As-S melts. Nevertheless, the segregation of arsenide melts is a rather uncommon process in the upper mantle owing the fact that most natural basalts are orders of magnitude below As saturation, even after 95% of crystallization (e.g., Wood, 2003). Additional supply of As to the ore-forming system would be required to achieve the segregation of arsenide melts coeval with or soon after the crystallization of chromite, orthopyroxene and/ or cordierite.

The assumption that the parental melts of the Cr-Ni and S-G ores derived from residual, volatile-rich small-volume melts migrating upwards through the spinel (± garnet) tectonite domain that occasionally were injected within opening fractures lead us to question why these small-volume melts sometimes form Cr-Ni ore bodies but in some others they form barren Cr-rich pyroxenites. The fractures where these small fractions of melt were injected corresponded to weak zones developed parallel

to the axial fold-thrust structure that aided the crustal emplacement of the attenuated SCLM into the Alborán wedge (Fig. 7.3; Hidas et al., 2013). In this scenario, the relatively hot emplacement of the peridotite may have promoted dehydration and subsequent anatexis of the enclosing crustal units (mainly metasediments) (Fig. 7.3a). Within such fold-related, opening fractures, the fluid-rich phase accompanying the anatectic melt could eventually infiltrate the ultramafic rocks and encounter the small fractions of highly fractionated mafic-ultramafic melt squeezed outwards from the recrystallization front (Fig. 7.3b). When these two very distinct types of melts mingle they could produce a suite of "exotic" mafic melts with exceptionally high content of Cr, Al, Ti, V, Fe, Ni, Co, Cu, Zn, S and As from which precipitate those cordierite-(Cr-Ni) ores found well above the recrystallization front in the spinel tectonite domain (Fig. 7.3b). The crustal-derived fluid-rich melts would supply the additional As required to achieve As saturation as well as the necessary C to form graphite with biogenic carbon signature (Crespo et al, 2006). Mingling of the highly fractionated mafic-ultramafic melts with the anatexis-related fluid-rich melts promoted the crystallization of chromite (Irvine, 1977; Ballhaus, 1998) and the subsequent segregation of immiscible arsenide melts (with variable S contents), which remained interstitial among chromite crystals and gave rise to the Ni arsenide assemblage on cooling, below 900ºC (Gervilla and Leblanc, 1990; Gervilla et al., 1996; Gervilla et al., 2002). These authors hypothesized that the arsenide-rich melt was segregated slightly before the sulfide melt, thus collecting most of the Ni and noble metals, which become concentrated along with chromite in the PGE- and Au-rich Cr-Ni ores. As a consequence, the immiscible sulfide melt that was segregated soon after was depleted in noble metals, thus explaining the formation of S-G ores poorer in noble metals. The observation of pyrrhotite-chromite and chalcopyrite-chromite layers within the chromite-nickelite ore (e.g., La Gallega) as well as the presence of arsenide blebs embedded in the matrix of Ni-Fe-Cu sulfide in transitional S-G ores (e.g., Los Jarales; Gervilla et al., 1996) clearly attest that the arsenide melt kept some amounts of S, which segregated as small volumes of sulfide melt during the crystallization of the Ni arsenides, and in turn, the sulfide melt locally entrained small volumes of the earlier segregated immiscible arsenide melt.

As noted above, this model assumes that Cr-Ni and S-G ores were genetically linked as the two immiscible arsenide and sulfide melt were segregated from a common precursor As- and S-, volatile-rich melt (Gervilla and Leblanc, 1990; Gervilla et al., 1996, 2002). Some evidence supporting this interpretation include: (1) the similar spatial distributions of Cr-Ni and S-G mineralization with respect to the zoning of the peridotite massifs, (2) textural evidence (composite exsolution lamellae of pyrrhotite, pentlandite and chalcopyrite in nickelite of Cr-Ni ores; nickelite and/or maucherite inclusions in Fe-Ni-Cu sulfides of S-G ores, (3) the existence of a few samples in which both assemblages coexist with PGE preferentially concentrted in arsenides relative to Fe-Ni-Cu sulfides (Piña et al., 2013, 2015), and (4) empirical and experimental studies suggesting that arsenide and sulfide melts are immiscible over a wide range of temperatures (~850–1,200 °C) with PGE preferentially partitioned into the arsenide melt (Merkle, 1992; Makovicky et al. 1990, 1992; Fleet et al. 1993; Gervilla et al., 1994, 2004; Wood, 2003; Hanley, 2007; Canali et al., 2017; Piña et al., 2013).
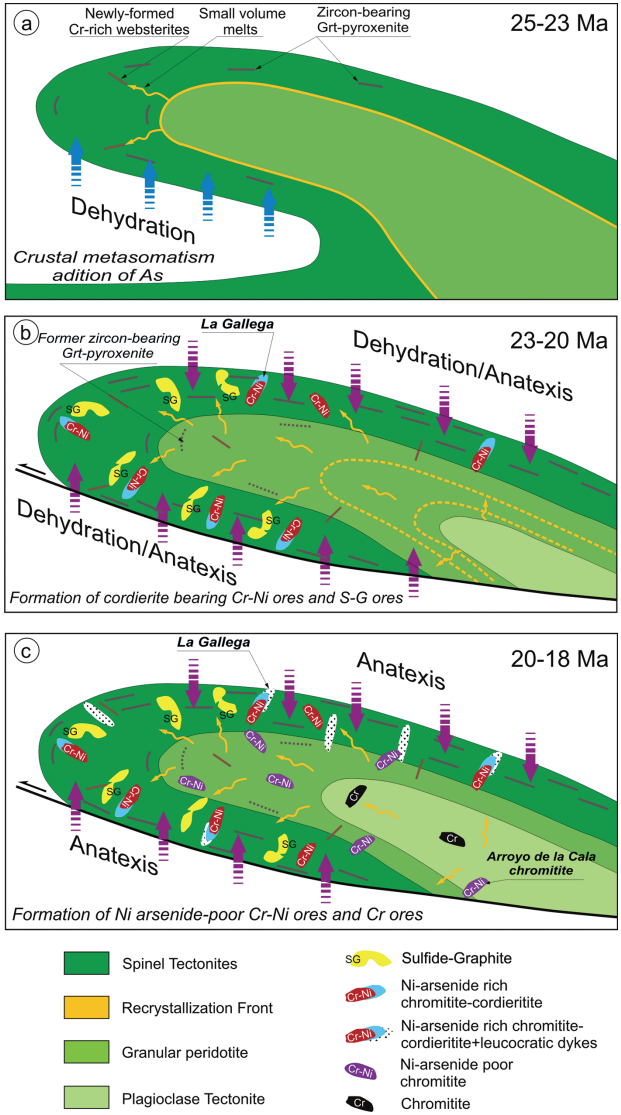
Figure 7.3. Genesis of the different ore types within the mantle peridotites during the development of the fold-thrust structure that aided the intra-crustal emplacement of the Serranía de Ronda Ultramafic massifs (mofied from Gonzalez-Jiménez et al.,2017). Legend inset in the figure.

Progressive penetration of the host peridotite slab into the crust further favored anatexis of the crustal units (mainly metasediments), giving rise to higher volumes of highly-peraluminous melts that intruded the peridotite at ca. 21-18 Ma through the aforementioned fracture system (Fig. 7.3c; González-Jiménez et al., 2017 and references therein). These melts formed the leucogranite dykes which eventually

cross-cut the already formed Cr-Ni ore veins as was observed in the El Sapo Mine where leucogranite dykes include fragments of orthopyroxene-bearing Cr-Ni ores surrounded by a reaction aureole mainly made up of antophyllite and phlogopite.

On the other hand, the observation that Cr-Ni ores located close to, or below, the recrystallization front (e.g., El Nebral and El Lentisco) do not contain cordierite and mostly consist of Cr-rich chromite associated with Mg-rich orthopyroxenite with very little amounts of Ni-arsenides (< 10 vol %) suggest less penetration of the anatectic acidic melts through the fractures should become towards the inner parts of the ultramafic bodies (Fig. 7.3c). In addition, one could expect that when peridotites rose up, they cooled down, enhancing the crystallization of the interstitial melt below the former recrystallization front, thus moving this partial melting and melt migration front to deeper horizons in the mantle (Fig. 7.3c). The melts originated in this stage derived by partial melting (and melt/rock reactions) of peridotites that already experienced high rates of melting and were progressively smaller in volume. As a consequence, these small-volume melts should be relatively richer in Cr and Mg but significantly more impoverished in Al_2O_3, V_2O_3, FeO, S and chalcophile elements. In fact, further uplift and cooling of the ultramafic body may have retracted the melt migration front towards the inner part of the fold-thrust structure (Fig. 7.3c), restricting the migration of melts through dunite channels representing zones of higher permeability. This may explain why Ni-arsenide-poor Cr-Ni ores (e.g., Arroyo de la Cala and Mina Baeza) and Ni-arsenide free Cr ores (e.g., Arroyo de los Caballos) are mainly found in dunites and shear zones of the plagioclase tectonite domain. Furthermore, the observation that the Arroyo de la Cala Cr-Ni ore (Fig. 6.5) exhibit deformation before its final consolidation (Gervilla and Leblanc, 1990) indicate that the injection of its parental melt through the shear zone was synchronous with the development of the plagioclase tectonite. However, isolation of the small-fraction of melts could not account only by their injection into opening fractures but also as a consequence of the rapid undercooling of the peridotites owing the high rates of the ascent of the peridotites during the latest stages of crustal emplacement. In a relatively cooled peridotite slab the migration of the very small-fractions of melt should have been taken place under non-equilibrium conditions, thus explaining the great variety of composition and thickness of the dunite envelope observed in this type of ores. Variable extents of melt-rock reaction may have resulted in different capacity of the small-fractions of melts to extract Cr and Al at distinctively different Cr_2O_3/Al_2O_3 ratios via dissolution of pyroxenes from the host rock (Arai and Yurimoto, 1994).

7.3   Origin of the Cr ores from small-volume of residual, volatile-rich melts

The Cr ores identified in the ultramafic rocks of the Serranía de Ronda contain abundant inclusions of hydrous silicates in chromite (these silicates are rich in Na, OH, K and Cl; Gutiérrez-Narbona et al., 2003). This suggests that their parental melts were particularly rich in volatile component and alkalis. One could expect a singular concentration of alkalis, halogens and volatiles (C-O-H) in order to produce small fractions of highly alkaline hydrous melts, considering the fact that

these very small fraction of melts were previously produced after extensive melt-rock and pervasive porous flow with decreasing melt volume and temperature. Relatively high concentrations of volatile probably favored the unmixing of a fluid-rich silicate phase that would concentrate chromite (Matveev and Balhaus, 2002) from a relatively drier silica-rich melt that would precipitate a new generation of Cr- and Mg-rich orthopyroxenites. For example, in the Arroyo de la Cala Cr-(Ni) ore, the generation of both chromitite and orthopyroxenite is suggested by the mutual transitional contacts between these two types of rocks. Additionally, the parental melt of the latter pyroxenites had a boninitic-like signature with a weaker imprint of crustal contamination (type D pyroxenites; Garrido and Bodinier, 1999; Marchesi et al., 2012), which is consistent with the Cr-rich composition of the chromite typical of chromite from arc-type melts of boninitic affinity. The observation that this Cr(-Ni) ore contain a population of zircons identical to that reported in garnet pyroxenites from the spinel (± garnet) tectonite domain (González-Jiménez et al. 2017), allow to track the origin of these parental melts as related to the product of the reaction of upwelling asthenosphere-melts and former garnet pyroxenites.

A relatively high concentration of volatile not only favored the unmixing of a fluid-rich silicate phase from the latter small-volume melts but also hydraulic overpressure due to focused melt/fluid accumulation and subsequent volume expansion, particularly in a relatively cold peridotite. At the P-T conditions (~1200ºC and ≤ 1GPa) under which the plagioclase tectonite domain was formed, it may have favored the replacement of neighboring (co-genetic pyroxenites) as indicated by the occurrence of the chromitites as entwined and contorted veins replacing clino- and ortho-pyroxenites (Gutiérrez-Narbona, 1999). The assimilation of pyroxenites may have further supplied silica and/or chromium required to move the hydrous melt into the chromite liquidus field (Bédard and Herbert, 1998), thus explaining the correlation between the chromite composition and type or pyroxenite relics found in chromitites: clinopyroxene for high-Al chromitites (e.g., CDA chromitite) versus orthopyroxene for high-Cr chromitite (e.g., ARC and ACA chromitites), which would reflect the Cr_2O_3/Al_2O_3 ratio of the mafic rock being assimilated. Further evidence for the unmixing of a water-rich fluid phase is provided by the late, discordant millimeter-thick veins of amphibolite that locally occur around the chromitite bodies. These discordant amphibolite have been interpreted as the product of reaction between the fluid and the host peridotite along the walls of narrow cracks (González-Jiménez et al., 2013).

The identification of PGM and BMS as euhedral inclusions in unaltered cores of chromite grains indicate their crystallization from melts and their later mechanical entrapment by crystallizing chromite. Torres-Ruiz et al. (1996), Gutiérrez-Narbona et al. (2003) and González-Jiménez et al. (2013) noted that Os-poor laurite crystals crystallized at ~1200ºC, at very low sulfur fugacity conditions (log fS_2 < -2), although the coexistence of these laurite with some grains of erlichmanite (OsS_2) in some zoned grains indicate local variations of temperature and/or fS_2 (González-Jiménez et al., 2009). González-Jiménez et al. (2013) suggested that local changes of temperature and fS_2 could be achieved during the injection of different batches of small-volume melts within the dunite channels/fractures/shear zones where the chromitite were formed. Initial (or local) low fS_2 may also explain why some of the

Cr ores contain Os-rich alloys coexisting with laurite-erlichmanite and PGE alloys, which might also have been formed by sulfurization of pre-exiting Os-Ir-(Ru) alloys when the activity of S (or As) rose up (e.g., Bockrath et al., 2004). This is consistent with the extensive solid solution between laurite-erlichmanite and PGE-sulfarsenides in the studied chromitites (Torres-Ruiz et al., 1996; Gutiérrez-Narbona et al., 2003). It is also worth to note that the Cr ores hosted in the SCLM of the Serranía de Ronda contain an abnormally high number of grains of Fe-Ni-(Cu)-bearing sulfides and sulpharsenides, which can also be forming triple junctions along chromite grains. The textural position of these latter minerals suggest the possible segregation of small fractions of immiscible S-As-rich melts enriched in base metals as a result of oversaturation in volatile and subsequent ummixing from a silicate melt. This is a very uncommon feature of chromitites hosted in either oceanic or subcontinental mantle, which attest to the relatively high As in the melts that have precipitated these chromitites. As noted above, these relatively high As contents in the parental melts of the Cr ores can be explained by considering that their parental melts were small-volume melts formed after extensive reaction between migrating melts and a SCLM polluted with crustal material.

References

Arai, S. and Yurimoto, H. (1994). Podiform chromitites of the Tari-Misaka ultramafic complex, Southwest Japan, as mantle-melt interaction products. *Economic Geology* 89, 1279-1288.

Ballhaus, C. (1998). Origin of podiform chromite deposits by magma mingling. *Earth and Planetary Science Letters* 156, 185-193.

Bédar, J.H. and Hébert, R. (1998). Formation of chromitites by assimilation of crustal pyroxenites and gabbros into peridotitic intrusions: North Arm Mountain massif, Bay of Island ophiolite, Newfounland, Canada. *Journal of Geophysical Research* 103, 5165-5184.

Bockrath, C., Ballhaus, C. and Holzheid, A. (2004). Stabilities of laurite RuS2 and monosulphide liquid solution at magmatic temperature. Chemical Geology 208, 265-271.

Canali, A.C., Brenan, J.M. and Sullivan, N.A. (2017). Solubility of platinum-arsenide melt and sperrylite in synthetic basalt at 0.1 MPa and 1200ºC with implications for arsenic speciation and platinum sequestration in mafic igneous systems. *Geochimica et Cosmochimica Acta* 216, 153-168.

Crespo, E., Luque, F.J., Rodas, M., Wada, H. and Gervilla, F. (2006). Graphite-sulfide veins in Ronda and Beni Bousera orogenic lherzolites (Spain and Morocco) and the origin of Carbon in mantle-derived rocks. *Gondwana Research* 9, 279-290.

Fleet, M.E., Chryssoulis, S.L., Stone, W.E. and Weisener, C.G. (1993). Partitioning of platinum-group elements and Au in the Fe-Ni-Cu-S system: experiments on the fractional crystallization of sulfide melt. *Contributions to Mineralogy and Petrology* 115, 36-44

Garrido, C.J. (1995). Estudio geoquímico de las capas máficas del Macizo Ultrmáfico de Ronda. Ph. D. Thesis, University of Granada.

Garrido, C.J. and Bodinier, J.L. (1999). Diversity of mafic rocks in the Ronda peridotite: evidence for pervasive melt/rock reaction during heating of subcontinental lithosphere by upwelling asthenosphere. *Journal of Petrology* 40, 729-754.

Garrido, C.J., Gueydan, F., Booth-Rea, G., Precigout, J., Hidas, K., Padron-Navarta, J.A. and Marchesi, C. (2011). Garnet lherzolite and garnet-spinel mylonite in the Ronda peridotite: vestiges of Oligocene backarc mantle lithospheric extension in the western Mediterranean. *Geology* 39, 927–930.

Gervilla, F. (1990). Mineralizaciones magmáticas ligadas a la evolución de las rocas ultramáficas de la Serranía de Ronda (Málaga, España). Ph. D. Thesis, University of Granada.

Gervilla, F., Cabri, L.J., Kojonen, K., Oberthür, T., Weiser, T.W., Johanson, B., Sie, S.H., Campbell, J.L., Teesdale, W.J. and Laflamme, J.H.G. (2004). Platinum-group element distribution in some ore deposits: results of EPMA and micro-PIXE analyses. *Microchimica Acta* 147, 163-173.

Gervilla, F., Gutiérrez-Narbona, R. y Fenoll Hach-Alí, P. (2002). The origin of different types of magmatic mineralizations from small-volume melts in the lherzolite massifs from the Serranía de Ronda (Málaga, Spain). *Boletín de la Sociedad Española de Mineralogía* 25, 79-96.

Gervilla, F. and Leblanc, M. (1990). Magmatic ores in high-temperature Alpine-type lherzolite massifs (Ronda, Spain) and Beni Bousera, Morocco). *Economic Geology* 85, 112-132.

Gervilla, F., Leblanc, M., Torres-Ruiz, J. and Fenoll Hach-Alí, P. (1996). Immiscibility between arsenide and sulfide melts: a mechanism for the concentration of noble metals. *Canadian Mineralogist*, 34, 485-502.

Gervilla, F., Makovicky, E., Makovicky, M. y Rose-Hansen, J. (1994). The system Pd-Ni-As at 790° and 450°C. *Economic Geology*, 89, 1630-1639.

González-Jiménez, J.M., Gervilla, F., Proenza, J.A., Kerestedjian, T., Augé, T. y Bailly, L. (2009). Zoning of laurite (RuS_2)-erlichmanite(OsS_2): Implications for the origin of PGM in ophiolitic chromitites. *European Journal of Mineralogy* 21, 419-432

González-Jiménez, J.M., Marchesi, C., Griffin, W.L., Gervilla, F., Belousova, E.A., Garrido, C.J., Romero, R., Talavera, C., Leisen, M., O'Reilly, S.Y., Barra, F. and Martin, L. (2017). Zircon recycling and crystallization during formation of chromite- and Ni-arsenide ores in the subcontinental lithospheric mantle (Serranía de Ronda, Spain). *Ore Geology Reviews* 90, 193-209.

González-Jiménez, J.M., Marchesi, C., Griffin, W.L., Gutiérrez-Narbona, R., Lorand, J.P., O'Reilly, S.Y., Garrido, C.J., Gervilla, F., Pearson, N.J. and Hidas, K. (2013). Transfer of Os isotopic signatures from peridotite to chromitite in the subcontinental mantle: insights from in situ analysis of platinum-group and base-metal minerals (Ojén peridotite massif, southern Spain). *Lithos* 164-167, 74-85.

Gutiérrez-Narbona, R. (1999). Implicaciones metalogénicas (cromo y elementos del grupo del platino) de los magmas/fluidos residuales de un proceso de percolación a gran escala en los macizos ultramáficos de Ronda y Ojén (Béticas, Sur de España). Ph. D. Thesis, University of Granada. Spain.

Gutiérrez-Narbona, R., Lorand, J.P., Gervilla, F. and Gros, M. (2003). New data on base metal mineralogy and platinum-group minerals in the Ojén chromitites (Serranía de Ronda, Betic Cordillera, Southern Spain). *Neues Jahrbuch für Mineralogie Abhandlungen* 179 (2), 143-173.

Hanley J. (2007). The role of Arsenic-rich melts and mineral phases in the development of high grade Pt-Pd mineralization within komatiite-associated magmatic Ni-Cu sulfide horizons at Dundonald Beach South, Abitibi Subprovince, Ontario, Canada. *Economic Geology* 102, 305–317.

Hidas, K., Booth-Rea, G., Garrido, C.J., Martínez-Martínez, J.M., Padrón-Navarta, J.A., Konc, Z., Giaconia, F., Frets, E. and Marchesi, C. (2013). Backarc basin inversion and subcontinental mantle emplacement in the crust: kilometre-scale folding and shearing at the base of the proto-Alborán lithospheric mantle (Betic Cordillera,southern Spain). *Journal of the Geological Society* 170, 47–55.

Irvine, T.N. (1967). Chromian spinel as petrogenetic indicator. Part II: petrologic aplications. Canadian Journal of Earth Sciences 4, 71-103.

Irvine, T.N. (1977). Origin of chromite layers in the Muskox intrusion and other stratiform intrusions: A new interpretation. *Geology* 5, 273-277.

Lenoir, X., Garrido, C.J., Bodinier, J.-L., Dautria, J.-M. y Gervilla, F. (2001). The recrystallization front of the Ronda peridotite: Evidence for melting and thermal erosion of subcontinental lithospheric mantle beneath the Alborán basin. *Journal of Petrology,* 42 (1), 141-158.

Lorand, J.P. (1987). Sur Lòrigine mantellaire d l'arsenic dans les roches du manteaux: Example des pyroxénites à grenat du massif lherzolitique des Beni-Bousera (Rif. Maroc). *Comptes Rendus de l'Academie de Sciences de París* 305, 383-386.

Makovicky, E., Karup-Møller, S., Makovicky, M. and Rose-Hansen, J. (1990). Experimental studies on the phase systems Fe-Ni-Pd-S and Fe-Pt-Pd-As-S applied to PGE deposits. *Minealogy and Petrology* 42, 307-319.

Makovicky, E., Makovicky, M. and Rose-Hansen, J. (1992). The phase system Pt-Fe-As-S at 850ºC and 470ºC. *Neues Jahrbuch für Mineralogie Monatshefte*, 441-457.

Marchesi, C., Garrido, C.J., Bosch, D., Bodinier, J.-L., Hidas, K., Padrón-Navarta, J.A. and Gervilla, F. (2012). A late oligocene suprasubduction setting in the westernmost mediterranean revealed by intrusive pyroxenite dikes in the ronda peridotite (Southern Spain). *Journal of Geology* 120, 237–247.

Matveed, S. and Ballhaus, C. (2002). Role of water in the origin of podiform chromitite deposits. *Earth and Planetary Science Letters* 203, 235-243.

Merkle, R.K. (1992). Platinum-group minerals in the middle group of chromitite layers at Marinkana, western Bushveld Complex: Indications for collection mechanisms and postmagmatic modifications. *Canadian Journal of Earth Sciences* 29, 209-221.

Naldrett, A.J. and Duke, J.M. (1980). Pt metals in magmatic sulfide ores: the occurrence of these metals is discussed in relation to the formation and importance of these ores. Science 208, 1417-1424.

O'Driscoll, B. and Gonzalez-Jiménez, J.M. (2016). Petrogenesis of the Platinum-Group Minerals. Reviews in Mineralogy and Geochemistry 81, 489-578.

Oen, I.S. (1973). A peculiar type of Ce-Ni mineralization; cordierite-chromite-niccolite ores of Málaga, Spain, and their possible origin by liquid unmixing. *Economic Geology* 68, 831-842.

Platt, J.P., Soto, J.I., Whitehouse, M.J., Hurford, A.J. and Kelley, S.P. (1998). Thermal evolution, rate of exhumation, and tectonic significance of metamorphic rocks from the floor of the Alboran extensional basin, western Mediterranean. *Tectonics* 17(5), 671–689

Piña, R., Gervilla, F., Barnes, S.-J., Ortega, L. y Lunar, R. (2013). Partition coefficients of platinum-group and chalcophile elements between arsenide and sulfide phases as determined in the Amasined sulfide-graphite mineralization (Beni Bousera, North Morocco). *Economic Geology* 108, 935-951

Piña, R., Gervilla, F., Barnes, S.-J, Ortega, L. and Lunar, R. (2015). Liquid immiscibility between arsenide and sulfide melts: evidence from LA-ICP-MS study in magmatic deposits from Serranía de Ronda (Spain). *Mineralium Deposita* 50, 265-279.

Torres-Ruiz, J., Garuti, G., Gazzoti, M., Gervilla, F. and Fenoll Hach-Alí, P. (1996). Platinum-group minerals in chromitites from the Ojén lherzolite massif (Serranía de Ronda, Betic Cordillera, Southern Spain). *Mineralogy and Petrology*, 56, 25-50.

Van der Wal, D. and Bodinier, J.L. (1996). Origin of the recrystallization front in the Ronda peridotite by km-scale pervasive porous flow. *Contributions to Mineralogy and Petrology* 122, 387-405

Van der Val, D. and Vissers, R.L.M. (1993). Uplift and emplacement of upper mantle rocks in the western Mediterranean. *Geology* 21, 1119-1122.

Wood, M. (2003). Arsenic in igneous systems: An experimental investigation. BA Science Thesis, University of Toronto. Canada.

Chapter 8
Field-trip guide

8.1 <u>Stop</u> 1: Overview of the field trip to the Ronda Peridotite

<u>Locality</u>: Lookout located along the Estepona to Jubrique road at Cerro del Porrejón (Fig. 8.1).
<u>Geographical coordinates</u>: 36°31'20.89"N / 5°11'22.34"<u>W</u>
<u>Tectonic Domai</u>n: Recrystallization front – spinel tectonite.
<u>Goals</u>:
- Overview of the regional geology.
- Overview of the structure of the peridotite.
- Understand the structure of the field trip to illustrate older to younger structures in the peridotite.

In this field trip, we are going to see some of the main petrological and structural features on the Ronda peridotite exposed in the western Sierra Bermeja. In view of its geologically young emplacement age (ca. 22 Ma) (Priem et al., 1979) in the Alborán area, showing significant gravity anomalies scattered but frequent seismic activity, high thermal anomalies (Cermák, 1982) an upper mantle with low seismic velocities (Banda and Deichmann, 1983), high subsidence rates since Miocene, and postorogenic calc-alkaline volcanism (Duggen et al., 2004, 2005), it is envisaged that Western Mediterranean ultramafic massifs allow a unique opportunity to interpret upper mantle structures, metamorphic assemblages and magmatic features in terms of ongoing tectonic and magmatic processes probably still active today.

The emphasis of this field trip will be to illustrate the different tectonic and metamorphic domains in the Ronda peridotites, as well as their magmatic features, in chronological order as deduced from their structural and metamorphic history, namely from an older domain represented by the spinel tectonites, situated to the NW in the visited area, to a younger plagioclase tectonite domain situated SE. The structural and metamorphic constraints provide a temporal and spatial framework for the geochemical studies and allow: (i) interpretation in terms of temporal magmatic events recorded in both peridotites and pyroxenites; (ii) relation to
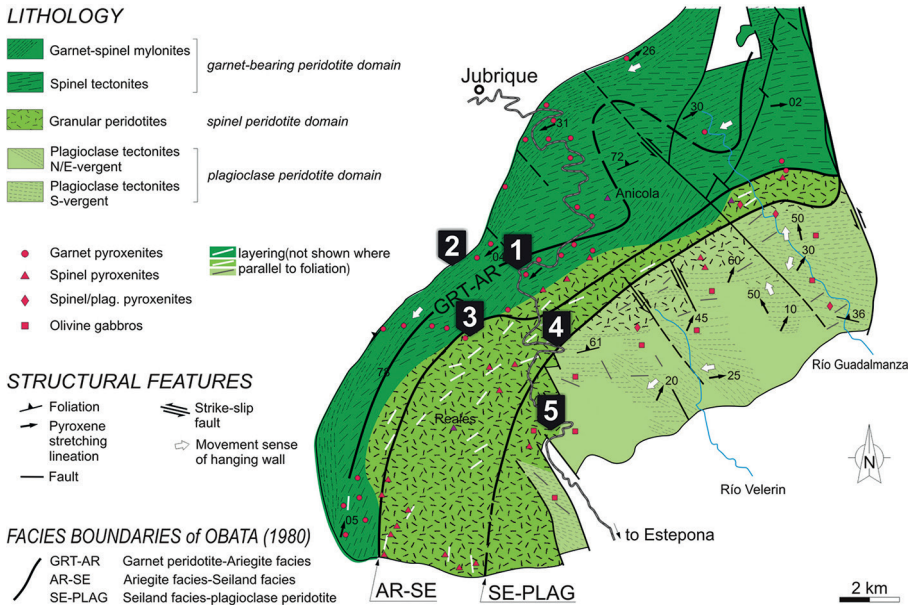
Figure 8.1. Location of outcrops provided in the field guide to characterize the different tectono-metamorphic domains of the Ronda ultramafic massif.

the development of the different tectonic domains; (iii) and study of magmatic mechanisms and the scale at which they occur in the upper mantle. Furthermore, the overprinting relationships identified in the field are used to test current working hypotheses for the uplift and emplacement of upper mantle rock in the Betic-Rifean orogen.

8.2   Stop 2: Thinning of the subcontinental lithospheric mantle, the crust-mantle detachment

Locality: Road to Genalguacil, stop near the contact with overlying Los Reales crustal units.
Geographical coordinates: Stop 2A (36°31'33.67"N / 5°12'38.12"W) Stop 2B (36°31'27.19"N / 5°12'31.32"W)

8.2.1 Stop 2A: Kinzigites

Tectonic Domain: kinzigites (mylonitic granulites).
Goal:
- See outcrop of the overlying kinzigites from the Los Reales Unit.

At the NW part of the Sierra Bermeja, a sequence of continental crust (los Reales unit) overlies the Ronda peridotite massif. This metapelitic unite belongs to the upper Alpujárride complex and displays a metamorphic imprint that grades from medium pressure – high temperature in felsic granulite facies (kinzigites) at the contact with the peridotite to low pressure – low temperature in phyllites below the low-grade Maláguide complex. From bottom to top –and lying between the kinzigites and phyllites– migmatites, gneisses, and schists occur structurally parallel to the northern contact of the massif (Balanyá et al., 1997; Negro et al., 2006) (Fig. 8.2).

In this outcrop, we will visit fresh kinzigites with large garnets that are crustal rocks overlying the garnet-spinel mylonite domain (Stop 2B).

8.2.2   Stop 2B: Garnet-spinel mylonites and ultramylonites

Tectonic Domain: Garnet-spinel mylonites.
Goal:
- Observe the mylonitic nature of garnet-spinel peridotite, and discuss the origin and geodynamic interpretation.

The NW part of the Ronda peridotite is bounded by a tectonic domain of foliated spinel- and garnet-bearing porphyroclastic to mylonitic peridotite (Fig. 8.2B). The existence of true garnet and garnet-spinel peridotite assemblages and their significance in terms of the internal structure and exhumation of Ronda peridotite has long been a matter of intense debate because of the lack of quantitative estimates of P-T pre-shearing and syn-shearing conditions due to the strong overprint of low-pressure assemblages and recrystallization (Obata, 1982; Platt et al., 2003; Schubert, 1982; Van der Wal and Vissers, 1996, 1997; Zeck, 1997).

Figure 8.2. (A) Field view of the contact between the Ronda ultramafic massif (left) and the overlying metamorphic units (right). (B) Garnet-Spinel mylonite outcrop with parallel S_0 compositional layering and S_1 tectonite foliation. Inset shows a garnet porphyroclasts.

Graphitized diamond in pyroxenite layers (Davies et al., 1993) is the earliest assemblage indicating an ultra-deep provenance of the Ronda peridotite (>4.5 GPa). All later studies agree that, before the deformation events recorded in the spinel tectonites and garnet-spinel mylonites, the Ronda peridotite was equilibrated at some "Primary conditions" at the graphite stability field; however, they differ in unambiguously establishing whether pre-shearing primary conditions were in the spinel (Van der Wal and Vissers, 1993, 1996) or in the garnet lherzolite facies (Obata, 1980). The strong overprint of low-pressure assemblages has precluded accurate determination of the P and T conditions for the onset of exhumation that formed the spinel tectonite and spinel-garnet mylonite domain occurring in the northern part of this massif.

Garrido et al. (2011) reported for the first time in Ronda unequivocal petrographic evidence for the existence of pre-shearing, coarse-grained garnet lherzolite assemblages from the spinel-garnet mylonite domain of the Ronda peridotite. Application of well-calibrated geothermobarometers yields pre-shearing minimum equilibration conditions of 1150 °C and 2.4-2.7 GPa (Figure 5.3.) demonstrating that the Ronda peridotite equilibrated at ca. 100 km before shearing. These authors show further evidence for the existence of syn-shearing spinel-garnet assemblages that overprinted garnet lherzolite assemblages at 900 °C and 1.9 GPa. The decompressive path and high-pressure recorded by the Ronda spinel-garnet mylonites rule out that they were formed by near-isobaric cooling right above a subduction-collision wedge or through (or after) the emplacement of the peridotite massif into the crust. Ronda spinel-garnet mylonites represent the vestiges of subcontinental mantle ductile shear zones formed at early stages of lithosphere extension. The presence of graphite pseudomorphs after diamond in garnet pyroxenites and the established "primary conditions" in garnet lherzolite facies likely record the end of an early extensional thinning from a thick diamond-bearing cratonic lithosphere (>150 km) to a thinner subcontinental mantle during the Mesozoic (Sánchez-Rodriguez and Gebauer, 2000). South-to-westward retreat of the African slab during the Oligocene-Early Miocene accounts for intense back-arc lithosphere extension and development of Ronda extensional shear zone coeval with extreme thinning of the Alborán domain overlying crust likely associated with lateral excision or flow of the lower crust. In contrast to other Alpine-type peridotite massifs that underwent extreme thinning towards plagioclase conditions during Tethyan extension, the Ronda peridotite was exhumed to garnet lherzolite facies (c. to 100 km).

The Garrido et al. (2011) P-T estimates of primary conditions differ significantly from those of Van der Wal and Vissers (1993, 1996) who established ad hoc pressure equilibration for primary conditions in the range of 1.8-2.0 GPa assuming that primary conditions reflected an earlier equilibrium in the spinel lherzolites facies after exhumation from diamond facies during the Mesozoic. These authors ascribed formation of garnet-spinel mylonites to cooling and compression of spinel peridotites in an Alpine subduction zone. The cooling and compressional nature of their P-T path strongly relied on their choices of temperature and pressure conditions for the primary conditions. New estimates of the primary conditions and the evidence of pre-shearing garnet lherzolites invalidate such P-T path and their

proposed tectonic scenario during the development of garnet-spinel mylonites. In addition, detailed mapping and fabric analysis shows that both garnet-spinel mylonites and spinel tectonites formed coevally during extension and progressive strain localization (Precigout et al., 2007, 2013).

New P-T estimates imply decompression of about 1.0 GPa from primary conditions to the frozen equilibration pressure recorded in garnet-spinel mylonites (Figure 5.3.). This decompression path is in good agreement with the breakdown of eclogite to garnet granulite observed in pyroxenitic boudins enclosed within the spinel-garnet mylonites (Morishita et al., 2001). Due to the fine-grained nature of mylonites, the isothermal or cooling nature of the path cannot easily be constrained from geothermometry. The equilibrium temperatures of garnet-spinel mylonites depend on whether compositions of neoblast reflect syntectonic equilibration temperatures or post-tectonic diffusional equilibration due to late cooling during the final emplacement of the massif into the crust. Several independent arguments support cooling during shearing. First, strain localization in garnet-spinel mylonites requires cooler conditions during shearing relative to primary conditions (Precigout et al., 2007). Second, elongated sapphirine-anorthite assemblages after high-pressure eclogite require both cooling and decompression (Morishita et al., 2001) from primary conditions.

A potential mechanism to account for cooling of garnet-spinel mylonites during exhumation and the pressure gap with the overlying felsic crustal section would be excision of the thickened lower mafic crust, which is totally absent in the Alpujárrides units, and the juxtaposition of the lithospheric mantle with cooler middle crust that presently overlies the peridotites along the Jubrique shear zone. This mechanism would explain the pressure gap between the primary conditions of the peridotites (c. 2.4-2.7 GPa) and the peak metamorphic pressure of the overlying granulites (1.5-1.8 GPa) and the preservation of the frozen garnet-spinel mylonites at the top of the mantle lithospheric section. Further extension during the late Oligocene to early Miocene lead to high temperature conditions and melting at the base of an extremely attenuated subcontinental lithospheric mantle (Garrido and Bodinier, 1999; Lenoir et al., 2001; Précigout et al., 2013). This event was likely coeval with tholeiitic dike intrusion in the Maláguide complex at the top of the overlying crustal envelope (Torres Roldán et al., 1986). This extensional event took place in a back-arc setting developed upon the previous Alpujárride-Maláguide orogenic wedge in a region situated several hundred km eastwards of their present emplacement (Booth-Rea et al., 2007).

8.3   Stop 3: Partial melting of the subcontinental lithospheric mantle

Locality: Road to Genalguacil, stop at "Peñas Blancas" (road MA-8301).
Geographical coordinates: from 36°29'52.94"N / 5°11'54.89"W boulders along a ca. 1 km path.
Tectonic Domain: Transition from the overlying spinel tectonite to the underlying granular spinel peridotite domain (Fig. 8.3).

Figure 8.3. Field view of the transition from overlying spinel tectonite to underlying coarse granular spinel peridotite domain across the recrystallization front. Note the parallel S_0 compositional layering and S_1 tectonite foliation (cf. Fig. 8.2B); the latter one disappears in the seemingly undeformed granular peridotites.

Goals:
- Recognize the main structures at the transition from the spinel tectonite to the granular spinel peridotite domains of the Ronda massif.
- Understanding the formation of coarse-granular spinel peridotite by recrystallization (grain growth) and melting of a previously deformed peridotite domain represented by the spinel tectonites.
- Recognize that the recrystallization front is a melting front associated to asthenospheric heating and decompression, leading to melting of an old subcontinental mantle lithosphere.

8.3.1 Microstructure of spinel tectonites

The spinel tectonites preserved in the Ronda peridotite occur on the northwestern part of the Ronda massif. This domain is dominated by porphyroclastic spinel peridotites. Their maximum dimension is >7 km measured perpendicular to the foliation. They are bound by granular peridotites to the south and southeast, and by a 500-750 m thick garnet-spinel mylonite to the northwest.

The outcrops visited is along the recrystallization front but peridotite still shows the porphyroclastic structure typical of the spinel tectonites; this microstructure is

marked by elongated pyroxenes in an olivine-dominated matrix. Throughout this domain, the intensity of the foliation is homogeneous but, locally, there are 100 m-scale discontinuous lens-shaped domains of less deformed rocks with a coarse-grained granular structure. The spinel tectonite microstructure is dominated by large elongated olivines (1-2 mm) surrounded by small olivine neoblasts (200-400 µm). Deformation-induced extinction and deformation bands are common. Elongate orthopyroxene porphyroclasts are occasionally surrounded by polygonal orthopyroxene and clinopyroxene neoblasts, suggesting deformation-induced dynamic recrystallization of the pyroxenes.

8.3.2   Transition from foliated to seemingly undeformed peridotites

Virtually undeformed granular peridotites define a second structural domain dominating the central part of the massif. This domain is bound by spinel tectonites to the north and northwest and by porphyroclastic plagioclase peridotites to the south and southeast. Spinel tectonites and granular peridotites are separated by a transition zone, about 200 m wide, which will be referred to as the "recrystallization front" (Lenoir et al., 2001; Van der Wal and Vissers, 1993, 1996; Vauchez and Garrido, 2001). The characteristics of the recrystallization front illustrate the nature and relative age of this boundary and some of its aspects can be seen at the locality visited, although continuity of the transition zone is largely lost due to late brecciation and poor outcrop conditions. This stop illustrates general features of the granular domain.

Features critical to the nature of the recrystallization front as well as to the relative age of the granular rocks with respect to the spinel tectonites are (Lenoir et al., 2001; Van der Wal and Vissers, 1993, 1996; Vauchez and Garrido, 2001). (i) the high relief in the area of up to 900 m allows assessment of the three-dimensional shape of the boundary by field mapping, indicating that this boundary is curved and that it forms part of a km-scale dome shaped surface; (ii) the transition from "typical" spinel tectonites to clearly granular peridotites occurs within a narrow zone of 200 m at most, marked by the disappearance of fabric elements such as foliation and mineral elongation, i.e., across the transition the shape-preferred orientations of olivine and pyroxene disappear and evolve towards a coarse equigranular microstructure; (iii) as evident from the map the boundary is markedly oblique to the structural trend of the spinel tectonites; (iv) the compositional layering and pyroxenite layers, are essentially continuous across the transition, and the orientation of the layering in the spinel tectonites is parallel to that in the granular domain; and (v) the alignment of spinel grains in trails, parallel to the foliation in the spinel tectonites, is also observed in the NW part of the granular domain and, across the transition, remains constant in orientation and parallel to the layering.

In the outcrop visited there are some fabric elements preserved which can be related to previous deformation in the spinel tectonite domain north of the recrystallization front. One such fabric element is spinel trails similar to those is the spinel tectonites.

8.3.3   Textural and microstructural variations of peridotites

Lenoir et al. (2001) classified peridotites across the recrystallization front into three textural groups:

1. *Porphyroclastic peridotites*, representing the deformed peridotite facies predominant in the spinel tectonite domain;
2. *Transitional peridotites*, which define the recrystallization front itself. This textural group occurs in a narrow band, a few hundred meters thick, between the porphyroclastic peridotites of the spinel tectonite domain to the NW and the recrystallized, coarse-granular peridotites to the SE. Its texture is distinguished by the presence of undeformed aggregates of clinopyroxene (cpx). These aggregates, made of equant (>0.5 mm) cpx grains with a cloudy appearance, coexist with clean cpx neoblasts and deformed cpx porphyroclasts. These undeformed aggregates of cpx are interpreted as newly formed, secondary clinopyroxene formed by cpx-forming reactions ("refertilization") that overprinted the porphyroclastic textures typical of peridotites from the spinel tectonite domain.
3. *Coarse-granular peridotites* characterized by very coarse and completely annealed microstructures. This textural facies defines within the granular domain the coarse-granular subdomain, which is spatially associated with the recrystallization front.

8.3.4   Geothermometry of peridotites at the recrystallization front

Lenoir et al. (2001) estimated the equilibration temperature in five samples -across the recrystallization front- using the compositions of unmixed cores and three thermometric formulations involving pyroxenes: (1) the Ca-in-cpx ['BKN' formulation of Brey and Köhler (1990)] and (2) the Ca-in-opx geothermometers ['Ca-in-opx' formulation Brey and Köhler (1990)] based on the two-pyroxene solvus; and (3) the Al-in-opx thermometer based on the Al solubility in orthopyroxene in the spinel lherzolite facies [opx-sp formulation of Witt-Eickschen and Seck (1991)]. The three formulations yield similar temperatures for the two samples of spinel tectonites, indicating relatively low temperatures in the range 1050–1100°C. The BKN formulation provides significantly higher temperatures for the three transitional and coarse-granular peridotites (1180–1225 °C). The Ca-in-opx formulation also provides similar results for the transitional and coarse-granular peridotites, but the temperature range is lower (1140–1150 °C). Finally, the opx–sp formulation yields a temperature similar to that obtained with the Ca-in-opx method for the coarse-granular peridotite (1155°C ±33 °C), but provides lower temperatures— indistinguishable from those obtained for the spinel tectonites— for the two transitional peridotites (1050–1110 °C).

In summary, their results indicate that the development of the recrystallization front was associated with a heating event in the temperature range of 1180–1225 °C, as recorded by the BKN geothermometer in the transitional and coarse-granular peridotites. This thermal event postponed the decompression cooling recorded by the spinel tectonites and spinel-garnet mylonites preserved in peridotites NW part of the Ronda peridotite (Figure 5.3.).

8.3.5   *Compositional variations of peridotites across the recrystallization front*

Lenoir et al. (2001) demonstrated the existence of compositional differences between the spinel tectonites and the transitional peridotites, and more important variations between the transitional peridotites and the coarse-granular ones. In contrast to the spinel tectonites, which include extremely variable compositions, from very fertile lherzolites (CaO/MgO >0.08) to refractory harzburgites (CaO/MgO <0.02), the transitional peridotites tend to be more homogeneous and dominated by mildly fertile lherzolites (CaO/MgO=0.06–0.08). The coarse-granular peridotites also tend to be more homogeneous than the spinel tectonites, but they are dominated by more refractory compositions (CaO/MgO=0.02–0.04), compared with the transitional peridotites. Statistical analysis indicates that the transitional peridotites are significantly more fertile (CaO/ MgO=0.072 ±0.009) than the spinel tectonite (CaO/MgO=0.048 ±0.027) and the coarse-granular textural facies (CaO/MgO=0.030 ±0.012). Conversely, the coarse-granular facies is significantly more refractory than the two other facies. The high average fertility and the elevated CaO/MgO ratio of the transitional peridotites is connected with the presence of secondary cpx aggregates characteristic of this textural facies.

In addition to major element variations, the study of Lenoir et al. (2001) revealed changes in REE contents and ratio of LREE across the recrystallization front. REE show subtle differences between the spinel tectonites and the transitional peridotites, and more important variations between the transitional peridotites and the coarse-granular ones. In general, the spinel tectonites have slightly more variable MREE and HREE contents than the other two textural groups. The transitional peridotites show slightly higher MREE and HREE contents than the spinel tectonites. The transitional peridotites show, on average, a significantly smaller Ce_N/Sm_N ratio and have a much more homogeneous LREE/MREE ratio than the spinel tectonites. On average, the coarse-granular peridotites are significantly more homogeneous and depleted in terms of REE contents than spinel tectonites and transitional peridotites, but show a range of Ce_N/Sm_N variation similar to that of transitional peridotites

As they are correlated with Ca content, variations of HREE and MREE abundances across the front are essentially controlled by the fertility of the peridotites, which increases from the spinel tectonites to the transitional peridotites, and then decreases abruptly in the coarse-granular subdomain. The higher HREE and MREE contents of the transitional peridotites are in good agreement with cpx-forming reactions as inferred from their greater CaO/MgO ratio. The mean Ce_N/Sm_N ratio shows an overall decrease across the recrystallization front, unrelated to peridotite fertility, and it is significantly more homogeneous in the transitional and coarse-granular peridotites compared with spinel tectonites.

Lenoir et al. (2001) interpreted REE variations of peridotites across the recrystallization front as a record of coeval partial melting (coarse-grained peridotites) and melt-consuming reactions ("refertilization" reactions; transitional peridotites), spatially separated by a few hundred meters. The extraction of partial melts from the coarse-granular peridotites is indicated by the abrupt decrease of peridotite fertility degree and REE contents in the few hundred meters (200 m)

separating this facies from the transitional peridotites. Using the mean Yb content of the spinel tectonites as the source composition the estimated melt extraction degree varies between 2.5% for fractional melting and 3.5% for batch melting.

Geochemical variations of peridotites indicate that the recrystallization front is the narrow boundary of a partial melting domain (the coarse-granular peridotites) formed at the expense of subcontinental lithospheric mantle (the spinel tectonites). The presence of secondary cpx related to melt-consuming reactions in the transitional peridotites, a few hundred meters ahead of the melting front, demonstrates that the development of the front was thermally controlled. It implies that smooth thermal gradient existed across the Ronda massif during the formation of the recrystallization front. The melting event inferred from the geochemical variation of peridotites across the front is recorded by differences in pyroxene compositions on either side of the front, probably implying a rapid, transient heating event at (1200 °C and >1.5 GPa). The sharpness of geochemical and textural variations occurring at the Ronda recrystallization front strongly indicates coupling between melting and textural coarsening processes during asthenosphere–lithosphere interaction.

This thermal event took place in the late geodynamic evolution of the Alborán domain (Garrido and Bodinier, 1999; Garrido et al., 2011; Hidas et al., 2013a; 2015; Lenoir et al., 2001; Van der Wal and Vissers, 1993), likely in the late Cenozoic evolution of Ronda, and was aborted by the emplacement of the massif in the crust (Hidas et al., 2013a). The recrystallization front indicates that a heating event caused pervasive shallow melting of the thinned lithospheric roots beneath the Alborán domain during thinning in a back-arc setting due to subduction rollback (Garrido et al., 2011; Hidas et al., 2013b; 2015).

8.4   Stop 4: Intracrustal emplacement – Part A.

Locality: Leaving "Peñas Blancas" on the road MA-8301, direction Estepona.
Geographical coordinates: Stop 4A (36°30'17.02"N / 5°10'39.24"W) and Stop 4B (36°30'23.18"N / 5°10'40.47"W).
Tectonic Domain: Coarse-granular spinel peridotite domain.

8.4.1   Stop 4A. Intrusive leucogranite dykes and bodies in serpentinite fault gauges

Goals:
- See outcrops of intrusive leucogranites and their relation with late serpentinite faults.
- Age of leucogranite intrusions and their relation with the intracrustal emplacement of the Ronda peridotite.

At this stop, we will visit an outcrop (picture above; white network in a dark-blueish serpentinite matrix) of a dyke swarm of leucogranites intruding along a

Figure 8.4. Leucogranite dyke swarm (white) along a serpentinite fault gauge. The leucogranite formed at the dynamothermal aureole below the peridotites during the intracrustal emplacement of the Ronda ultramafic massif, and intruded in the overlying peridotites along late brittle serpentinite faults.

serpentinite fault gauge (Fig. 8.4). The origin of these leucogranite dykes and bodies are ascribed to be formed at the dynamothermal aureole below the peridotite that produced partial melts that generated the intrusion of granite dykes in the Ronda peridotite during the its hot intracrustal emplacement (Cuevas et al., 2006; and references therein). Geochronological data place rather broad limits for this event between 22 and 19 Ma (Esteban et al., 2007, 2011; Priem et al., 1979). Analyses of neocrystalline zircon rims from large zircon populations yield a U–Pb SHRIMP age of 22.3 ±0.7 Ma for the dynamothermal aureole formation, and intrusion ages of granite dykes between 22.6 ±1.8 Ma and 21.5 ±3.8 Ma support that conclusion (Esteban et al., 2011). Granite dykes were crystallized from felsic magmas derived by partial melting of the continental crust related to the formation of this dynamothermal aureole. They emanate from the aureole and intrude within the overlying peridotites (Cuevas et al., 2006; and references therein). Moreover, their [87]Sr/[86]Sr signature (Priem et al., 1979) also confirms their crustal affinity. Dykes are slightly deformed and porphyritic dyke containing euhedral to subhedral crystals of plagioclase, cordierite and K-feldspar immersed in a euhedral and fine-grained cordierite–plagioclase–quartz matrix. This interpretation has been challenged by recent U-Pb zircon ages that demonstrate a Variscan age for the genesis of the dynamothermal aureole (Acosta-Vigil et al., 2014) implying that leucogranites formed in an unrelated melting event.

8.4.2 Stop 4B. Group-D pyroxenites

Goal:
• See Group-D (Cr-rich) pyroxenites.

In this locality, we will visit a remarkable outcrop of a thick Cr-rich pyroxenite (group D of Garrido and Bodinier, 1999). These pyroxenites are common in the coarse-granular domain, a few hundred of meters behind the recrystallization front, and the plagioclase tectonite domain of Ronda. The outcrop visited here shows a very coarse-grained, Cr-rich websterite (up to several cm-wide diopside and enstatite). Here, group D pyroxenites are "concordant" and parallel to other pyroxenite layers in the Ronda peridotite. A close inspection of the outcrop reveals that Cr-rich pyroxenite actually replaces an Al-rich pyroxenite (group B of Garrido and Bodinier, 1999) preserving clusters of spinel-orthopyroxene-plagioclase interpreted as formed after garnet breakdown. In terms of their geochemistry, Group B pyroxenites are interpreted as melting residues of garnet pyroxenites in an open system related to the development of the recrystallization front (Garrido and Bodinier, 1999). Textural and field relationships indicate that Cr-rich pyroxenite such as the one observed in this outcrop fully replaced group B pyroxenites. This replacement took place after melting of garnet pyroxenites recorded in the recrystallization front, likely in the waning magmatic stages of the Ronda peridotites before its final emplacement into the crust. This would explain the predominance of group D pyroxenites in the Ronda coarse-granular and plagioclase tectonite domains.

From a geochemical point of view, Cr-suite pyroxenites are characterized by high but nearly constant Mg# (85-95), high Cr (up to 15,000 ppm) and Ni (up to 2500 ppm) contents, and low Al_2O_3 (2-8 wt%) and TiO_2 (<0.34 wt%) contents. In terms of major and transition elements, Cr-suite pyroxenites are similar to igneous cumulates occurring in the mantle section of some ophiolites. Chondrite-normalized REE patterns of group D pyroxenites show sigmoidal patterns characterized by relatively high-LREE contents compare to other Cr- suite mafic layers, and very low HREE contents. However, the most striking geochemical feature of group D pyroxenites as exemplified by the crosscutting dikes is their HFSE depletion relative to trace element of similar compatibility. This depletion is illustrated by strong negatives anomalies of Zr and Hf relative to Sm and Nd, and Nb and Ta relative to Th and La, in primitive-mantle (PM)-normalized compatibility diagrams.

Critical features of Cr-suite parental melts (group D) which provide insight into their geochemical nature are: (i) high but relatively constant Mg# (65-75); (ii) high Cr and Ni contents; (iii) low variance primary mineralogy dominated by clinopyroxene and orthopyroxene (± olivine); (iv) enrichment in LILE and LREE relative to N-MORB, but HFSE contents similar to N-MORB; and (v) HREE contents lower than N-MORB. These geochemical features not only indicate that Cr-suite parental melt had an arc-like geochemical signature but also suggest that they were similar to High Magnesium Andesites (HMA) occurring in current arc and back-arc tectonic settings (Crawford, 1989; Kelemen et al., 2003). High Mg#, as well as high Ni and Cr contents, indicates that these melts were equilibrated with refractory peridotites. These observations corroborated a Cenozoic supra-subduction evolution of the Ronda peridotite.

8.5   Stop 5: Intracrustal emplacement – Part B.

Locality: Stop on the road MA-8301, direction Estepona. Walk along unpaved road in the Arroyo de la Cala area (ca. 20 min in one direction).

Geographical coordinates: from 36°29'6.76"N / 5°10'41.92"W to 36°28'58.94"N / 5°11'6.63"W

Tectonic Domain: Plagioclase tectonite domain.

Goals:

- Observe the transition from coarse-granular spinel peridotites to plagioclase-bearing peridotites. Development of a new ductile deformation.
- Understand the relationship of plagioclase tectonites with the intracrustal emplacement of the peridotite massif.

8.5.1   *Transition from granular spinel peridotites to plagioclase tectonites*

Compositional layering (S_0), represented by spinel pyroxenite at the recrystallization front has similar orientation to garnet pyroxenite layering and tectonic foliation (S_1) of the spinel tectonite domain (dipping N70-80° to NW) (Hidas et al., 2013a; Lenoir et al., 2001; Soustelle et al., 2009; Van der Wal and Vissers, 1996). However, down the lithospheric section from the granular peridotites to the plagioclase tectonites the layering is rotated gradually, at the base of the Ronda SCLM section ending up in a N40-60º to E-NE position that is almost perpendicular to the compositional layering of the spinel tectonite domain. Weak tectonic foliation (S_2) is seen in spinel lherzolite (Fig. 8.5) immediately below the recrystallization front with a N60-80° to N-NW structure slightly oblique to both local S_0 and to the garnet pyroxenite layering of the overlying spinel tectonite domain (Hidas et al., 2013a).

Further down section the plagioclase tectonite domain exhibits a quite uniform N50-70° to N-NE foliation that is intense in lherzolite and weaker in the more refractory peridotites, crosscutting local S_0 layering and isoclinal folds and, at the same time, striking oblique to the S_1 foliation and S_0 compositional layering of the spinel tectonite domain. The microstructure of porphyroclastic plagioclase lherzolite is characterized by the occurrence of elongated symmetric tails of metamorphic plagioclase rims around spinel in the foliation plane suggesting that foliation is formed by pure flattening. Lineation is measured on aggregates of elongated spinel ±plagioclase crystals showing NE-SW trend within the northward dipping foliation plane. Crosscutting relationship between layering and S_2 foliation indicates an overall west-southwest vergence in the northeastern and east-southeast vergence in the southeastern part of the study area with local inversion of these vergence directions related to minor folds at a scale of 10-100 meters (Hidas et al., 2013a). Stereonets of structural data show that the compositional layering forms two limbs crosscut by the unfolded plagioclase tectonite foliation and the fold axis direction is estimated as the perpendicular to the plane that contains the poles of layering (Hidas et al., 2013a). Under present geographical coordinates, the fold axial surface dips 60° towards the north (average orientation of the plagioclase foliation) and the fold hinge (intersection
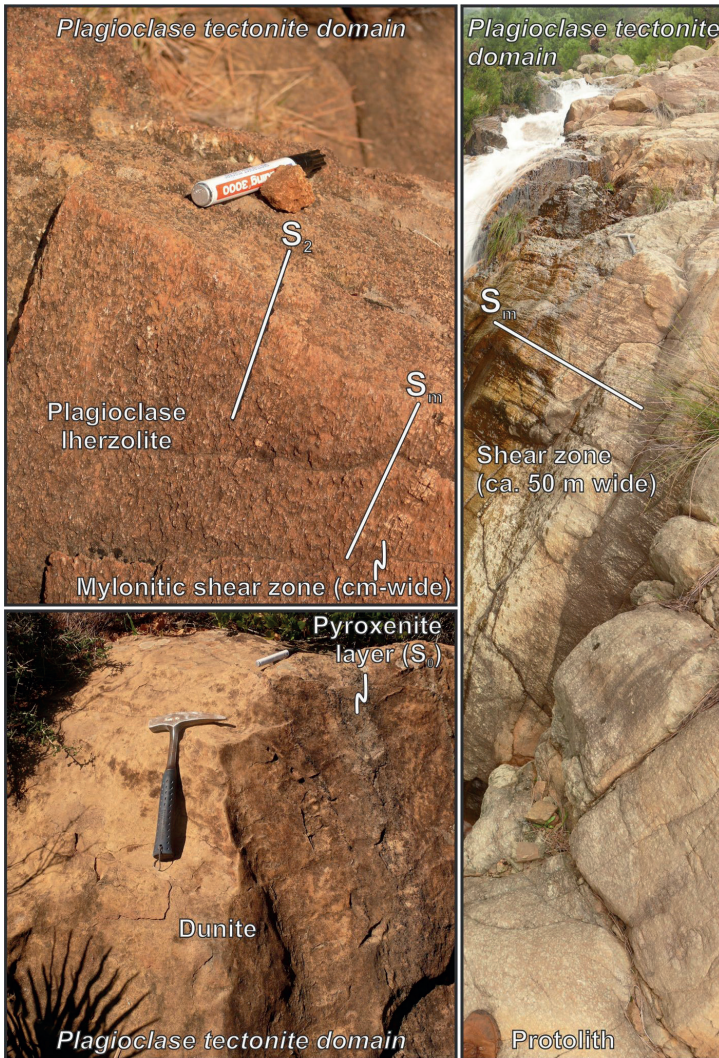
Figure 8.5. Plagioclase lherzolite (top-left), dunite (bottom-left) and late ductile shear zone (right) in the plagioclase tectonite domain of the Ronda ultramafic massif. Note that S_2 high-T plagioclase tectonite foliation and S_m low-T mylonite foliation are subparallel to each other but they have a distinctly different orientation from S_0-S_1 of the overlying tectono-metamorphic domains (cf. Figs. 5.2, 8.2. and 8.3.).

between the layering in both limbs and between the foliation and the layering) plunges approx. 45° towards the NE.

Numerous shear zones ranging from several tens of centimeters to several-meters width occur in the plagioclase tectonite domain (Hidas et al., 2013a; 2013b; 2016) (Fig. 8.5). The strike of the shear zone foliation (S_m) usually follows that of the tectonic foliation but with a more gentle dip (30-50º towards N-NE). Besides,

the mylonites develop spinel porphyroclast aggregate lineation trending in the same direction as in S$_2$ tectonites (NE-SW), which direction also correlates with the top-to-the-SW sense of shear deducted from S-C structures observed in some shear zones (Hidas et al., 2013a; 2016).

8.5.2   *The Arroyo de la Cala chromitite*

This mineralization can be classified within the Ni arsenide-poor Cr-Ni ore type (see Chapter 6). The chromitite occurs associated with one of the low-temperature shear zones mapped in the Arroyo de la Cala area (Fig. 4.2.), located at the transition between the granular domain and the plagioclase tectonite domain and shows internal foliation parallel to the shear zone. This area is characterized by the presence of lens-like bodies of dunite with an orientation parallel to the foliation of the plagioclase tectonite domain (N50-70° to N-NE), enveloped by harzburgite and olivine-rich lherzolite within plagioclase lherzolite. It consists of chromitite ore veins of variable thickness (from 1 to 20 cm) arranged in a stockwork-like pattern hosted in sheared harzburgite (locally containing Group D pyroxenite layers) and minor dunite (Fig. 8.6.). The latter
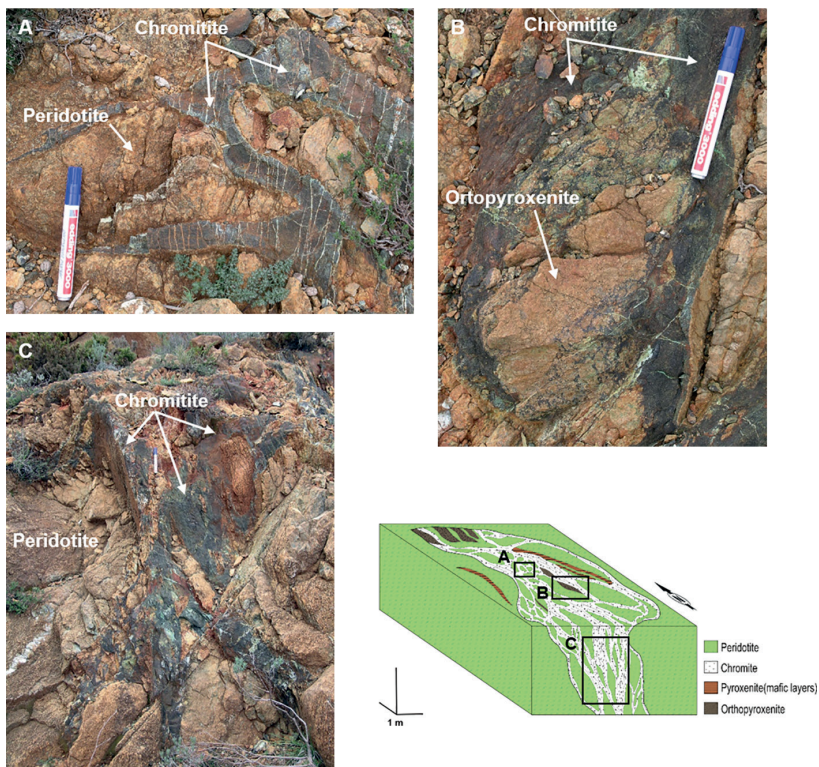

Figure 8.6. Mesostructure of the chromitite pod (Cr-Ni ore) cropping at the Arroyo de la Cala area, showing contact relationships between chromitite and host peridotite (A and C), and between chromitite and included lenses of orthopyroxenite (B).

peridotites remain as angular blocks within the chromitite stock work, showing sharp contacts. This ore occurrence has a sigmoidal morphology and is small in size (surface projection 9 x 5 m). The chromitite contains very small amounts of Ni arsenides (<1 % volume) although there are abundant green and blue-greenish-white patinas of Ni silicates (garnierite) and Ni arseniates (annabergite) formed by weathering of the primary Ni arsenides. The ore veins enclose and grade into lenticular bodies of cumulus orthopyroxenite.

The foliated nature of this chromitite (the associated orthopyroxenite is locally foliated too) with internal lineation and foliation subparallel to that of the low T shear zones developed during the crustal emplacement of the massif (see Chapter 5) shows that it formed by syntectonic magmatic crystallization coeval with such emplacement. These internal structures would result from the deformation of partially consolidated ore consisting of chromite crystals with minor amounts of intergranular arsenide melt associated with solid orthopyroxenite. Deformation was favored by the presence of the intergranular melt and the generated foliation planes later acted as pathways for the meteoric fluids which weathered and lixiviated the Ni arsenides.
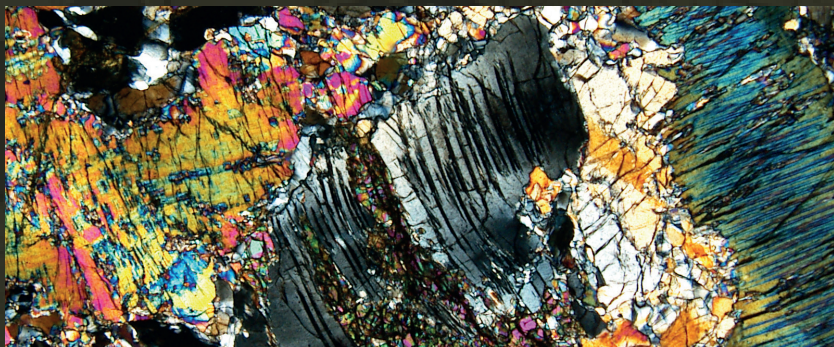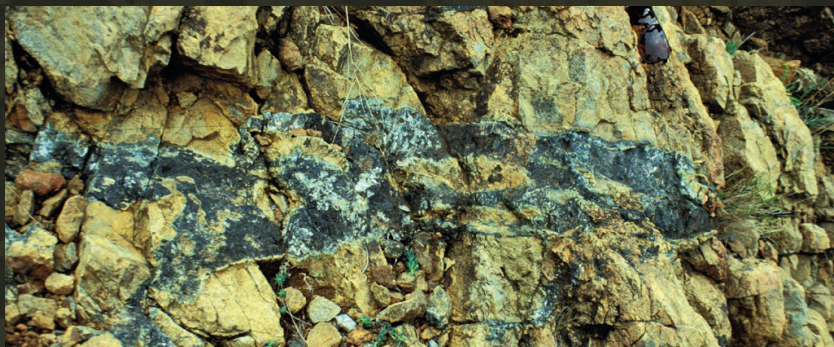
References

Acosta-Vigil, A., Rubatto, D., Bartoli, O., Cesare, B., Meli, S., Pedrera, A., Azor, A. and Tajcmanova, L. (2014). Age of anatexis in the crustal footwall of the Ronda peridotites, S Spain. *Lithos* 210, 147-167.

Balanyá, J.C., García Dueñas, V., Azañón, J.M. and Sánchez Gómez, M. (1997). Alternating contractional and extensional events in the Alpujarride Nappes of the Alboran domain (Betics, Gibraltar arc). *Tectonics* 16, 226-238.

Banda, E. and Deichmann, N. (1983). Low-velocity zone reflections observed in geometrical shadows of refraction profiles - comment. Geophysical Journal of the Royal Astronomical Society 74, 633-636.

Booth-Rea, G., Ranero, C.R., Martínez-Martínez, J.M. and Grevemeyer, I. (2007). Crustal types and Tertiary tectonic evolution of the Alborán Sea, western Mediterranean. *Geochemistry Geophysics Geosystems* 8, 10.1029/2007gc001639.

Brey, G.P. and Köhler, T. (1990). Geothermobarometry in four-phase lherzolites. II. New thermobarometers, and practical assessment of existing thermobarometers. *Journal of Petrology* 31, 1353-1378.

Cermák, V. (1982). Crustal temperature and mantle heat flow in Europe. *Tectonophysics* 83, 123-142.

Crawford, A.J. (1989). Boninites and Related Rocks. Unwin Hyman, London, p. 446.

Cuevas, J., Esteban, J.J. and Tubía, J.M. (2006). Tectonic implications of the granite dyke swarm in the Ronda peridotites (Betic Cordilleras, Southern Spain). *Journal of the Geological Society* 163, 631-640.

Davies, G.R., Nixon, P.H., Pearson, D.G. and Obata, M. (1993). Tectonic implications of graphitized diamonds from the Ronda Peridotite massif, Southern Spain. *Geology* 21, 471-474.

Duggen, S., Hoernle, K., Van den Bogaard, P. and Garbe-Schonberg, D. (2005). Post-collisional transition from subduction- to intraplate-type magmatism in the westernmost Mediterranean: Evidence for continental-edge delamination of subcontinental lithosphere. *Journal of Petrology* 46, 1155-1201.

Duggen, S., Hoernle, K., van den Bogaard, P. and Harris, C. (2004). Magmatic evolution of the Alboran region: The role of subduction in forming the western Mediterranean and causing the Messinian Salinity Crisis. *Earth and Planetary Science Letters* 218, 91-108.

Esteban, J.J., Cuevas, J., Tubia, J.M., Liati, A., Seward, D. and Gebauer, D. (2007). Timing and origin of zircon-bearing chlorite schists in the Ronda peridotites (Betic Cordilleras, Southern Spain). *Lithos* 99, 121-135.

Esteban, J.J., Cuevas, J., Tubía, J.M., Sergeev, S. and Larionov, A. (2011). A revised Aquitanian age for the emplacement of the Ronda peridotites (Betic Cordilleras, southern Spain). *Geological Magazine* 148, 183-187.

Garrido, C.J. and Bodinier, J.L. (1999). Diversity of mafic rocks in the Ronda peridotite: Evidence for pervasive melt-rock reaction during heating of subcontinental lithosphere by upwelling asthenosphere. *Journal of Petrology* 40, 729-754.

Garrido, C.J., Gueydan, F., Booth-Rea, G., Precigout, J., Hidas, K., Padron-Navarta, J.A. and Marchesi, C. (2011). Garnet lherzolite and garnet-spinel mylonite in the Ronda peridotite: Vestiges of Oligocene backarc mantle lithospheric extension in the western Mediterranean. *Geology* 39, 927-930.

Hidas, K., Booth-Rea, G., Garrido, C.J., Martínez-Martínez, J.M., Padrón-Navarta, J.A., Konc, Z., Giaconia, F., Frets, E. and Marchesi, C. (2013a). Back-arc basin inversion and subcontinental mantle emplacement in the crust: kilometre-scale folding and shearing at the base of the proto-Alborán lithospheric mantle (Betic Cordillera, southern Spain). *Journal of the Geological Society* 170, 47-55.

Hidas, K., Garrido, C.J., Tommasi, A., Padrón-Navarta, J.A., Thielmann, M., Konc, Z., Frets, E. and Marchesi, C. (2013b). Strain localization in pyroxenite by reaction-enhanced softening in the shallow subcontinental lithospheric mantle. *Journal of Petrology* 54, 1997-2031.

Hidas, K., Tommasi, A., Garrido, C.J., Padrón-Navarta, J.A., Mainprice, D., Vauchez, A., Barou, F. and Marchesi, C. (2016). Fluid-assisted strain localization in the shallow subcontinental lithospheric mantle. *Lithos* 262, 636-650.

Hidas, K., Varas-Reus, M.I., Garrido, C.J., Marchesi, C., Acosta-Vigil, A., Padrón-Navarta, J.A., Targuisti, K. and Konc, Z. (2015). Hyperextension of continental to oceanic-like lithosphere: The record of late gabbros in the shallow subcontinental lithospheric mantle of the westernmost Mediterranean. *Tectonophysics* 650, 65-79.

Kelemen, P.B., Hanghøj, K. and Greene, A.R. (2003). One view of the geochemistry of subduction-related magmatic arcs, with emphasis on primitive andesite and Lower crust. In: Rudnick, R.L. (Ed.), *Geochemistry of the Crust*. Elsevier-Pergamon, Oxford, pp. 593-659.

Lenoir, X., Garrido, C., Bodinier, J., Dautria, J. and Gervilla, F. (2001). The recrystallization front of the Ronda peridotite: Evidence for melting and thermal erosion of subcontinental lithospheric mantle beneath the Alboran basin. *Journal of Petrology* 42, 141-158.

Morishita, T., Arai, S. and Gervilla, F. (2001). High-pressure aluminous mafic rocks from the Ronda peridotite massif, southern Spain: significance of sapphirine- and corundum-bearing mineral assemblages. *Lithos* 57, 143-161.

Negro, F., Beyssac, O., Goffe, B., Saddiqi, O. and Bouybaouene, M.L. (2006). Thermal structure of the Alborán Domain in the Rif (northern Morocco) and the Western Betics (southern Spain). Constraints from Raman spectroscopy of carbonaceous material. *Journal of Metamorphic Geology* 24, 309-327.

Obata, M. (1980). The Ronda peridotite - garnet-lherzolite, spinel-lherzolite, and plagioclase-lherzolite facies and the P-T trajectories of a high-temperature mantle Intrusion. *Journal of Petrology* 21, 533-572.

Obata, M. (1982). Reply to W. Schubert's comments on "The Ronda peridotite - garnet-lherzolite, spinel-lherzolite, and plagioclase-lherzolite facies and the P-T trajectories of a high-temperature mantle intrusion". *Journal of Petrology* 23, 296-298.

Platt, J.P., Argles, T.W., Carter, A., Kelley, S.P., Whitehouse, M.J. and Lonergan, L. (2003). Exhumation of the Ronda peridotite and its crustal envelope: constraints from thermal modelling of a P-T-time array. *Journal of the Geological Society* 160, 655-676.

Precigout, J., Gueydan, F., Gapais, D., Garrido, C.J. and Essaifi, A. (2007). Strain localization in the subcontinental mantle - a ductile alternative to the brittle mantle. *Tectonophysics* 445, 318-336.

Précigout, J., Gueydan, F., Garrido, C.J., Cogné, N. and Booth-Rea, G. (2013). Deformation and exhumation of the Ronda peridotite (Spain). *Tectonics* 32, 1011-1025.

Priem, H.N.A.K., Hebeda, E.H., Boelrijk, N.A.I.M., Verdurmen, T.E.A. and Oen, I.S. (1979). Isotopic dating of the emplacement of the ultramafic masses in the Serrania de Ronda, Southern Spain. *Contribution to Mineralogy and Petrology* 70, 103-109.

Sánchez-Rodriguez, L. and Gebauer, D. (2000). Mesozoic formation of pyroxenites and gabbros in the Ronda area (southern Spain), followed by Early Miocene subduction metamorphism and emplacement into the middle crust: U-Pb sensitive high-resolution ion microprobe dating of zircon. *Tectonophysics* 316, 19-44.

Schubert, W. (1982). Comments on "The Ronda peridotite - garnet-lherzolite, gpinel-lherzolite, and plagioclase-pherzolite facies and the P-T trajectories of a high-temperature mantle iuntrusion" by M. Obata (J. Petrol., 21, 553-572, 1980). *Journal of Petrology* 23, 293-295.

Soustelle, V., Tommasi, A., Bodinier, J.L., Garrido, C.J. and Vauchez, A. (2009). Deformation and reactive melt transport in the mantle lithosphere above a large-scale partial melting domain: the Ronda Peridotite Massif, southern Spain. *Journal of Petrology* 50, 1235-1266.

Torres Roldán, R.L., Poli, G. and Peccerillo, A. (1986). An early Miocene arc-tholeitic magmatic dike event from the Albora Sea - Evidence for precollisional subduction and back arc crustal extension in the westernmost mediterranean. *Geologische Rundschau* 75, 219-234.

Van der Wal, D. and Vissers, R.L.M. (1993). Uplift and Emplacement of Upper-Mantle Rocks in the Western Mediterranean. *Geology* 21, 1119-1122.

Van der Wal, D. and Vissers, R.L.M. (1996). Structural petrology of the Ronda peridotite, SW Spain: Deformation history. *Journal of Petrology* 37, 23-43.

Van der Wal, D. and Vissers, R.L.M. (1997). Reply to Discussion by H. P: Zeck of 'Structural petrology of the Ronda Peridotite, SW Spain; deformation history'. *Journal of Petrology* 36, 534-536.

Vauchez, A. and Garrido, C.J. (2001). Seismic properties of an asthenospherized lithospheric mantle: constraints from lattice preferred orientations in peridotite from the Ronda massif. *Earth and Planetary Science Letters* 192, 235-249.

Witt-Eickschen, G. and Seck, H.A. (1991). Solubility of Ca and Al in Ortho-pyroxene from spinel peridotite - an improved version of empirical geothermometer. *Contributions to Mineralogy and Petrology* 106, 431-439.

Zeck, H.P. (1997). Discussion of 'Structural petrology of the Ronda Peridotite, SW Spain: Deformation History' by D. Van der Wal and R. L. M Vissers. *Journal of Petrology* 38, 529-531.

Geology and Metallogeny

of the upper mantle rocks from the

Serranía de Ronda

SEM
Sociedad Española de Mineralogía

UNIVERSIDAD
DE GRANADA

Ronda
SUERTE NATURAL
www.turismoderonda.es

IACT
INSTITUTO ANDALUZ DE CIENCIAS DE LA TIERRA